12.812: THE GENERAL CIRCULATION OF THE ATMOSPHERE AND CLIMATE CHANGE

Paul O'Gorman

April 9, 2010

Contents

1 Introduction

1.1 Lorenz's view

> During the past three centuries, the prevailing ideas about the general circulation of the earth's atmosphere have evolved in a stepwise manner. Early in each step, a new theoretical idea is formulated. Late in each step, the idea gains general acceptance, but, more or less concurrently, new observations show that the idea is wrong. (Lorenz, 1983)

1.2 The general circulation: 1735 (Hadley)

See sketches in Lorenz (1983)

- Zonal Coriolis force
- Surface easterly and westerly winds
- Angular momentum balance
- Equatorward drift in midlatitudes!

1.3 The general circulation: 1857 (Thompson)

- Meridional Coriolis force
- Indirect cell
- Also Ferrel 1859
- 1900 cloud study: no upper level poleward flow in extratropics!

... more cells(!), then angular momentum and heat transport by *eddies* (Jeffries 1926, Starr 1948, and others)...

1.4 The general circulation: 1980-2001 (ERA40)

See Figure 1.1.

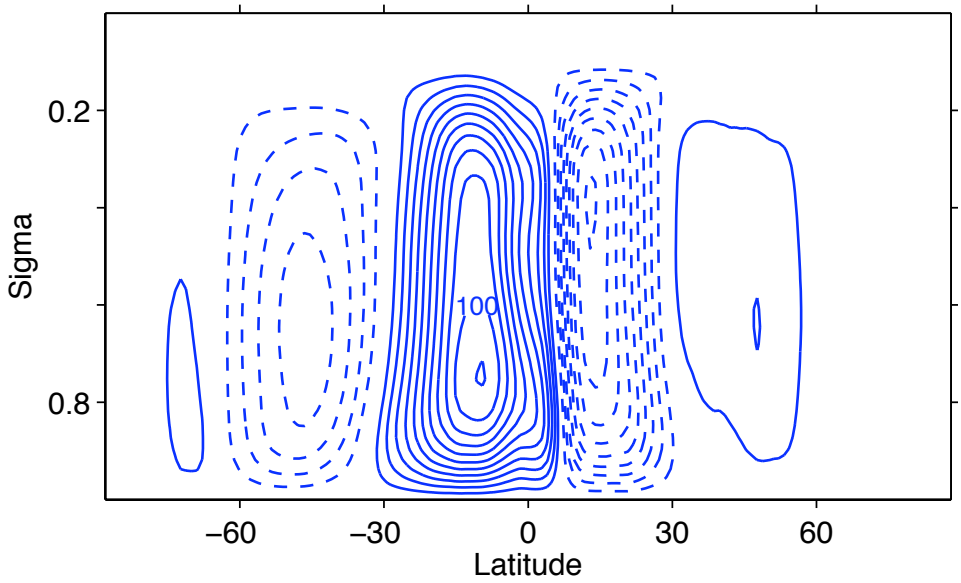

Figure 1.1: Based on data from ERA40

1.5 The general circulation: recent trends (1980-2005)

- See Figure 2 of Siedel et al. (2008)
- An update to Lorenz's epistomological theory?

1.6 Course aim

Characterize the mean circulations, variability, and energy, momentum, water, and entropy budgets of the atmosphere and how they may change.

2 Some mathematical machinery

2.1 Transient and Stationary eddies

Note: this section follows Peixoto and Oort (1992), section 4.1

We will denote the time mean of any quantity A as

$$\overline{A} = \frac{1}{\tau}\int_0^\tau A dt$$

where the time interval τ could be a month, a season, a year, etc. We can always express A as the sum of the mean plus an anomaly:

$$A = \overline{A} + A'$$

It follows that the mean of the anomaly must be zero:

$$\overline{A'} = 0$$

.

We will frequently be taking the mean of the product of two quantities, which we can write

$$\begin{aligned}\overline{AB} &= (\overline{A} + A')(\overline{B} + B') \\ &= \overline{AB} + \overline{A'B'}\end{aligned}$$

The second term on the RHS above is the covariance of A and B, which can also be written

$$\overline{A'B'} = r(A,B)\sigma(A)\sigma(B) \tag{2.1}$$

where $r(A,B)$ is the correlation coefficient and $\sigma(A), \sigma(B)$ are the standard deviations of A and B.

Most atmospheric fields are more uniform (in a statistical sense) along latitude circles than meridionally (with some notable exceptions such as the Walker circulation). We will therefore assume a zonally symmetric distribution as a first approximation, and take averages around latitude circles. Note that the fundamental basis for this assumption is Earth's rotation, which ensures that the daily-averaged insolation is zonally symmetric. (This would not be a good average for a tidally-locked planet, for example).

We denote the zonal mean with square brackets $[A]$, and note that we can decompose A into mean and anomaly in the same way as we did for the time mean:

$$\begin{aligned}[A] &= \frac{1}{2\pi}\int_0^{2\pi} A d\lambda \\ A &= [A] + A^* \\ [A^*] &= 0\end{aligned}$$

Now combining the two averaging operators, we can decompose A into four components:

$$\begin{aligned}A &= [A] + A^* \\ &= [\overline{A} + A'] + (\overline{A} + A')^* \\ &= [\overline{A}] + [A'] + \overline{A^*} + A'^*\end{aligned}$$

where $[\overline{A}]$ is the zonally symmetric part of the time averaged quantity; $\overline{A^*} = \overline{A} - [\overline{A}]$ is the asymmetric part of the time averaged quantity (e.g. stationary eddies or land-ocean contrast); $[A'] = [A] - [\overline{A}]$ represents instantaneous fluctuations of the symmetric part (e.g. fluctuations of the zonal-mean circulation); and finally A'^* represents transient, asymmetric eddies.

Now consider $[\overline{AB}]$ (e.g. the total flux or variance), noting that $[\overline{AB}] = \overline{[AB]}$. As an example, take $[\overline{vT}]$, the poleward heat flux. First, decompose each term into mean and anomaly in time, and expand:

$$\begin{aligned}vT &= (\overline{v} + v')(\overline{T} + T') \\ &= \overline{v}\overline{T} + v'T' + v'\overline{T} + \overline{v}T'\end{aligned}$$

Now take the time average:

$$\overline{vT} = \overline{v}\overline{T} + \overline{v'T'}$$

(the other terms drop out of the average).

But we can also decompose the time-mean terms into zonal mean and anomaly:

$$\begin{aligned}\overline{v} &= [\overline{v}] + \overline{v}^* \\ \overline{T} &= [\overline{T}] + \overline{T}^*\end{aligned}$$

so we can write

$$\overline{vT} = [\overline{v}][\overline{T}] + \overline{v}^*\overline{T}^* + \overline{v}^*[\overline{T}] + [\overline{v}]\overline{T}^* + \overline{v'T'}$$

and finally, taking the zonal mean, once again the cross terms drop out of the average:

$$[\overline{vT}] = [\overline{v}][\overline{T}] + [\overline{v}^*\overline{T}^*] + [\overline{v'T'}]$$

We will use this decomposition often. We will refer to the various terms as follows:

$[\overline{vT}]$ Flux by all motions

$[\overline{v}][\overline{T}]$ Flux by steady symmetric circulations

$[\overline{v}^*\overline{T}^*]$ Flux by stationary eddies

$[\overline{v'T'}]$ Flux by transient eddies

Note that this expression is not fully decomposed: the transient eddy term $[\overline{v'T'}]$ can be rewritten using

$$\begin{aligned} v' &= [v'] + v'^* \\ T' &= [T'] + T'^* \\ v'T' &= [v'][T'] + v'^*T'^* + v'^*[T'] + [v']T'^* \\ [\overline{v'T'}] &= \overline{[v'][T']} + [\overline{v'^*T'^*}] \end{aligned}$$

In word form, we can say that the flux by transient eddies is comprised of the flux by transient meridional circulations and transient asymmetric eddies.

Putting this all together, the full decomposition of the flux is therefore

$$[\overline{vT}] = [\overline{v}][\overline{T}] + [\overline{v}^*\overline{T}^*] + \overline{[v'][T']} + [\overline{v'^*T'^*}]$$

and we identify the four terms on the RHS as, respectively, the flux by steady symmetric circulation, the flux by stationary eddies, the flux by transient symmetric circulations, and the flux by transient asymmetric eddies.

An alternative decomposition can be derived by reversing the order we followed above, and decomposing first with respect to zonal mean:

$$[\overline{vT}] = [\overline{v}][\overline{T}] + \overline{[v]'[T]'} + \overline{[v^*T^*]}$$

where the terms of the RHS are respectively the flux by steady symmetric circulations, the flux by transient symmetric circulations, and the flux by asymmetric eddies (both transient and steady).

The generic decomposition of $[\overline{AB}]$ becomes slightly simpler when $A = B$. For example, we might consider the meridional wind variance (which contributes to kinetic energy):

$$[\overline{v^2}] = [\overline{v}]^2 + [\overline{v}^{*2}] + [\overline{v'^2}]$$

where the terms on the RHS are the contributions due to, respectively, steady symmetric circulation, stationary eddies, and transient eddies. The transient eddy term can be decomposed further into a transient symmetric and transient asymmetric component:

$$[\overline{v'^2}] = \overline{[v']^2} + [\overline{v'^{*2}}]$$

Decomposition allows us to ascribe physical mechanisms to processes (e.g. the contribution of stationary waves). A few points to keep in mind:

- Decomposition into stationary and transient components is influenced by our choice of τ, the averaging interval.
- We will also later use spectral decomposition (for decomposition over different length scales) and EOF's (for analysis of low-frequency variability)[1]
- The heat flux by mean symmetric motions $\int_0^{p_s}[\overline{v}][\overline{T}]\frac{dp}{g}$ can be in serious error if $\int_0^{p_s}[\overline{v}]\frac{dp}{g}$ is inaccurate in the data source (the error would be $\mathcal{O}(1)$). Peixoto and Oort actually used the angular momentum budget to estimate $[v]$ for their analysis.

2.2 The Dynamical Equations

2.2.1 Coordinates

We will work primarily with pressure p as the vertical coordinate, but not always (note $\sigma = p/p_s$ is used in some figures). As we are mostly interested in large-scale circulations and budgets, we will use a spherical coordinate system (λ, ϕ) with λ the longitude and ϕ the latitude.

We will use the so-called thin shell approximation: the radial coordinate $r = z + R$ where R is the Earth's radius, and $z \ll R$ for any atmospheric motion. We will often make use of the hydrostatic approximation

$$\frac{\partial p}{\partial z} \simeq -\rho g$$

which implies that the surface pressure is directly related to the mass of the air column (per unit area):

$$p_s = g\int_0^\infty \rho dz$$

2.2.2 Continuity equation

The conservation of mass in a fluid is expressed per unit area as

$$\frac{d\rho}{dt} + \rho\nabla\cdot\underline{c} = 0$$

where $\underline{c} = (u, v, w)$ is the 3d velocity field, and the total derivative can be written (in height coordinates)

$$\frac{d}{dt} = \frac{\partial}{\partial t} + \frac{u}{R\cos\phi}\frac{\partial}{\partial\lambda} + \frac{v}{R}\frac{\partial}{\partial\phi} + w\frac{\partial}{\partial z}$$

We can convert to pressure coordinates assuming hydrostatic balance. Consider a mass element δm with dimensions $\delta x, \delta y, \delta z$:

$$\delta m = \rho\delta x\delta y\delta z$$

[1] EOF = Empirical Orthogonal Function

The hydrostatic relation is

$$\delta p = -\rho g \delta z$$

and thus the mass can be written

$$\delta m = -\delta x \delta y \delta p / g$$

Conservation of mass for the parcel can be expressed as $\frac{d}{dt}\delta m = 0$. Therefore

$$\begin{aligned} 0 &= \frac{1}{\delta m}\frac{d}{dt}\delta m \\ &= \frac{1}{\delta x}\delta y \frac{d}{dt}\big(\delta x \delta y\big) + \frac{1}{\delta p}\frac{d}{dt}\big(\delta p\big) \end{aligned}$$

from which we get the continuity equation is pressure coordinates:

$$\nabla \cdot \underline{v} + \frac{\partial \omega}{\partial p} = 0$$

where $\underline{v} = (u, v)$ is the horizontal velocity vector with u the eastward wind and v the northward wind, and $\omega = \frac{dp}{dt}$ is the vertical velocity in pressure coordinates.

2.2.3 Momentum equations (in p coordinates)

We will work with this form of the horizontal momentum equations:

$$\begin{aligned} \frac{du}{dt} &= \frac{\tan\phi}{R}uv + fv - \frac{g}{R\cos\phi}\frac{\partial z}{\partial \lambda} + \text{ subgrid} \\ \frac{dv}{dt} &= -\frac{\tan\phi}{R}u^2 - fu - \frac{g}{R}\frac{\partial z}{\partial \phi} + \text{ subgrid} \end{aligned}$$

Here we keep the metric terms, as we are considering motions over the planetary scale. We have assumed hydrostatic balance in the vertical, allowing us to rewrite the pressure gradient force in terms of geopotential height gradients on pressure surfaces. We have also used the so-called "traditional approximations" (for example, neglecting the $\frac{du}{dt} = -f'\omega$ term). The Coriolis parameter is defined as $f = 2\Omega\sin\phi$ where $\Omega = 2\pi/day$ is the Earth's rotation rate.

To understand the meaning of the metric terms, consider an air parcel moving with $v = 0, u > 0$. The metric term proportional to $-u^2$ induces a southward acceleration. Thus the parcel would deviate from a latitude circle. The lines of motion are along great circles instead. Note that these metric terms, like the Coriolis terms, conserve kinetic energy, just redistributing momentum between the eastward and northward directions.

Note that the total derivative in pressure coordinates is expressed as

$$\frac{d}{dt} = \frac{\partial}{\partial t} + \frac{u}{R\cos\phi}\frac{\partial}{\partial \lambda} + \frac{v}{R}\frac{\partial}{\partial \phi} + \omega\frac{\partial}{\partial p}$$

2.2.4 Thermodynamic equation

The first law of thermodynamics for air can be expressed as

$$c_p \frac{dT}{dt} = Q + \alpha\omega$$

where Q is the diabatic heating rate from radiation, phase changes, etc., and the last term could also be written vdp for a volume v.

We define the potential temperature θ as

$$\theta = T\Big(\frac{p_0}{p}\Big)^{\kappa}$$

where $\kappa = \frac{R}{c_p}$. The first law then becomes

$$c_p \frac{T}{\theta}\frac{d\theta}{dt} = Q$$

from which it's clear that in the absence of a diabatic forcing Q, θ is conserved following an air parcel. On timescales of a few days, θ surfaces are therefore quasi-Lagrangian, and we will sometimes use θ as a vertical coordinate.

2.2.5 Water vapor

The specific humidity q is defined as the mass of water vapor per unit total mass of air. A conservation equation for q can be written

$$\frac{dq}{dt} = s + D$$

where s is the source term due to phase changes of water (evaporation + sublimation - condensation - deposition), and D accounts for sub-gridscale fluxes.

We will consider static stability, moist entropy, and the Clausius-Clapeyron relation as needed.

3 Observed mean state of the atmosphere

3.1 Mass

3.1.1 Geopotential height at 1000 hPa

By hydrostatic balance, height anomalies are related to sea-level pressure (SLP) anomalies, $\delta p_{sl} \sim 0.12 \delta Z_{1000}$, with pressure in hPa and height in m. See Figs. 3.1 and 3.2.

- Subtropical high pressure cells (anticyclonic)
- Low pressure near the equator (ITCZ)
- NH and SH quite different, even in annual mean. (From ERA40 data, NH

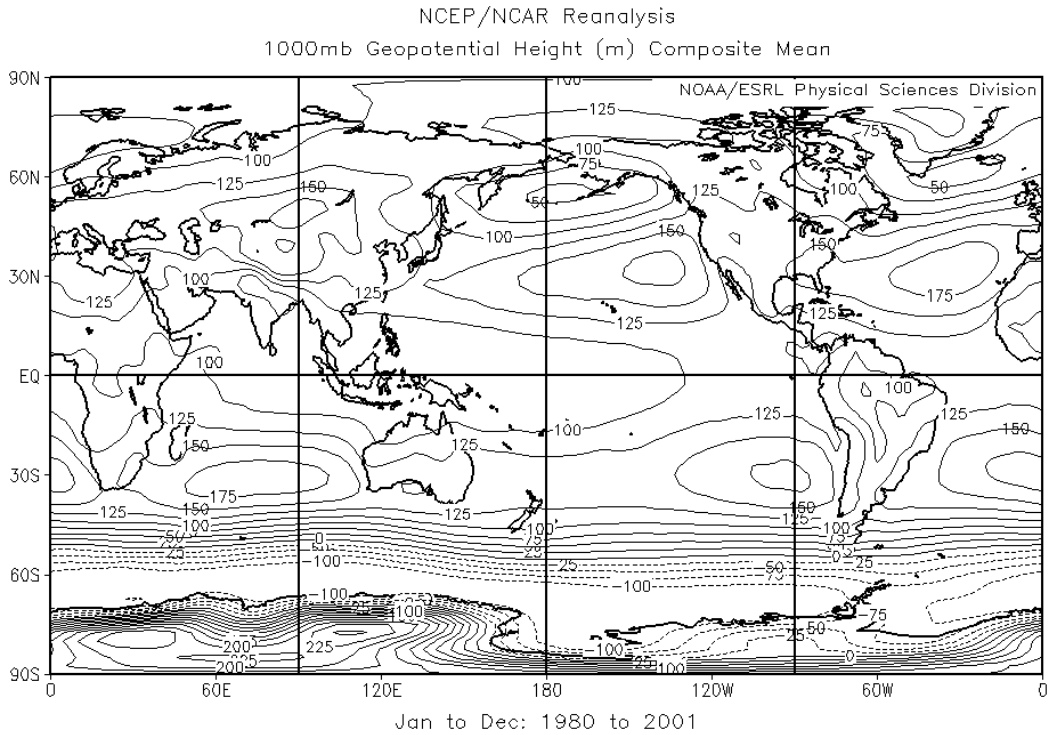

Figure 3.1: Geopotential height at 1000 hPa, annual mean

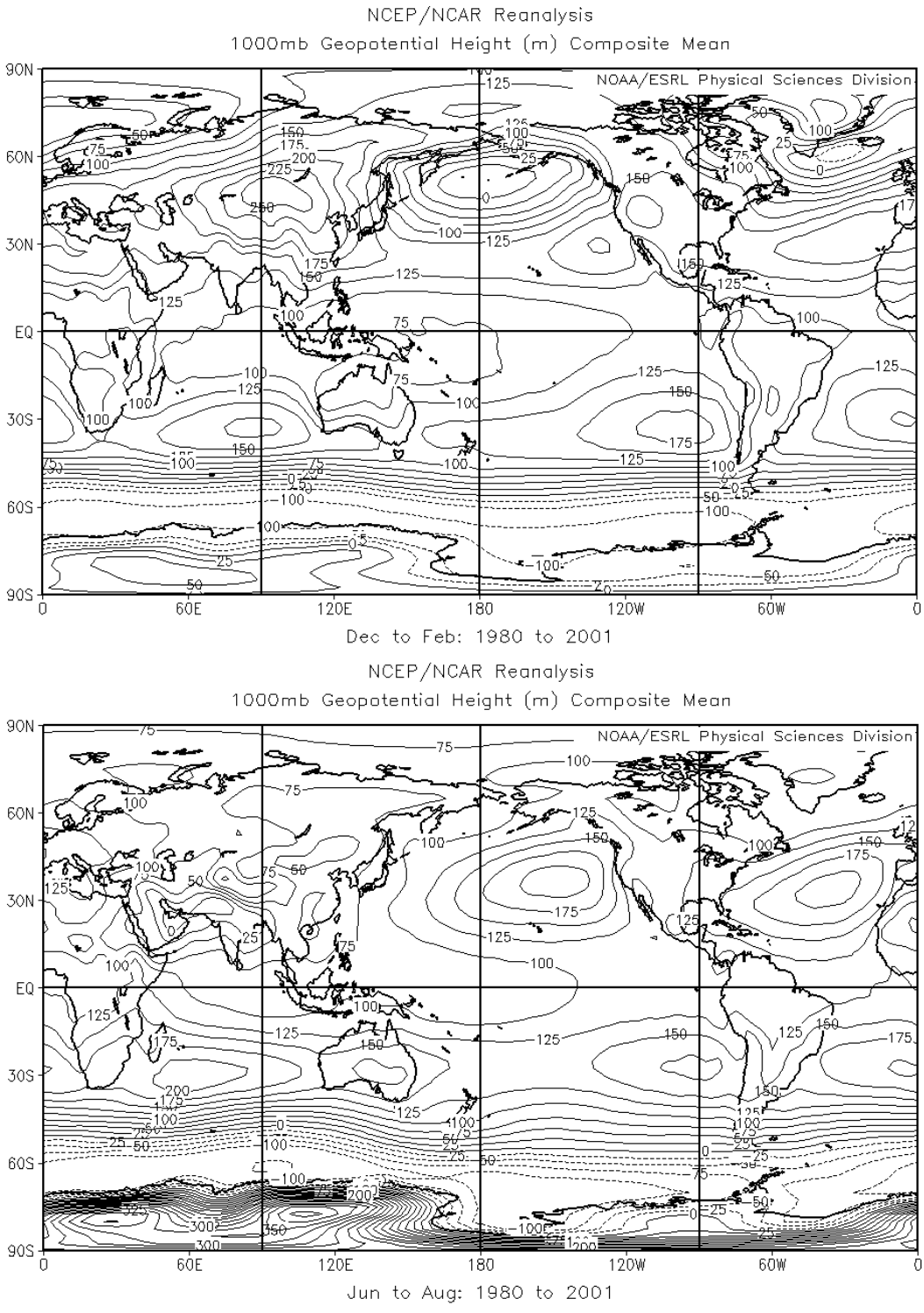

Figure 3.2: Geopotential height at 1000 hPa, NH winter (upper) and NH summer (lower)

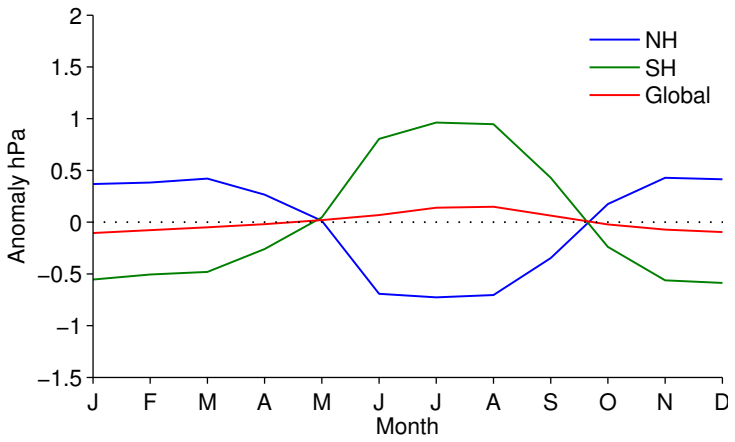

Figure 3.3: Seasonal cycle of sea-level pressure

mean $p_s = 983$ hPa, SH mean $p_s = 988$ hPa. Note that p_s and SLP will differ substantially wherever there is topography.)

- Subtropical highs move poleward in summer
- Low pressure regions at higher latitudes intensify in winter in NH, little change in SH
- Large seasonality over Asia: summer low north of India, winter high over Siberia.
- Very low pressure over belt around Antarctica

3.1.2 Zonal mean SLP

The geostrophic balance for near-surface zonal winds is

$$f u_g = -\frac{g}{R}\frac{\partial Z}{\partial \phi}$$

or, in height coordinates,

$$f u_g = -\frac{1}{\rho R}\frac{\partial p}{\partial \phi}$$

- Subtropical highs more intense and move equatorward during winter
- annular modes give rise to low-frequency variability in mass distribution

3.1.3 Seasonal cycle of mass

Refer to Fig. 3.3

- Trans-equatorial mass transport is implied

- Total mass varies (water vapor)

The rate of change of mass in a polar cap is related to the mass transport across the wall around a latitude circle, which we show by applying the divergence theorem to the integrated continuity equation:

$$\begin{aligned}\int_V \frac{\partial \rho}{\partial t} dV &= -\int_V div(\rho \underline{c}) dV \\ &= -\int_S \rho \underline{c} \cdot \underline{n} dS \\ &= \int_{wall} \rho v dS\end{aligned}$$

3.2 Thermal structure

3.2.1 Insolation: daily-mean and TOA

Refer to Fig. 2.6 of Hartmann (1994).

- Highest daily-mean insolation occurs at summer poles at solstice (24 hour daylight)
- Radiation also destabilizes the atmosphere in the vertical (most heating near the surface)

3.2.2 Surface air temperature

See Fig. 3.4.

- High topography and land masses are apparent
- Small gradients in tropics (reflects both insolation and dynamics)
- Strong gradients over land and water
- Ocean currents are important
- Strong seasonality in Siberia and northern Canada
- Zonal asymmetry decreases with height (not shown)

3.2.3 Latitude-σ plots of temperature

Recall that $\sigma = \frac{p}{p_s}$, thus always equals 1 at the surface regardless of topography. The zonal average in σ coordinates takes into account the mass weighting $dp = p_s d\sigma$, thus

$$\overline{A}^{\sigma} = \frac{\int \frac{d\phi}{2\pi} p_s A}{\int \frac{d\phi}{2\pi} p_s}$$

See Fig. **??**.

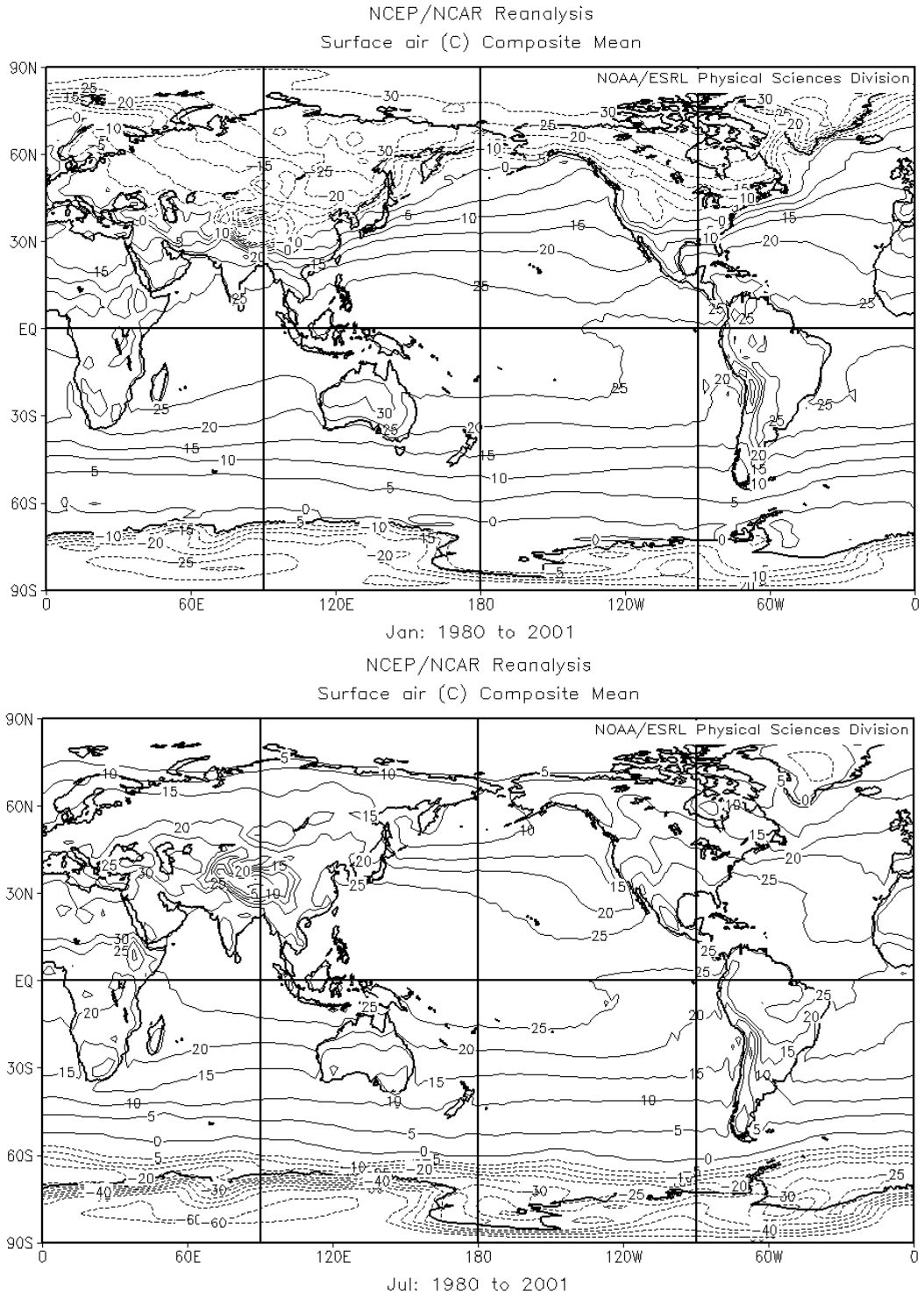

Figure 3.4: Surface air temperature in January (upper) and July (lower).

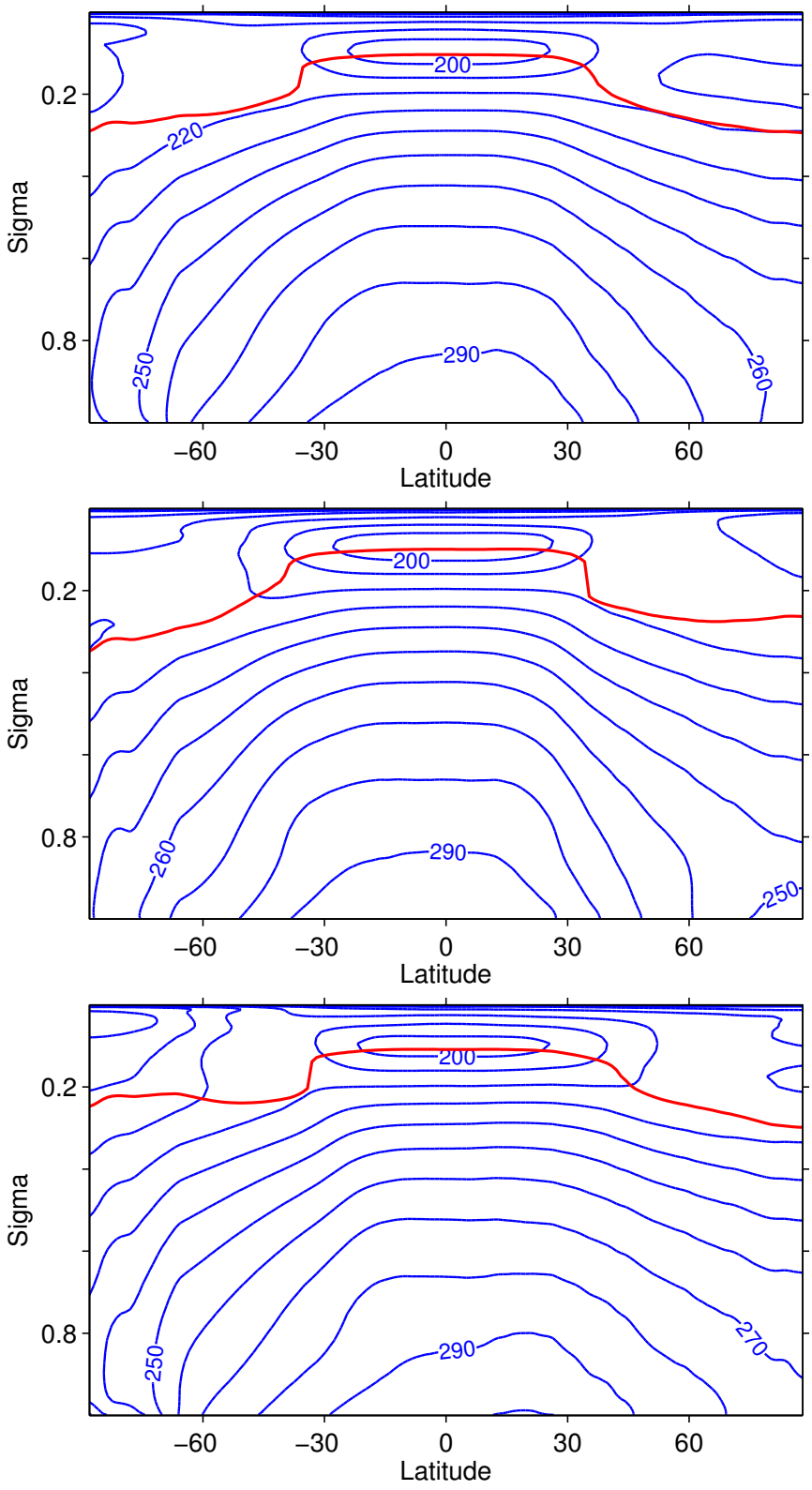

Figure 3.5: Temperature in σ coordinates from ERA-40: annual mean (upper), NH winter (middle), NH summer (lower)

- The tropopause is indicated by σ-level of mean temperature lapse rate 2 K/km.
- Temperature decreases with height in troposphere, increases with height in stratosphere
- Cold point above tropical tropopause

3.2.4 Potential temperature

Recall the definition

$$\theta = \left(\frac{p_0}{p}\right)^{\kappa}$$

with $\kappa = R/cp$. Potential temperature is related to the entropy s by

$$s = c_p \ln\theta + constant$$

Thus we often refer to surface of constant θ as *isentropes*.

See Fig. 3.6.

- NP and SP are similar (altitude, 'jet', continental vs. sea ice)
- Flat in tropics
- Isentropes from near-surface in the tropics to the tropopause near the poles.

3.2.5 Static stability

Consider a parcel of fluid with density ρ displaced from its resting position in the vertical. The vertical momentum equation for the parcel is

$$\frac{dw}{dt} = -g - \frac{1}{\rho}\frac{\partial p}{\partial z}$$

while the surrounding environment is assumed to be in hydrostatic balance, thus

$$0 = -g - \frac{1}{\rho_A}\frac{\partial p}{\partial z}$$

Therefore we can write, for the parcel

$$\frac{dw}{dt} = -g - \frac{1}{\rho}g\rho_A = g\frac{\rho_A - \rho}{\rho} = g\frac{T - T_A}{T_A}$$

(using the ideal gas law to relate density to temperature).

If the parcel is displaced adiabatically, its temperature will change by compression/expansion at the dry adiabatic lapse rate $\gamma_d = g/c_p \simeq 10$ K/km. We denote the environmental lapse rate $\gamma = -\partial T/\partial z$. Then for small displacements we can write

$$T(z) = T_A(z_0) - \gamma_d(z - z_0)$$
$$T_A(z) = T_A(z_0) - \gamma(z - z_0)$$

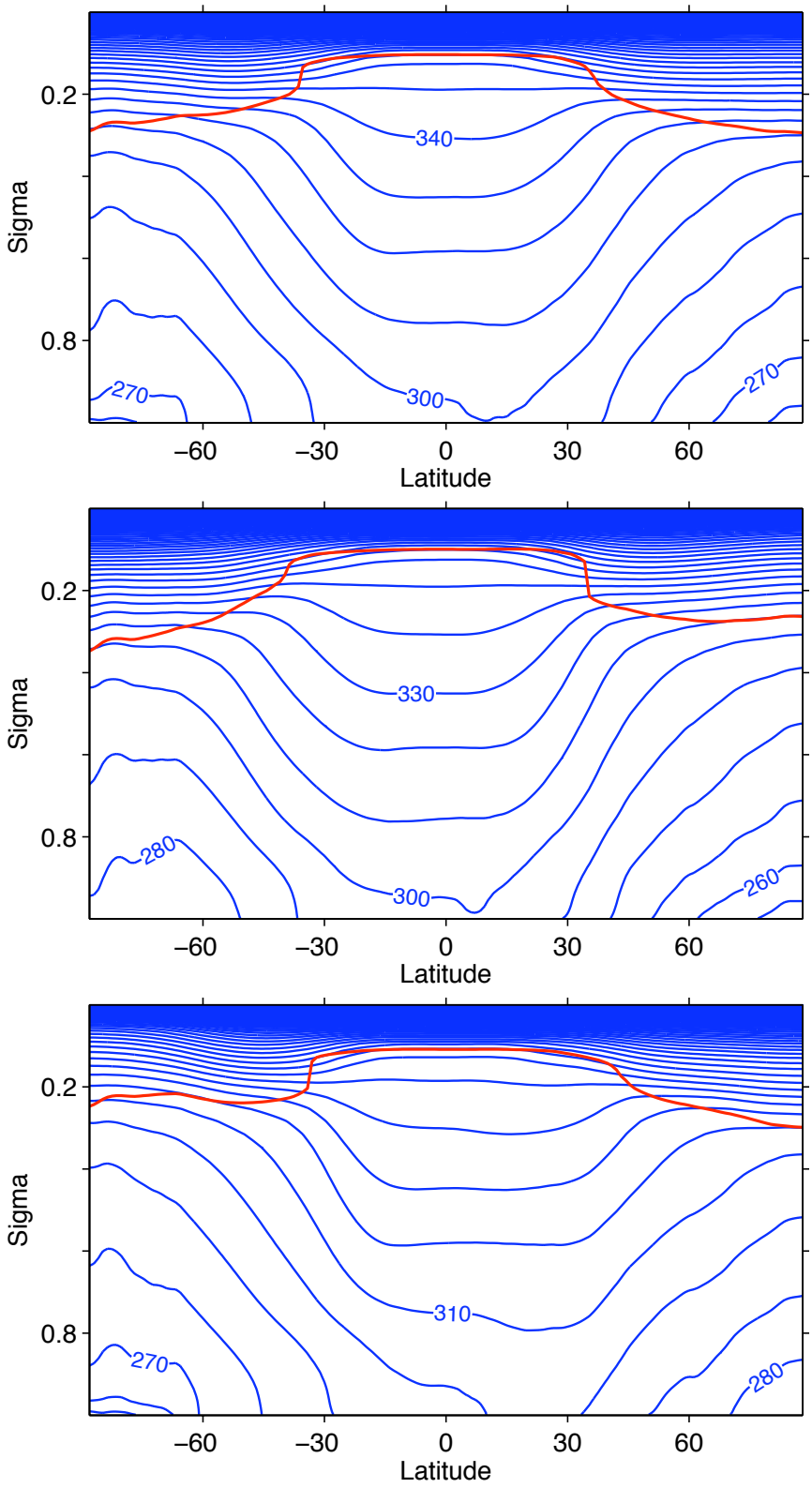

Figure 3.6: Potential emperature in σ coordinates from ERA-40: annual mean (upper), NH winter (middle), NH summer (lower)

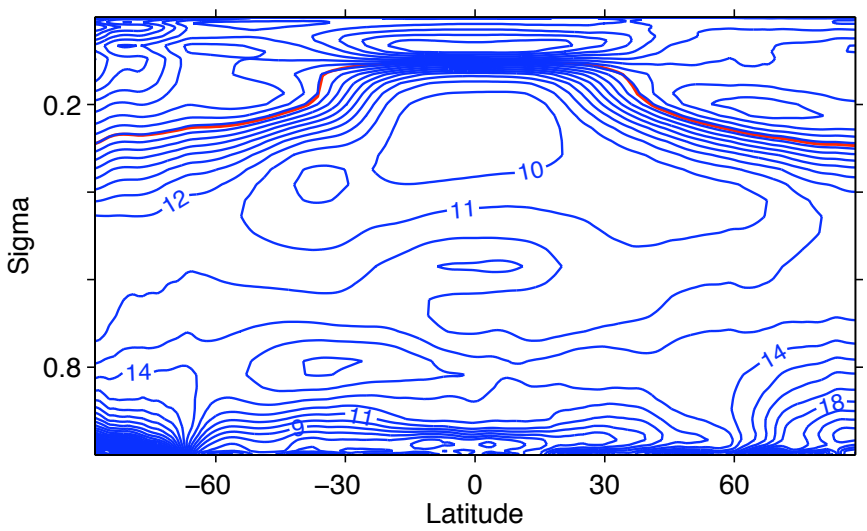

Figure 3.7: Buoyancy frequency N from ERA-40, in units of 10^{-3} s^{-1}.

and plugging these linearized expressions into the momentum equation above, we get

$$\frac{dw}{dt} = g\frac{z - z_0}{T_A}(\gamma - \gamma_d)$$

This gives us a condition for the stability of the parcel displacements: if $\gamma > \gamma_d$ then a parcel displaced upwards will accelerate upwards. On the other hand, if $\gamma < \gamma_d$ (which is almost always the case in the atmosphere), then the upwardly displaced parcel will accelerate downwards and oscillate about its initial position.

It can be shown that

$$-\gamma + \gamma_d = \frac{T_A}{\theta}\frac{\partial\theta}{\partial z}$$

and thus

$$\frac{dw}{dt} = \frac{d^2z}{dt^2} = -\frac{g}{\theta}\frac{\partial\theta}{\partial z}(z - z_0)$$

This is a wave equation with a "buoyancy frequency" N, defined as

$$N^2 = \frac{g}{\theta}\frac{\partial\theta}{\partial z}$$

The buoyancy frequency gives the timescale for gravity waves. As shown in Fig. 3.7, N is remarkably uniform with respect to latitude in the atmosphere, despite the fact that different processes at different latitudes contribute to the maintenance of the stratification.

If $N \simeq 10^{-2}$ s^{-1}, then the typical period of oscillation is $T = 2\pi/N \simeq 600$ s $\simeq 10$ mins. N is low near the surface and high in the stratosphere.

An alternative view of static stability in terms of potential temperature: Note that θ is conserved under dry adiabatic displacements, while in a stably stratified environment $\partial\theta_A/\partial z > 0$. If a parcel at potential temperature θ_A is displaced upwards by δz, it remains at θ_A but encounters an environmental potential temperature

$\theta_A + \frac{\partial \theta_A}{\partial z}\delta z > \theta_A$. The parcel is thus denser than its environment and accelerates downward.

3.2.6 Effects of moisture

Here we do a simple analysis that neglects effect on heat capacity, etc. For a more rigorous account, see e.g. Emanuel (1994), chapter 4.

We can define an "equivalent potential temperature" θ_e which is conserved by moist-adiabatic displacements. We also define the saturated equivalent potential temperature θ_e^* (the θ_e of a parcel with the same T, p but with $q = q_s$). An approximate derivation, neglecting variations of c_p, L:

$$\begin{aligned} Tds &= -Ldq_s \\ s &= c_p \ln\theta + constant \end{aligned}$$

(s is the dry entropy)

$$\begin{aligned} Tc_p\frac{d\theta}{\theta} &= -Ldq_s \\ \frac{d\theta}{\theta} &= -\frac{Ldq_s}{c_pT} \\ \ln\theta &= -\frac{Lq_s}{c_pT} + constant \\ \theta &= \theta_e^* \exp\Big(-\frac{Lq_s}{c_pT}\Big) \\ \theta_e^* &= \theta \exp\Big(\frac{Lq_s}{c_pT}\Big) \end{aligned}$$

θ_e^* is conserved for *saturated* moist-adiabatic displacements. A quantity conserved more generally is

$$\theta_e = \theta \exp\Big(\frac{Lq_s}{c_pT_{LCL}}\Big)$$

where T_{LCL} is the temperature at the lifting condensation level (where the parcel becomes saturated). θ_e is the potential temperature θ a parcel would have if it was lifted to $p \to 0$. In other words, θ_e is the temperature of a parcel after condensing out all the water vapor and bringing it adiabatically to the 1000 hPa. θ_e^* and θ_e are plotted in Fig. 3.8.

3.2.7 Moist static stability

There are several different measures of the static stability of a moist air column. The column is said to be *conditionally unstable* if $\partial\theta_e^*/\partial z < 0$ (the instability is conditional on the air parcels being saturated). If $\partial\theta_e/\partial z < 0$ then the column is *potentially unstable*, meaning that if a layer of air is lifted to saturation, then $\partial\theta_e^*/\partial z < 0$ and the layer becomes unstable.

Slantwise moist convective instability looks at θ_e^* along angular momentum surfaces.

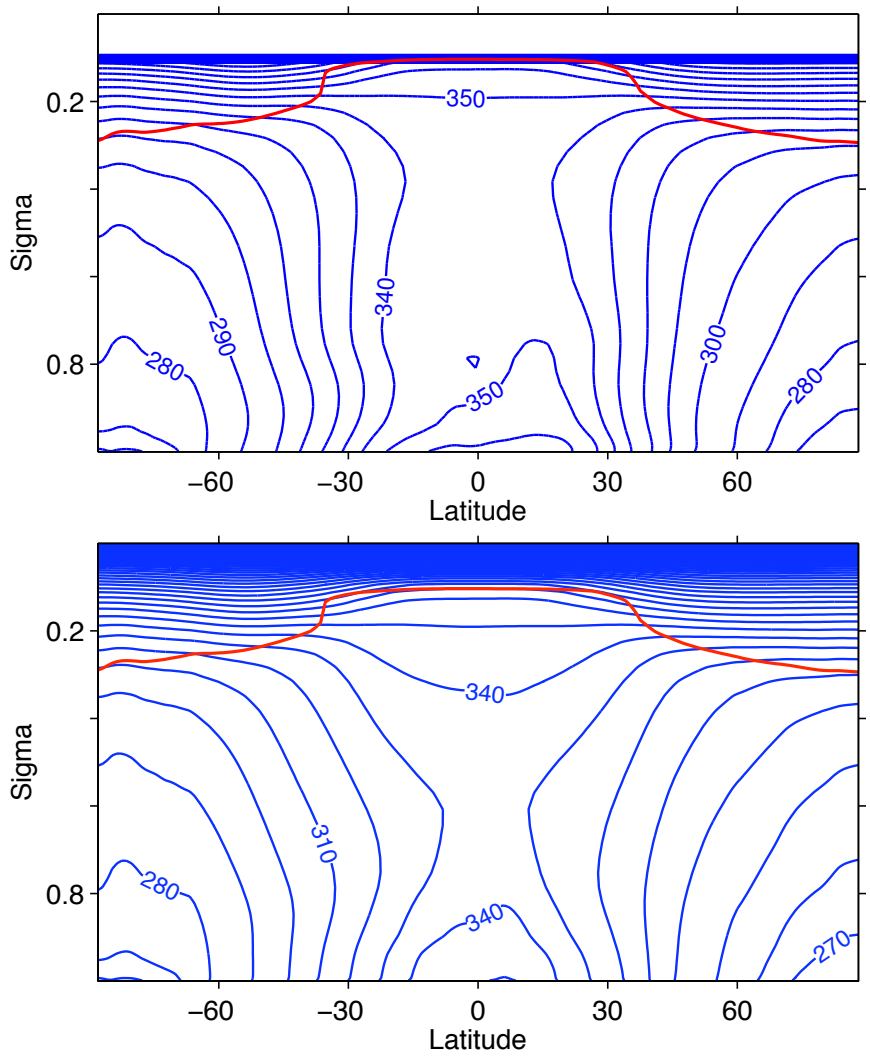

Figure 3.8: Saturated equivalent potential temperature θ_e^* (upper) and equivalent potential temperature θ_e (lower).

3.2.8 Meridional temperature gradient

A few points about $\partial\overline{T}/\partial y$:

- Strongest in winter and can reverse in stratosphere
- Indicative of APE (available potential energy), baroclinicity
- Can use to identify storm tracks?

The Eady growth rate for baroclinic instability is

$$\sigma_E \sim \frac{\partial\theta/\partial y}{N}$$

and as we saw previously, N is roughly constant with latitude.

3.2.9 Temperature variability

- ~ 5 K
- Upper troposphere variability partly from movement of the tropopause
- Small in tropics
- Seasonality is included in annual statistics (especially at high latitudes)
- Stationary eddies, land-ocean contrast

3.2.10 Theories for the thermal structure

It is an outstanding challenge to develop a theory for the thermal structure of the extratropical troposphere. One of the challenges is that the stratification is maintained by both moist convection and eddies, and their contributions vary with latitude.

A few notable papers:

Stone (1978) Baroclinic adjustment. E.g. Zhou and Stone (1993): isentropic slope roughly twice the neutral slope in a 2-level model where static stability can adjust. (Note that the mean state of the atmosphere is baroclinically unstable in general).

Juckes (2000) Moist convection and eddies. The vertical stratification is moist neutral + occasionally stable contribution from eddy advection of temperature and moisture.

$$\Delta_z \overline{\theta_e} \sim \partial_y \overline{T}_{500hPa}$$

Schneider (2006) Eddy diffusion of PV

$$S_c = \frac{f}{\beta} \frac{\partial_y \overline{\theta_s}}{2\partial_p(\overline{p}_s - \overline{p}_t)} \simeq 1$$

(the isentropic slope is $\partial p/\partial y|_\theta = \partial_y \theta / \partial_p \theta$).

Schneider and OGorman (2008) Dry theories and Juckes theory inadequate in aquaplanet simulations. All these theories are related to observations of the mean isentrope from near-surface in the tropics to the tropopause in polar regions.

$$\overline{\theta}_t - \overline{\theta}_s \sim |\partial_y \overline{\theta} \frac{f}{\beta}| \sim |\partial_y \overline{\theta} a \tan\phi| \sim \theta_{eq} - \theta_{pole}$$

3.3 Mean state of the circulation

- Vertical: close to hydrostatic, relatively small velocities and accelerations
- Horizontal: Coriolis and pressure gradient balance

3.3.1 Surface winds and geopotential height

See P&O figure 7.1

- Winds and height contours almost parallel
- But some ageostrophic flow into lows and out of subtropical highs (Ekman balance with friction, smaller-scale turbulent fluxes).

3.3.2 Upper-level flow

See P&O figure 7.13

- Parallel to height contours (geostrophic)
- Long planetary waves superimposed on zonal flow
- More zonal in SH
- Seasonal: summer-NH jet stream move north and closed circulation over Asia
- Standing waves: wavenumber 2, strongest in NH winter (depends on surface forcing)

3.3.3 200 hPa $\overline{u}$ (CDC)

See Fig. 3.9.

- Strong jet streams, split in SH, superrotation of global average winds
- NH jet maxima over Eastern North America and Asia (and adjacent oceans)
- Tropical easterlies (westerly duct)
- Seasonal:
  - shifts equatorward in winter
  - winter jets stronger

3.3.4 Latitude-σ $\overline{u}$ (era40)

See Fig. 3.10

- Similar maximum in NH and SH in annual mean, although generally stronger in SH.
- Weak easterlies in tropics
- Surface easterlies and westerlies cover similar area (come back to this later)
- Max. in $[\overline{u}]$ above max. in $[\partial\overline{T}/\partial y]$ (cf. earlier figure)

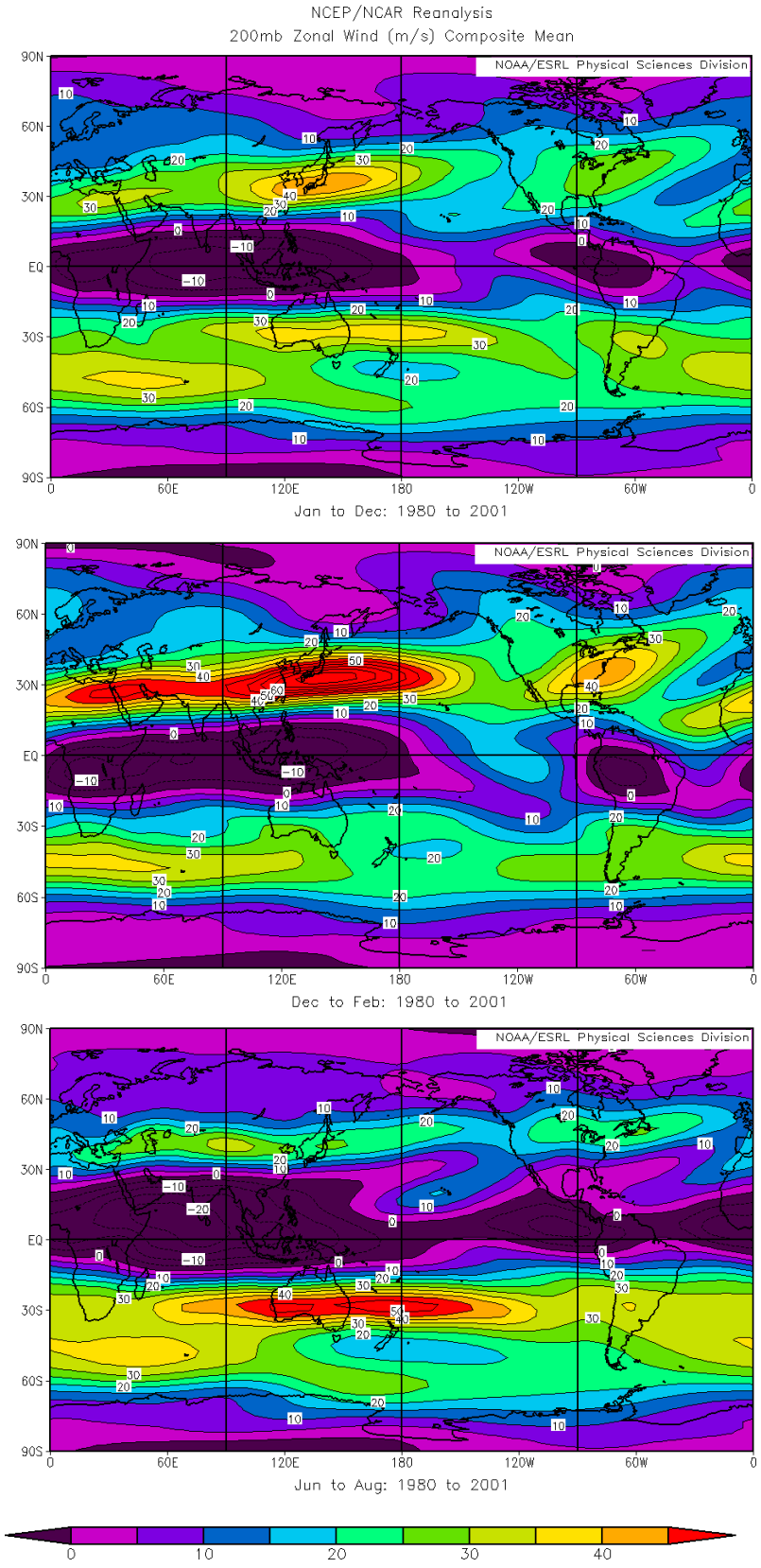

Figure 3.9: Zonal wind at 200 hPa, annual mean (upper), NH winter (middle) and NH summer (lower).

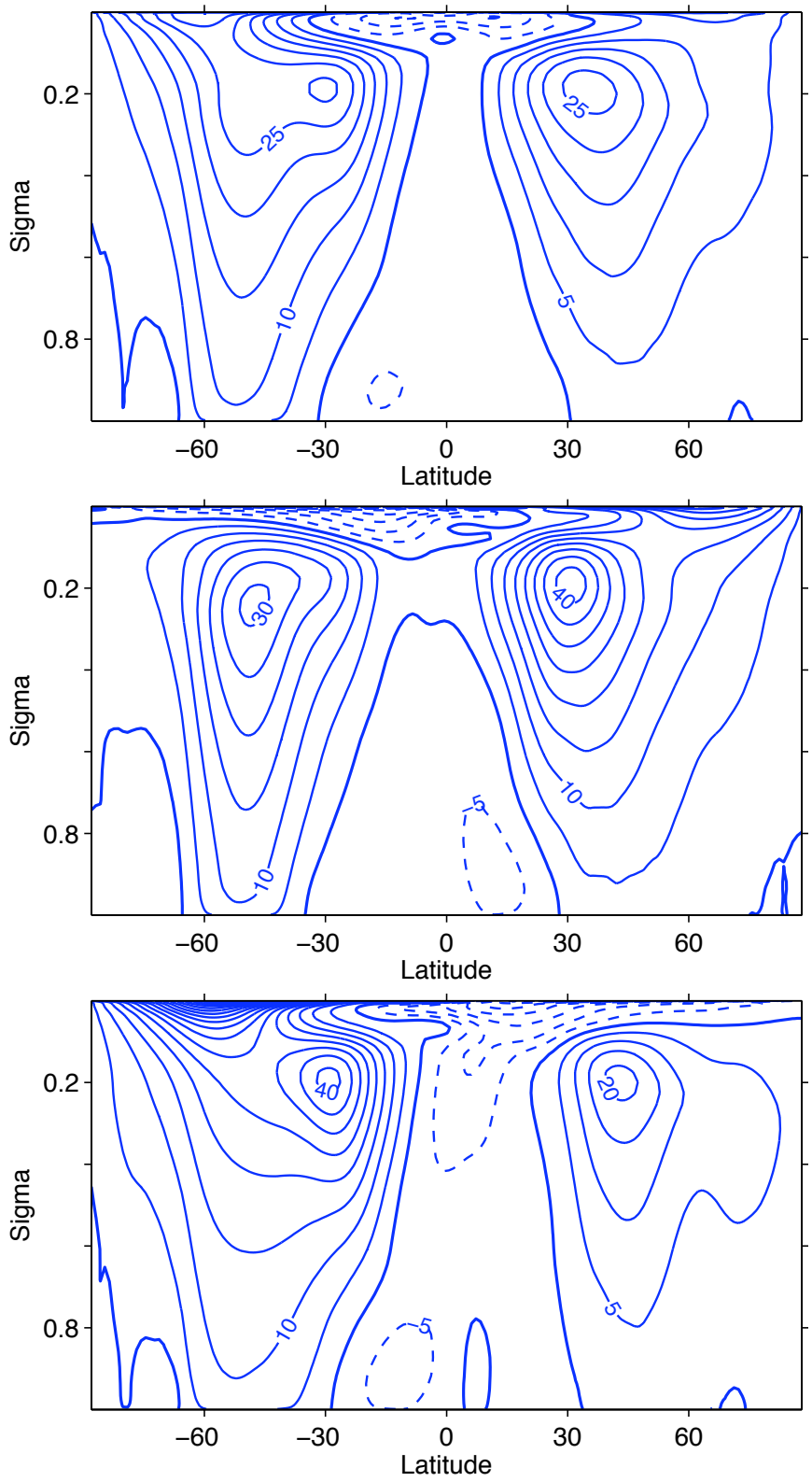

Figure 3.10: Zonal wind in σ coordinates from ERA-40: annual mean (upper), NH winter (middle), NH summer (lower)

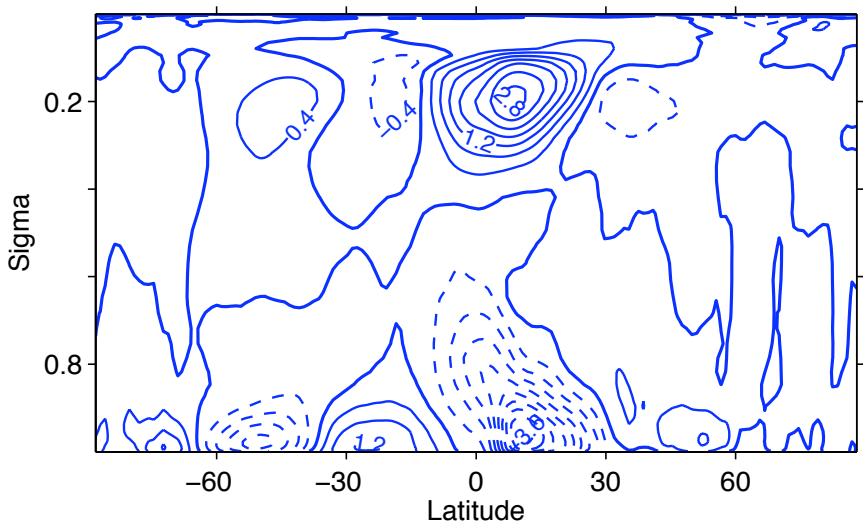

Figure 3.11: Meridional wind in σ coordinates from ERA-40: NH winter

3.3.5 Zonal wind shear $\partial\overline{u}/\partial z$

Derive the thermal wind relation:

$$
\begin{aligned}
f u_g &= -\frac{g}{R}\frac{\partial Z}{\partial \phi}\Big|_p \\
f\frac{\partial u_g}{\partial p} &= -\frac{g}{R}\frac{\partial}{\partial \phi}\Big|_p \frac{\partial Z}{\partial p} \\
&= \frac{g}{R}\frac{\partial}{\partial \phi}\Big|_p \frac{1}{\rho g} \\
&= \frac{1}{R}\frac{\partial}{\partial \phi}\Big|_p \frac{R_g T}{p} \\
\frac{\partial u_g}{\partial p} &= \frac{R_g}{f R p}\frac{\partial T}{\partial \phi}\Big|_p
\end{aligned}
$$

The flow is barotropic if $\partial\overline{u}/\partial z = \partial_y T|_p = 0$. But generally T varies on p surfaces so the flow is baroclinic. (c.f. equivalent barotropic $\underline{v} \propto \partial\underline{v}/\partial z$)

So upper level and surface zonal winds differ by an amount that depends on the meridional temperature gradients.

3.3.6 Mean meridional flow $[\overline{v}]$ (era40)

See Fig. 3.11

- Small values relative to $[\overline{u}]$
- Note $[v_g] = 0$ (there is no zonal-mean zonal pressure gradient).
- Since fv appears as an force in the zonal momentum equation, $[\overline{v}]$ is important in Eulerian momentum balance (e.g. at the surface).

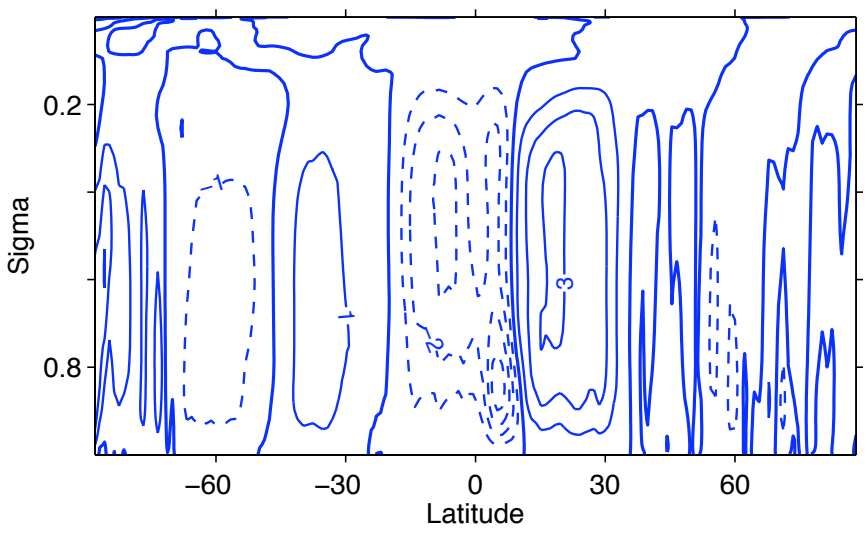

Figure 3.12: Vertical motion in σ coordinates, NH winter.

3.3.7 Vertical motion is σ coords, $[d\overline{\sigma}/dt]$ (era40)

See Fig. 3.12

- Strongest at mid-troposphere
- Annual mean ascent centered near 5°N (mean ITCZ).
- Values: 2×10^{-4} hPa s^{-1} $\sim$ 3 mm s^{-1}
- Cross cells for solstices
- ω strongly related to precip (or absence of it).
- Better visualization from mean meridional (Stokes) streamfunction

3.3.8 Definition of mean meridional streamfunction ψ

Continuity equation for the mean flow:

$$\frac{1}{R\cos\phi}\frac{\partial}{\partial\phi}\cos\phi[\overline{v}] + \frac{\partial[\overline{\omega}]}{\partial p} = 0$$

Since the mean flow is divergence-less in the $p-\phi$ plane, we can introduce a streamfunction ψ defined by:

$$[\overline{v}] = \frac{g}{2\pi R\cos\phi}\frac{\partial\psi}{\partial p}$$
$$[\overline{\omega}] = -\frac{g}{2\pi R^2}\frac{\partial\psi}{\partial\phi}$$

To calculate ψ, set $\psi = 0$ at the top boundary. Then integrate the first expression above to get

$$\psi = \int_0^p dp \frac{2\pi R \cos\phi}{g} [\overline{v}] = \int_0^p \frac{dp}{g} \int_0^{2\pi} d\lambda R \cos\phi \overline{v}$$

In other words, ψ is the mass transported northwards above pressure level p per unit time. The units of ψ are kg s^{-1}. In oceanic context, such transports are usually expressed in volumetric terms using the Sverdrup, where 1 Sv = 10^6 m^3 s^{-1}. Since the density of water is roughly 10^3 kg m^{-3}, the equivalent "mass Sverdrup" is 10^9 kg s^{-1}. These units are sometimes applied to atmospheric transports in order to explicitly compare and contrast with oceanic mass transport.

For long-time averages we should expect $\psi = 0$ at the lower boundary as well. We can use this as a check of accuracy (similarly for polar boundaries, although the factor of $\cos\phi$ ensures this).

Close vertical spacing of ψ contours implies large $[\overline{v}]$. Close horizontal spacing implies large $[\overline{\omega}]$.

3.3.9 Mean meridional streamfunction ψ from era40 data

See Fig. 3.13.

- Annual mean ascent north of equator (c.f. land masses and Asian monsoon)
- Strong seasonal cycle so that annual mean is not very representative
- Hadley, Ferrel, Polar cells
- Winter Hadley cell dominates at solstice
- Indirect Ferrel cells occur at latitudes where eddies are important, suggesting that ψ is an incomplete description of the flow
- Hadley cell important for dry and moist climate zones, e.g. desert regions, ITCZ, etc. (see later)
- If eddies unimportant for Hadley cell then streamfunction contours would coincide with angular momentum contours – this is not the case generally.

See Schneider figure.

Angular momentum per unit mass about the Earth's axis can be written

$$[\overline{M}] = \big(\Omega R \cos\phi + [\overline{u}]\big) R \cos\phi$$

M is conserved by symmetric circulations.

Different cells occur on other planets, e.g Venus has a slow rotation rate (253 day period), and its Hadley cell extends to 60°. Large planets like Jupiter also have different cells.

Note also that the mean circulation looks different if a different vertical coordinate is used. As an example, take potential temperature θ. For approximately

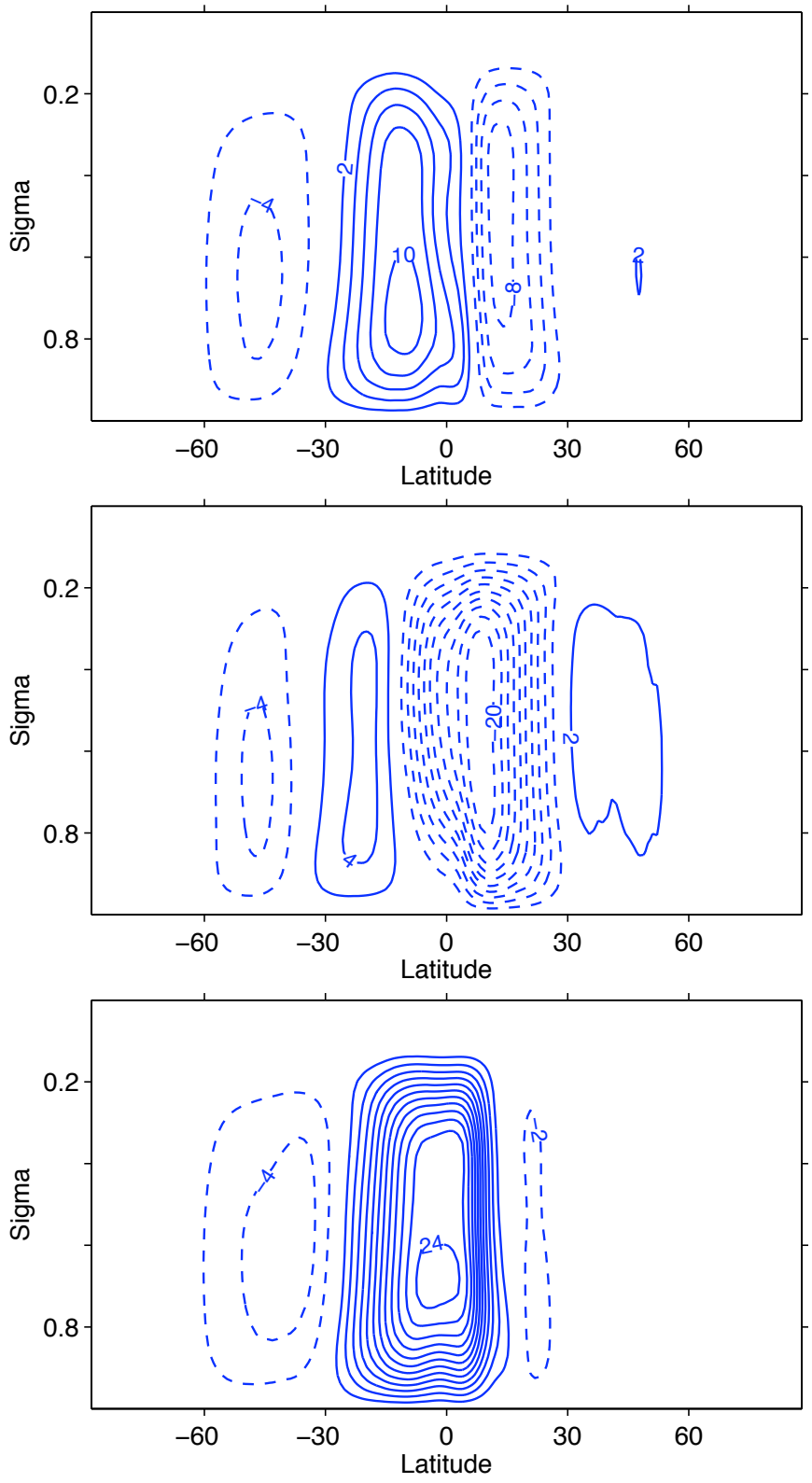

Figure 3.13: Mean meridional streamfunction ψ from ERA-40: annual mean (upper), NH winter (middle), NH summer (lower)

adiabatic motions, $d\theta/dt \simeq 0$, so θ is a quasi-Lagrangian coordinate. We can write the dynamical equations in this coordinate system.

Mass conservation in θ coordinates looks like (see Schneider, 2004):

$$\frac{\partial}{\partial t}\rho_\theta + \nabla_h \cdot \big(\rho_\theta \underline{v}\big) + \frac{\partial}{\partial \theta}\big(\rho_\theta Q\big) = 0$$

where

$$\begin{aligned} \underline{v} &= \big(u, v\big) \\ u &= \frac{dx}{dt} \qquad\qquad v = \frac{dy}{dt} \\ \nabla_h &= \Big(\frac{\partial}{\partial x}\big|_\theta, \frac{\partial}{\partial y}\big|_\theta\Big) \\ Q &= \frac{D\theta}{dt} \end{aligned}$$

and ρ_θ is the equivalent of density in θ coordinates in units of kg m^{-2} K^{-1}, with

$$\rho_\theta = -\frac{1}{g}\frac{\partial p}{\partial \theta}$$

(note $\rho_\theta dxdyd\theta = \rho dxdydz = -g^{-1}dxdydp$, these are all equivalent expressions for a mass element in the fluid).

The mass transport in θ coordinates is the same as the entropy transport. We can define the tropopause as the level to which entropy is redistributed by the circulation.

Averaging the above we find

$$\frac{\partial}{\partial y}\Big([\overline{\rho_\theta}]\overline{v}^\theta\Big) + \frac{\partial}{\partial \theta}\Big([\overline{\rho_\theta}]\overline{Q}^\theta\Big) = 0$$

where we use a density-weighted average

$$\overline{(\cdot)}^\theta = \frac{[\overline{(\rho_\theta \cdot)}]}{[\overline{\rho_\theta}]}$$

We can then define a streamfunction (just as before):

$$\begin{aligned} \overline{\rho_\theta}\overline{v}^\theta &= \frac{g}{2\pi R\cos\phi}\frac{\partial \psi}{\partial \theta} \\ \overline{\rho_\theta}\overline{Q}^\theta &= -\frac{g}{2\pi R^2}\frac{\partial \psi}{\partial \phi} \end{aligned}$$

so that ψ retains the same mass transport units of kg s^{-1}.

Alternatively, one can estimate from p-coordinates as

$$\psi\big(\theta_0, \phi\big) = \frac{1}{\tau}\int_0^\tau dt \int_0^{2\pi} d\lambda \int_0^{p_s} \frac{dp}{g} v R\cos\phi H\big(\theta_0 - \theta\big)$$

where we have written the Heaviside function:

$$H(x) = \begin{cases} 0 & x < 0 \\ 1 & x \geq 0 \end{cases}$$

(c.f. Pauluis et al., 2008)

Can do the same for equivalent potential temperature θ_e.

3.3.10 Mean meridional streamfunction ψ from era40 data

See Fig. 3.14.

- Takes into account latent heat release
- No indirect cells in isentropic coordinate circulations
- θ_e coordinate gives the overturning circulation with the simplest structure (if we used moist static energy as the vertical coordinate then this would be a description of the energy transport).
- θ circulation: can see latent heating in storm tracks.
- mass circulation in θ or θ_e coordinates related to entropy transport
- θ coordinate circulation related to residual circulation in Transformed Eulerian Mean.
- Return flow is predominantly in the surface layer, i.e. eddy fluctuations such as cold air outbreaks. (The surface layer is defined as the range of θ or θ_e where the surface θ or θ_e is mostly in).
- Can define the troposphere as a boundary layer in which the bulk of entropy is redistributed by the circulation.

3.3.11 Variability of the circulation

Decompose the circulation and its variance:

$$\begin{aligned} u &= [\overline{u}] + \overline{u}^* + u' \\ v &= [\overline{u}] + \overline{v}^* + v' \\ [\overline{u^2}] &= [\overline{u}]^2 + [\overline{u}^{*2}] + [\overline{u'^2}] \\ [\overline{v^2}] &= [\overline{v}]^2 + [\overline{v}^{*2}] + [\overline{v'^2}] \end{aligned}$$

Decompose the kinetic energy (per unit mass) as

$$K = K_{TE} + K_{SE} + K_M$$

with each term defined as follows:

$$\begin{aligned} K &= \frac{1}{2}\left[\overline{u^2 + v^2}\right] \\ K_{TE} &= \frac{1}{2}\left[\overline{u'^2}\right] \\ K_{SE} &= \frac{1}{2}\left[\overline{u^*}^2 + \overline{v^*}^2\right] \\ K_M &= \frac{1}{2}\Big(\left[\overline{u}^2\right] + \left[\overline{v}^2\right]\Big) \end{aligned}$$

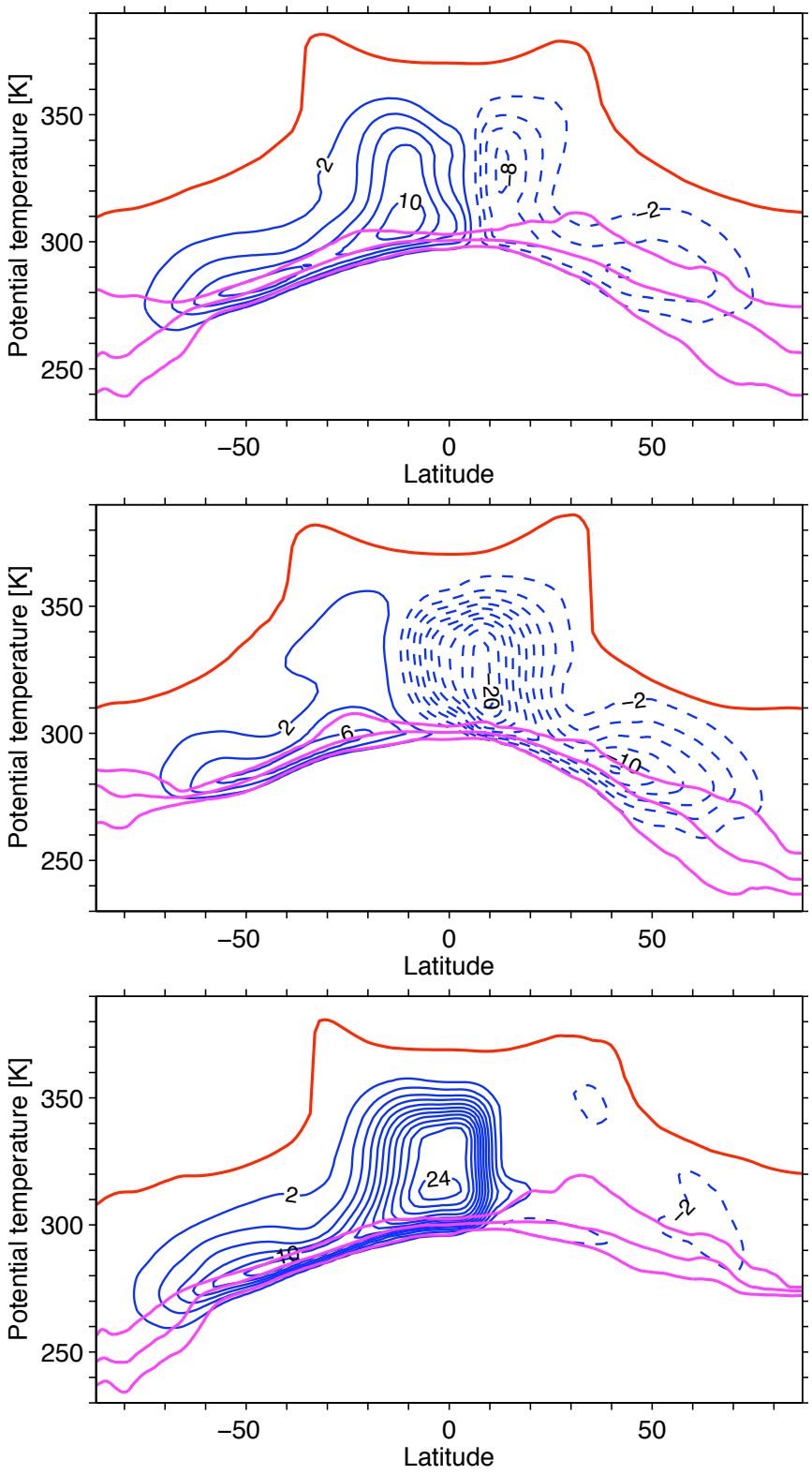

Figure 3.14: Meridional overturning streamfunction in dry isentropic coordinates from ERA-40: annual mean (upper), NH winter (middle), NH summer (lower).

3.3.12 Observed variability of the circulation

Refer to figures in Peixoto and Oort (1992):

Fig. 7.20

Vertical and zonal mean of standard deviations of components of u and v

- Fairly symmetric between hemispheres
- Temporal standard deviations same order of magnitude as $[\overline{u}]$, much bigger than $[\overline{v}]$
- $\sqrt{\overline{u'^2}}$ and $\sqrt{\overline{v'^2}}$ of comparable size and distribution
- Implies an equipartion of energy, $\overline{u'^2}/2 \sim \overline{v'^2}/2$, which suggests a turbulent flow.
- Winter standard deviations larger. Stronger eddies from stronger pole-to-equator temperature gradients
- Annual curves include variance from seasonal cycle
- Greater seasonal cycle in NH is evident.

Fig. 7.21

- (a) shows storm tracks, while (b) shows total KE which includes subtropical and midlatitude mean jet streams
- Peaks east of North America and Japan, more zonal in SH (like precipitation features)

Fig. 7.22

The vertical – meridional cross-section of wind variability

- Maxima near 200 hPa (related to eddy temperature gradients)
- K_E and K_M are the main contributions
- The broadness of K_{TE} due to
  - seasonal variation
  - variations with longitude (in N.H.)
  - day-to-day variability

Fig. 7.23

Kinetic energy vs. latitude

- Similar to 7.20
- Summer to winter in N.H.: factor of 3 difference
- Summer to winter in S.H.: much smaller changes

3.3.13 Spectral decomposition

Work with horizontal length scales and global spectral decomposition

For 2D cartesian flow:

$$\frac{1}{2}\overline{\underline{v}\cdot\underline{v}} = \int E(k)dk$$

where $E(k)$ is the kinetic energy spectrum, $k = \sqrt{k_x^2 + k_y^2}$, $k_x = \frac{2\pi}{\lambda_x}$ and $k_y = \frac{2\pi}{\lambda_y}$. $E(k)$ has units $\mathrm{m}^3\ \mathrm{s}^{-2}$.

For a frictionless, unforced flow, both energy and *enstrophy* (mean squared vorticity) are conserved over the domain.

$$\begin{aligned}\frac{1}{2}\overline{\xi^2} &= \int G(k)dk \\ &= \int k^2 E(k)dk\end{aligned}$$

If the flow is non-divergent then we can express it in terms of a streamfunction

$$\underline{v} = \underline{k} \times \nabla\psi$$

and

$$E(k) = \pi k^3 \overline{|\psi(k)|^2}$$

On the sphere, use spherical harmonics to decompose the horizontal streamfunction ψ of the non-divergent part of the flow (see Boer, 1982):

$$\psi(\lambda,\phi) = \sum_{n=0}^{N}\sum_{m=-n}^{n} \psi_{n,m}\exp(im\lambda)P_n^m(\sin\phi)$$

where n is the total wavenumber, m is the zonal wavenumber, and P_n^m is the associated Legendre polynomial of order n. For example, (see figure)

P_n^m	$P_0^0 = 1$	$P_1^0 = x$	$P_1^1 = -\sqrt{(1-x^2)}$
$Re\big(\exp(im\lambda)P_n^m(\sin\phi)\big)$	1	$\sin\phi$	$-\cos\phi\cos\lambda$

Take the global mean kinetic energy

$$\begin{aligned} < \frac{1}{2}\underline{v}\cdot\underline{v} > &=< \nabla\cdot(\psi\nabla\psi) - \psi\nabla^2\psi > \\ &= \sum_{n=0}^{N} E_n \\ &= \frac{1}{4}\sum_{n=0}^{N}\sum_{m=-n}^{n}\frac{n(n+1)}{a^2}|\psi_{n,m}|^2 \end{aligned}$$

(note that $n(n+1)/a^2$ are the eigenvalues of ∇^2 - use for length scales).

3.3.14 The energy spectrum in spherical coordinates

E_n has units $\mathrm{m}^2\ \mathrm{s}^{-1}$ (n is dimensionless).

To convert length scales to total wavenumbers consider that the eigenvalue of ∇^2 is $n(n+1)/a^2$, which is independent of zonal wavenumber m. That is,

$$\nabla^2 \exp(im\lambda)P_n^m(\sin\phi) = -\frac{n(n+1)}{a^2}\exp(im\lambda)P_n^m(\sin\phi)$$

So the length scale is

$$\begin{aligned} \frac{1}{L^2} &\sim \frac{n(n+1)}{a^2} \\ L &\sim \frac{a}{\sqrt{n(n+1)}} \end{aligned}$$

Note that for a sine wave we would say $L = 2\pi a/\sqrt{n(n+1)}$, so in this case L is the wavelength.

See Fig. 3.15

- The energy spectrum E_n includes contributions from all m for a given n (and thus all 'effective' meridional wavenumbers $l = n - m$).
- If the field is isotropic then $\psi_{n,m} = \psi_n$
- Water vapor movie shows turbulent flow
- Figure shows E_n on log-log scale from ERA40
- Peak at $n \simeq 7$
  - $L = \frac{a}{\sqrt{n(n+1)}} \sim 850$ km, but often include $\mathcal{O}(1)$ factors e.g. 2π
- If exclude $m = 0$ get spectrum of eddy kinetic energy. If include $m = 0$ then get large contribution for small wavenumbers from the zonal jets (large-scale features). Alternate approach is to time-filter the fields to pick out 2-8 day contribution.

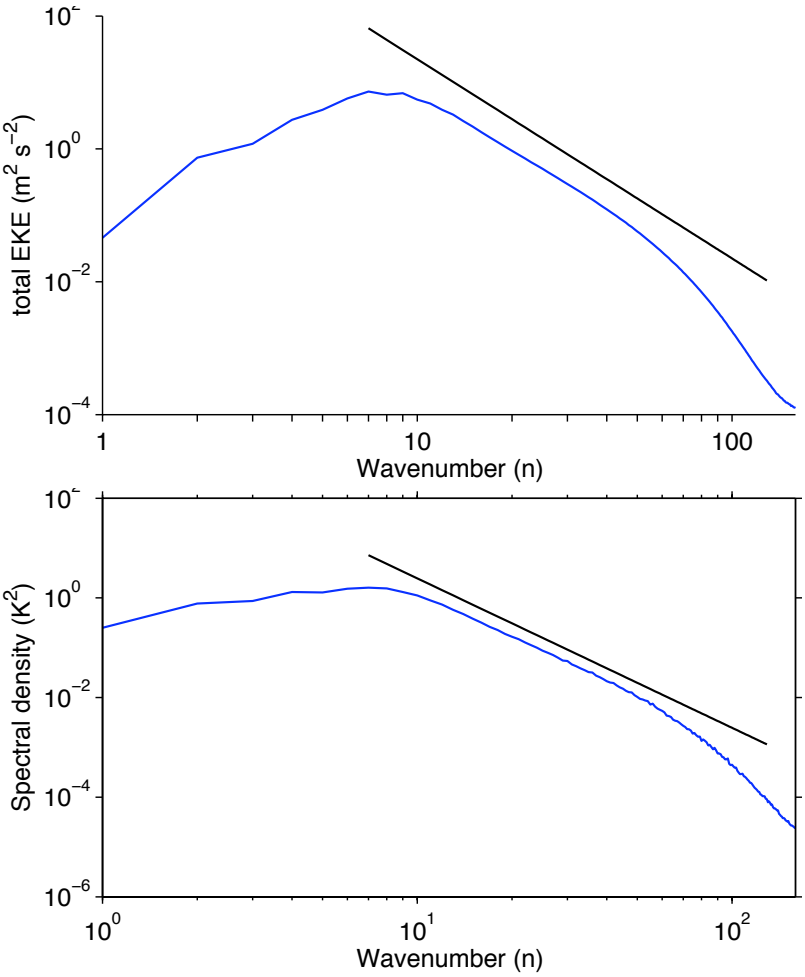

Figure 3.15: Spectra for total EKE (upper) and potential temperature (lower) (both annual mean). n^{-3} shown for comparison.

- See discussion of 2D turbulence in keynote
- Spectrum is roughly n^{-3} from $n \simeq 8$ to $n \simeq 50$.
  - same as enstrophy cascade, but will see later that no inertial range occurs
- Figure: potential temperature also close to n^{-3} as would be predicted for available potential energy (Charney, 1971)
- Can also define 1D spectra, e.g. $E(m)$ at a given latitude.
- Figure: aircraft data (flown near tropopause) suggest spectrum change to shallower slope at smaller scales. (This figure is for a 1D spectrum but not at one latitude).

3.4 Water vapor and the hydrological cycle

Highly variable in space and time.

3.4.1 Fig. 3.16: GPCP (Global Precipitation Climatology Project) mean precipitation rate vs. latitude and longitude in mm/day

- High precipitation in equatorial zone in ITCZ (note SPCZ in the Pacific)
- Seasonal maps show major differences over Monsoon regions (essentially, wherever there is a subtropical land mass) e.g. the Asian monsoon.
- Major dry regions where subsidence occurs (subtropical highs)
- Secondary maxima in midlatitude storm tracks

3.4.2 Fig. 3.17: time and zonal mean specific humidity (ERA40)

- Most water vapor near surface and in the tropics
- Saturation specific humidity $q_s \geq q$, largely determines structure of specific humidity, determined by T, p.

3.4.3 Fig. 3.18: time and zonal mean relative humidity

- Subtropical minima at ~ 500 hPa or higher.
- Even in zonal and time mean, values as low as 30%
- Close to 80% near surface
- Seasonal migration of dry zones is evident
- Observations and reanalysis may be unreliable, e.g. numerical model used in ERA40 has a critical value of 80% built-in for development of stratiform clouds in the free troposphere.

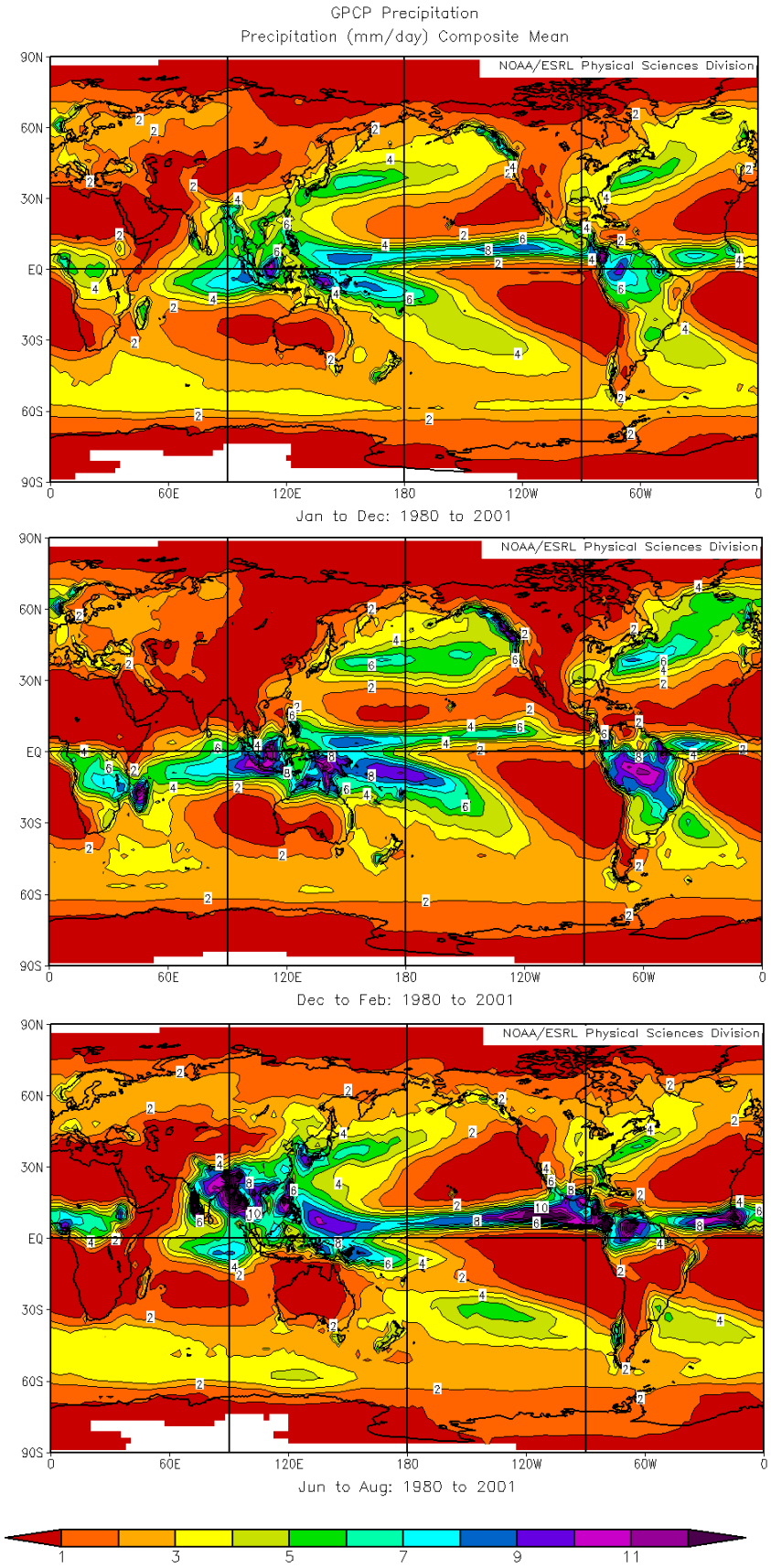

Figure 3.16: GPCP mean precipitation rate in mm/day: annual (upper), NH winter (middle) and NH summer (lower).

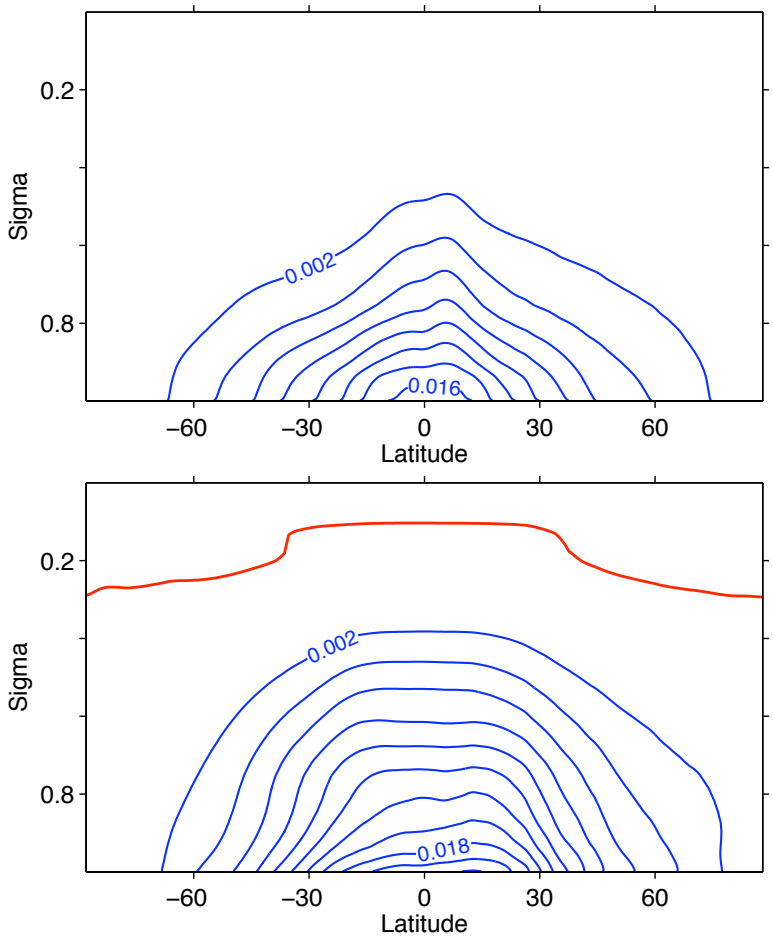

Figure 3.17: Time and zonal mean specific humidity (upper) and saturated specific humidity (lower).

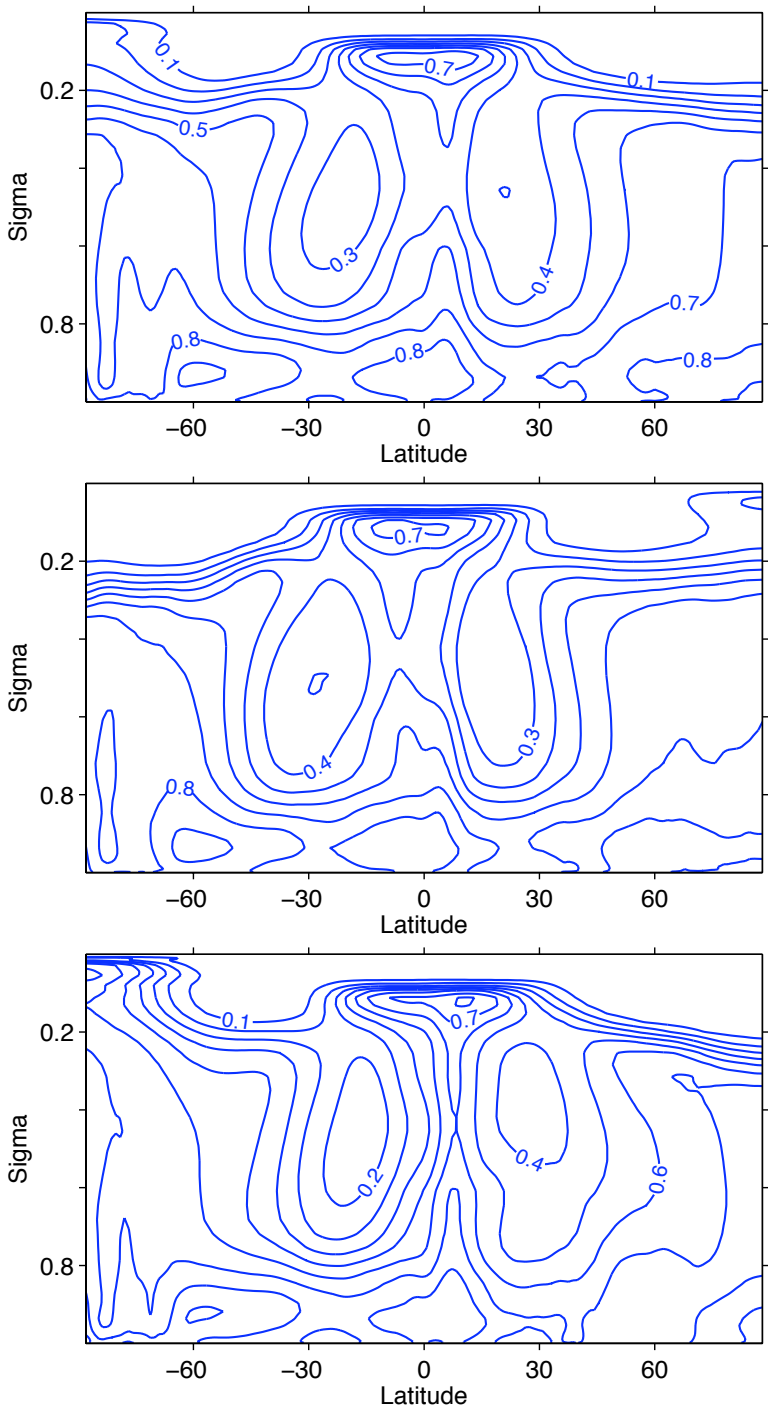

Figure 3.18: Zonal mean relative humidity: Annual mean (upper), NH winter (middle) and NH summer (lower).

4 Energetics

The goal of this section is to characterize the energy balance of the atmosphere and how energy is transported. Refer to the numbered figures in Peixoto and Oort (1992) unless otherwise stated.

4.1 Forms of energy

Internal $I = c_v T$ (with c_v the specific heat capacity at constant volume)

Potential $\Phi = gZ$

Kinetic $K = \frac{1}{2}\big(u^2 + v^2 + w^2\big) = \frac{1}{2}\underline{c} \cdot \underline{c}$

Latent $LH = Lq$

Note the latent heat of evaporation is $L = 2501$ J/g while the latent heat of sublimation is $L = 2835$ J/g, but we will neglect ice.

The total energy is thus $E = I + \Phi + LH + K$.

4.1.1 Total potential energy

The hydrostatic approximation means that internal and potential energy are related.

The internal energy per unit area is

$$\int_0^\infty \rho I dz = \int_0^\infty \rho c_v T dz = \int_0^{p_0} c_v T \frac{dp}{g}$$

while the potential energy per unit area is

$$\int_0^\infty \rho \Phi dz = \int_0^\infty \rho g z dz = \int_0^{p_0} z dp = \int_0^\infty p dz + \Big[pz\Big]_0^{p_0} = \int_0^\infty p dz$$

$$= \int_0^\infty \rho R_g T dz = \frac{R_g}{c_p} \int_0^{p_0} c_v T \frac{dp}{g} = \frac{R_g}{c_v} \int_0^\infty \rho I dz$$

So define the total potential energy (= grav. potential energy plus internal energy)

$$\int_0^\infty \rho\big(\Phi + I\big) dz = \int_0^\infty \rho c_p T dz = \int_0^{p_0} c_p T \frac{dp}{g}$$

using $c_p = c_v + R_g = c_v\big(1 + \frac{R_g}{c_v}\big)$.

4.1.2 Speed of sound

The speed of sound is c_s where

$$c_s^2 = \Big(\frac{\partial p}{\partial \rho}\Big)_\theta = \frac{c_p}{c_v} R_g T$$

Derivation:

$$\theta = T\Big(\frac{p_0}{p}\Big)^\kappa \rightarrow p = p_0\Big(\frac{T}{\theta}\Big)^{\frac{1}{\kappa}} = \frac{p_0}{\theta^{\frac{1}{\kappa}}}\Big(\frac{p}{\rho R_g}\Big)^{\frac{1}{\kappa}}$$

$$p^{1-\frac{1}{\kappa}} = p^{\frac{\kappa-1}{\kappa}} = \frac{p_0}{\theta^{\frac{1}{\kappa}}}\rho^{-\frac{1}{\kappa}} R_g^{-\frac{1}{\kappa}}$$

$$p = \left[\frac{p_0^{\frac{\kappa-1}{\kappa}}}{(\theta R_g)^{\frac{1}{\kappa-1}}}\right]\rho^{-\frac{1}{\kappa-1}}$$

$$\Big(\frac{\partial p}{\partial \rho}\Big)_\theta = -\left[\frac{p_0^{\frac{\kappa-1}{\kappa}}}{(\theta R_g)^{\frac{1}{\kappa-1}}}\right]\frac{1}{\kappa-1}\rho^{-\frac{1}{\kappa-1}-1} = -\frac{p}{\kappa-1}\rho^{-1} = -\frac{R_g T}{\kappa-1}$$

But $\kappa = R_g/c_p$ by definition, so

$$\kappa - 1 = \frac{R_g}{c_p} - 1 = \frac{R_g - c_p}{c_p} = -\frac{c_v}{c_p}$$

whence

$$\Big(\frac{\partial p}{\partial \rho}\Big)_\theta = \frac{c_p}{c_v} R_g T$$

4.1.3 Magnitude of kinetic energy

The kinetic energy per unit area is

$$\int_0^{p_0} K\frac{dp}{g} = \frac{1}{2g}\int_0^{p_0} |\underline{c}|^2 dp$$

while the total potential energy is

$$\int_0^{p_0} c_p T\frac{dp}{g} = \int_0^{p_0} c_s^2\Big(\frac{c_v}{R_g}\Big)\frac{dp}{g}$$

$$\rightarrow \frac{K}{\Phi + I} \sim \frac{1}{2}\frac{|\underline{c}|^2}{c_s^2}\frac{c_v}{R_g}$$

If $c \sim 15$ m/s and $c_s \sim 300$ m/s, then

$$\frac{K}{\Phi + I} \sim \frac{1}{2}\frac{15^2}{300^2}\frac{5}{2} \sim 0.003$$

So the kinetic energy is a small fraction of the total energy (but see later for available energy).

4.1.4 Fig 13.3: Meridional profiles of energy components

Note these are zonal, time and vertically averaged values. Kinetic energy is not plotted because the values are negligible.

Total 2.6×10^5 J/kg

Internal 1.8×10^5 J/kg, or 70% of total

Potential 0.7×10^5 J/kg, or 27% of total

Latent 0.1×10^5 J/kg, or 2.5% of total

Kinetic 180 J/kg, or 0.05% of total

(data from Oort and Peixoto, 1983)

- Latent energy has strong seasonal cycle at low latitudes (unlike I and Φ).
- Maximum at S.P. due to topography
- High latitude S.H. less energy than N.H. (colder) (but potential temperature similar!)
- Bigger seasonal cycle in N.H. (as usual).

4.2 Lagrangian rates of change of energy for air parcels

We will work in z coordinates for the moment.

4.2.1 Potential

$$\frac{d\Phi}{dt} = gw$$

4.2.2 Internal

$$\frac{dI}{dt} = Q - p\alpha\nabla\cdot\underline{c}$$

This follows from the 1st law and continuity:

$$c_v dT = Q - pd\alpha$$

$$-\frac{1}{\rho}\frac{d\rho}{dt} = \nabla\cdot\underline{c}$$

$$\rho = \frac{1}{\alpha} \rightarrow -\alpha\frac{d}{dt}\frac{1}{\alpha} = \nabla\cdot\underline{c}$$

$$\frac{1}{\alpha}\frac{d\alpha}{dt} = \nabla\cdot\underline{c}$$

$$\frac{d\alpha}{dt} = \alpha\nabla\cdot\underline{c}$$

The diabatic heating can be decomposed into radiative, latent and frictional heating:

$$Q = Q_h + Q_f$$
$$Q_h = -\alpha\nabla\cdot\underline{F}_{rad} - L(e-c) - \alpha\nabla\cdot\underline{J}_H^D$$

where $\underline{F}_{rad}$ is the radiative flux, e is evaporation per unit mass, and $\underline{J}_H^D$ is the diffusive heat flux.

The frictional contribution can be written

$$Q_f = -\alpha\underline{\underline{\tau}} : \nabla\times\underline{c}$$

where $\underline{\underline{\tau}}$ is the frictional stress tensor (e.g. $\overline{\rho c_i' u_i'}$, subgrid momentum contribution). The component τ_{zy} is the stress (force per unit area) in the y direction on the z=constant plane.

The tensor inner product is

$$\underline{\underline{\tau}} : \nabla\cdot\underline{c} = \tau_{ij}\delta_i c_j$$

So the total Lagrangian rate of change of internal energy is

$$\frac{dI}{dt} = -\alpha\nabla\cdot\underline{F}_{rad} - L(e-c) - \alpha\nabla\cdot\underline{J}_H^D - \alpha\underline{\underline{\tau}} : \nabla\underline{c} - p\alpha\nabla\cdot\underline{c}$$

4.2.3 Kinetic energy

For kinetic energy we use the vector momentum equation

$$\frac{d\underline{c}}{dt} = -2\Omega\times\underline{c} - \alpha\nabla p + \underline{g} + \underline{F}$$

Dot with $\underline{c}$:

$$\underline{c}\cdot\frac{d\underline{c}}{dt} = \underline{c}\cdot\big(-2\Omega\times\underline{c}\big) - \alpha\underline{c}\cdot\nabla p + \underline{g}\cdot\underline{c} + \underline{F}\cdot\underline{c}$$

$$\frac{d}{dt}\frac{1}{2}|\underline{c}|^2 = -\alpha\underline{c}\cdot\nabla p - gw - \alpha\underline{c}\cdot\nabla\cdot\underline{\underline{\tau}}$$

or

$$\frac{dK}{dt} = -gw - \alpha\nabla\cdot\Big(\underline{c}p + \underline{\underline{\tau}}\cdot\underline{c}\Big) + \alpha p\nabla\cdot\underline{c} + \alpha\underline{\underline{\tau}} : \nabla\underline{c}$$

For the hydrostatic case

$$-gw - \alpha\underline{c}\cdot\nabla p = -\alpha\underline{v}\cdot\nabla p$$

4.2.4 Latent heat

$$L\frac{dq}{dt} = L(e-c) - \alpha L\nabla\cdot J_q$$

where the last term represents subgrid and molecular diffusion processes.

4.2.5 Conversion between different forms

In the above Lagrangian rates of changes we can see several terms in common which balance each other and represent conversion between different forms of energy. These include

- $\alpha\underline{\underline{\tau}} : \nabla\underline{c}$ (frictional dissipation) in $\frac{dI}{dt}$ and $\frac{dK}{dt}$
- gw (work done against gravity) in $\frac{d\Phi}{dt}$ and $\frac{dK}{dt}$
- $-p\alpha\nabla \cdot \underline{c}$ (work done against pressure field, i.e. compression) in $\frac{dI}{dt}$ and $\frac{dK}{dt}$
- $L(e-c)$ (latent heating) in $\frac{dq}{dt}$ and $\frac{dI}{dt}$ (really conversion between different forms of internal energy)

Some things to note: conversions from KE involve forces: pressure, gravity, friction (but not e.g. Coriolis). Pressure and gravity give rise to reversible conversions, while frictional dissipation is irreversible (comes up as Tds).

See Fig. 13.1 in Peixoto and Oort.

4.2.6 Total energy

When multiplied by ρ and integrated in space, terms of the form

$$\alpha\nabla \cdot (flux)$$

result in

$$\int (\rho\alpha)\nabla \cdot (flux)dV = \int \nabla \cdot (flux)dV = \int_S (flux) \cdot \underline{n}dS$$

and are thus interpreted as boundary forcing, e.g. sensible heat flux, work done on ocean, surface evaporation.

Can add different equations to get an equation for E, the total energy of the atmosphere.

$$\frac{dE}{dt} = -\alpha\nabla \cdot (p\underline{c}) - \alpha\underline{c} \cdot \nabla\underline{\underline{\tau}} + L(e-c) + Q - \alpha L\nabla \cdot J_q^D$$

(gw and $p\alpha(\nabla \cdot \underline{c})$ cancelled)

Or using

$$Q = -\alpha\nabla \cdot \underline{F}_{rad} - L(e-c) - \alpha\nabla \cdot \underline{J}_H^D - \alpha\underline{\underline{\tau}} : \nabla \times \underline{c}$$

we can write

$$\frac{dE}{dt} = -\alpha\nabla \cdot \left(\underline{F}_{rad} + p\underline{c} + \underline{J}_H^D + L\underline{J}_q^D + \underline{\underline{\tau}} \cdot \underline{c}\right)$$

4.3 Observed heating rates

4.3.1 Radiation

We make a distinction between the solar shortwave fluxes, centered on 0.6 μm, and terrestrial longwave fluxes roughly centered on 15 μm. The net radiative flux at the top of the atmosphere is

$$F_{TOA} = \int_{top} (1-\alpha) F^{\downarrow}_{SW} ds - \int_{top} F^{\uparrow}_{LW} ds \simeq 0$$

where α is the albedo, where $(1-\alpha)$ is defined as the fraction of radiation not scattered or reflected back to space.

Figure: daily averaged insolation

- stronger in DJF than JJA by about 7% (perihelion, or closest approach to the sun, occurs in January).
- Max. at summer pole (due to increasing length of day as one moves towards the summer pole.
- Weaker meridional gradient in summer – as move poleward the longer day offsets change in zenith angle (how high the sun is) in the summer hemisphere, but the shorter day and lower sun combine in the winter hemisphere.

Albedo is variable and depends on the solar zenith angle (higher albedo as Z increases).

- Clouds account for roughly half (about 50% cloud cover)
- Cumulus have high albedos, stratus have large area
- Albedo is generally highest over land and in polar regions (Stephen's figure)
- Hemispheric albedos show little seasonal cycle (see table).
- $\sim 30\%$ of $F^{\downarrow}_{SW}(1-\alpha)$ is absorbed in the atmosphere.
- comment on polar night: ice albedo irrelevant at time of year when 'polar amplification' occurs (ocean plays a role).

Absorbed solar radiation (Trenberth and Stepaniak figure)

- Most absorbed near equator away from deep convection (cooling effect of clouds in SW).
- OLR is largest in tropics away from deep convection (warming effect of clouds in LW). Note that max. OLR in zonal average is in the subtropics.
- Net radiation shows compensation for high clouds and implies energy transport polewards by the circulation.

4.3.2 Diabatic heating

Fig. 13.2: Diabatic heating vs. latitude

- Radiative heating is negative and of order -0.5 to 2 K/day, but some warming in tropical stratosphere due to SW absorption (ozone).
- Latent heating is positive, maxima in ITCZ and storm tracks.
  - distribution in figure is very approximate!
  - values of $\mathcal{O}(2$ K/day$)$
- 'boundary layer heating' results from turbulent fluxes of temperature (e.g. thermals). Mostly positive
- Net diabatic heating is both positive and negative
  - largely depends on whether close to latent heating maxima

4.4 Energy budgets in Eulerian reference frame

So far we have considered Lagrangian rates of change. Now move to Eulerian framework so as to consider transport across fixed boundaries. Also switch to pressure coordinates (λ, ϕ, p, t) – this avoids density factors after using hydrostatic approximation.

4.4.1 Sensible heat

The first law says

$$c_p \frac{dT}{dt} = Q + \alpha \frac{dp}{dt}$$

or, in Eulerian notation

$$c_p \Big(\frac{\partial T}{\partial t} + \frac{u}{R\cos\phi}\frac{\partial T}{\partial \lambda} + \frac{v}{R}\frac{\partial T}{\partial \phi} + \omega \frac{\partial T}{\partial p} \Big) = Q + \alpha\omega$$

but, invoking the continuity equation

$$\frac{1}{R\cos\phi}\frac{\partial u}{\partial \lambda} + \frac{1}{R\cos\phi}\frac{\partial}{\partial \phi}(v\cos\phi) + \frac{\partial \omega}{\partial p} = 0$$

we can write

$$c_p \Big(\frac{\partial T}{\partial t} + \frac{1}{R\cos\phi}\frac{\partial}{\partial \lambda}\big(uT\big) + \frac{1}{R\cos\phi}\frac{\partial}{\partial \phi}\big(vT\cos\phi\big) + \omega \frac{\partial T}{\partial p} \Big) = Q + \alpha\omega$$

Now take the time average:

$$\frac{\partial}{\partial t}\Big(\overline{c_p T}\Big) = -\frac{1}{R\cos\phi}\Big(\frac{\partial}{\partial \lambda}\overline{\mathcal{F}_{H\lambda}} + \frac{\partial}{\partial \phi}\big(\overline{\mathcal{F}_{H\phi}}\cos\phi\big)\Big) - \frac{\partial}{\partial p}\overline{\mathcal{F}_{Hp}} + Q + \overline{\alpha\omega}$$

where we have defined the enthalpy flux $\overline{\mathcal{F}_H} = \big(c_pTu, c_pTv, c_pT\omega\big)$.

4.4.2 Latent heat

$$L\frac{dq}{dt} = L(e-c) - Lg\frac{\partial}{\partial p}J_q^D$$

(neglecting horizontal diffusion)

Following the same procedure as for the sensible heat above, we get

$$\frac{\partial}{\partial t}\overline{Lq} = -\frac{L}{R\cos\phi}\Big(\frac{\partial}{\partial\lambda}\overline{\mathcal{F}_{q\lambda}} + \frac{\partial}{\partial\phi}\big(\overline{\mathcal{F}_{q\phi}}\cos\phi\big)\Big) - L\frac{\partial}{\partial p}\big(\overline{\mathcal{F}_{qp}}\big) + L(\overline{e}-\overline{c}) - Lg\frac{\partial}{\partial p}\overline{J_q^D}$$

where we have defined the moisture flux as $\overline{\mathcal{F}_q} = \big(qu, qv, q\omega\big)$.

4.4.3 Kinetic energy

The kinetic energy flux is more subtle; we must exclude ω^2 to get conservation.

$$u\times\Big(\frac{du}{dt} = \frac{\tan\phi}{R}uv + fv - \frac{g}{R\cos\phi}\frac{\partial Z}{\partial\lambda} + F_\lambda\Big)$$
$$v\times\Big(\frac{dv}{dt} = \frac{\tan\phi}{R}u^2 - fu - \frac{g}{R}\frac{\partial Z}{\partial\phi} + F_\phi\Big)$$

$$\frac{\partial}{\partial t}\frac{1}{2}\big(u^2+v^2\big) = -\frac{1}{R\cos\phi}\Big(\frac{\partial}{\partial\lambda}\overline{\mathcal{F}_{K\lambda}} + \frac{\partial}{\partial\phi}\overline{\mathcal{F}_{K\phi}}\cos\phi\Big) - \frac{\partial}{\partial p}\overline{\mathcal{F}_{Kp}} + \overline{uF_\lambda} + \overline{vF_\phi} - \overline{\alpha\omega}$$

where the flux is defined as

$$\overline{\mathcal{F}_K} = \Big(\frac{1}{2}(u^2+v^2)u + gZu, \frac{1}{2}(u^2+v^2)v + gZv, \frac{1}{2}(u^2+v^2)\omega + gZ\omega\Big)$$

Note cancellation of metric terms, and cancellation of Coriolis terms, and that we have rewritten the pressure work term to give a flux of potential energy:

$$\begin{aligned}-\frac{gu}{R\cos\phi}\frac{\partial Z}{\partial\lambda} - \frac{gv}{R}\frac{\partial Z}{\partial\phi} =& -g\Big(\frac{1}{R\cos\phi}\frac{\partial}{\partial\lambda}uZ + \frac{1}{R\cos\phi}\frac{\partial}{\partial\phi}vZ\cos\phi + \frac{\partial}{\partial p}\omega Z\Big)\\ &+ g\omega\frac{\partial Z}{\partial p} + gZ\Big(\frac{1}{R\cos\phi}\frac{\partial u}{\partial\lambda} + \frac{1}{R\cos\phi}\frac{\partial}{\partial\phi}v\cos\phi + \frac{\partial\omega}{\partial p}\Big)\end{aligned}$$

The term in the second parentheses is zero by continuity, and

$$g\frac{\partial Z}{\partial p} = \frac{\alpha g}{g} = \alpha$$

4.4.4 Total energy

Adding the sensible, latent and mechanical energy equations gives

$$\begin{aligned}\frac{\partial\overline{E}}{\partial t} =& -\frac{1}{R\cos\phi}\Big(\frac{\partial}{\partial\lambda}\big(\overline{\mathcal{F}_{E\lambda}}\big) + \frac{\partial}{\partial\phi}\big(\overline{\mathcal{F}_{E\phi}}\cos\phi\big)\Big) - \frac{\partial}{\partial p}\overline{\mathcal{F}_{Ep}}\\ &- g\frac{\partial}{\partial p}\Big(\overline{F}_{rad} + \overline{\mathcal{F}_{H\,p}^D} + \overline{\mathcal{F}_{q\;p}^D} + \overline{\underline{\tau}\cdot\underline{c}}\Big)\end{aligned}$$

where the total energy flux is

$$\mathcal{F}_E = \Big(\big[c_pT + gZ + Lq + \frac{1}{2}\big(u^2+v^2\big)\big]u, \\ \big[c_pT + gZ + Lq + \frac{1}{2}\big(u^2+v^2\big)\big]v, \\ \big[c_pT + gZ + Lq + \frac{1}{2}\big(u^2+v^2\big)\big]\omega \Big)$$

4.4.5 Connection to moist static energy

Extra term in energy flux compared with energy (g Z) arises from pressure work.

In tropical meteorology, traditionally use the so-called 'moist static energy budget', defined as $h = c_pT + gZ + Lq$. This is a source of confusion in the literature (see Trenberth and Neelin for discussions of the confusion).

h would be conserved for displacements where pressure changes are purely hydrostatic. This is not the case when there are pressure gradients in the horizontal (even when usual hydrostatic approximation is appropriate).

In the case when $\frac{\partial}{\partial t} = 0$, the approximation amounts to the neglect of (u^2+v^2) in the flux.

4.4.6 Average budgets

Often take the zonal average also, e.g.

$$\frac{\partial}{\partial t}\big[\overline{c_pT}\big] = -\frac{1}{R\cos\phi}\frac{\partial}{\partial\phi}\Big(\big[\overline{\mathcal{F}_{H\phi}}\big]\cos\phi\Big) - \frac{\partial}{\partial p}\Big(\big[\overline{\mathcal{F}_{Hp}}\big]\Big) + \big[\overline{Q}\big] + \big[\overline{\alpha\omega}\big] \\ \big[\overline{\mathcal{F}_{H\phi}}\big] = c_p\big[\overline{T}\big] + c_p\big[\overline{T}^*\overline{v}^*\big] + c_p\big[\overline{T'v'}\big]$$

and so on.

(Note the conversion from potential to kinetic energy is now in the term $\overline{\alpha\omega}$).

Integrating over a polar cap

$$\frac{\partial}{\partial t}\int_M \overline{c_pT}dm = \int_M \overline{Q}dm + \int_M \overline{\alpha\omega}dm - \int_{\partial M}\overline{\underline{\mathcal{F}}_H}\cdot\underline{n}ds$$

where the polar cap integral is

$$\int_M dm = \int_0^{p_0}\frac{dp}{g}\int_0^{2\pi}d\lambda R\cos\phi\int_{\phi_0}^{\pi/2}d\phi R$$

Since there are no fluxes at TOA and surface contributing to the boundary term, we get

$$\frac{\partial}{\partial t}\int_M \overline{c_pT}dm = \int_M\big(\overline{Q}+\overline{\alpha\omega}\big)dm + 2\pi R\cos\phi\int_0^{p_0}\big[\overline{\mathcal{F}_{H\phi}}\big]\frac{dp}{g}$$

For global integral

$$\frac{\partial}{\partial t}\int_M \overline{E}dm = \int_{top}\overline{F}^{\downarrow}_{rad}ds + \int_{sfc}\big(-\overline{F}^{\downarrow}_{rad} + \overline{F}^{\uparrow}_{SH} + \overline{F}^{\uparrow}_{LH}\big)ds$$

The total conversion from potential to kinetic energy is

$$C\big(P,K\big) = -\int_M \alpha\omega dm$$

which is positive for upward motion $\omega < 0$.

Note also that $\frac{\partial\omega}{\partial p} = -\nabla_h \cdot (u,v)$, so that ω and $C(P,K)$ is associated with divergent circulations.

(Recall that the geostrophic wind is non-divergent and thus doesn't contribute to this conversion. In other words, it doesn't do work against the pressure gradient.)

We get generation of K.E. when $\alpha\omega < 0$... this implies upward motion ($\omega < 0$) when α is large (low density), and vice-versa.

For global integrals

$$\frac{\partial}{\partial t}P = -C\big(P,K\big) + H$$
$$\frac{\partial}{\partial t}K = C\big(P,K\big) - D_A - D_{oc}$$

where

$$H = \int_M Q dm$$
$$D_A = -\int_M \big(\alpha\underline{\tau}\cdot\nabla\underline{c}\big)dm$$

is the dissipation rate in the atmosphere, and

$$D_{oc} = -\int_{sfc}\big(\omega Z - \underline{\tau}_o\cdot\underline{c}\big)$$

is the ocean forcing.

For the long term average

$$\overline{H} = D_A + D_{oc} > 0$$

because the dissipation is positive.

4.5 Fluxes of energy poleward

The total poleward energy flux is given by

$$\Big(c_pT + gZ + Lq + \frac{1}{2}\big(u^2+v^2\big)\Big)v$$

4.5.1 Fig. 13.4: Transient sensible heat

Mostly associated with extratropical storm tracks

$$\overline{v'T'} \sim -D\partial_y\overline{T_s}$$

and both D and $\partial_y\overline{T_s}$ are stronger in winter.

Also expect to be poleward if diffused, but this is not always the case in the subtropical upper troposphere (θ not conserved).

4.5.2 Fig. 13.5: Components of sensible heat flux vs. lat-σ

- Transient flux maximizes near 800 hPa in current climate, but second maximum near tropopause.
- Equatorward transient flux between -25° and 25° as mentioned earlier
- Stationary flux extends through troposphere in N.H.
- Mean meridional component → strong near surface and tropopause

4.5.3 Fig. 12.11: Latent heat flux

Focussed near surface where temperatures are higher.

4.5.4 Fig. 12.12

Transients extend into tropics

4.5.5 Fig. 13.6: Northward sensible flux vs. latitude

- Stationary flux is very strong in N.H. winter, exceeds transients
- $\overline{v^{*2}} \sim 0.5\overline{v'^2}$
- Strong seasonal cycle in mean meridional flux component in tropics

4.5.6 Fig. 13.7: Potential energy flux

- $\left[\overline{v'Z'}\right]$ is very small compared with contribution from $\left[\overline{v'T'}\right]$ → no geostrophic component.
- Large compensation in mean component with mean sensible component.
  - For dry adiabatic motions we expect $gdz \simeq -c_p dT$

In tropics, fluxes of gZ, c_pT and Lq all nearly cancel (as we will see later). Stability arguments suggest that θ_e is constrained. But $c_pTd(\log\theta_e) \simeq d(c_pT + Lq + gZ)$ (see homework). This is usually phrased as gross moist stability. It is nearly zero, but in fact it can have different signs depending on the circulation.

4.5.7 Fig. 13.8, 13.9: Transport of kinetic energy

- Mostly at the jet stream level
- Transient eddies dominate except in N.H. winter
- Not always poleward, and get convergence in mid-latitudes
- Values are small compared with other components

4.5.8 Fig. 13.10, 13.11: Total energy flux

- Mean meridional in tropics, transients in extratropics.
- Seamless transport!

4.5.9 Fig. 13.12: Divergence of the poleward energy flux

Bi-modal structure in tropics (c.f. the TOA radiative fluxes from earlier).

4.5.10 Comparison of different components of the total energy flux

[see figure 1, Trenberth and Stepaniak, upper panel]

- Latent flux equatorward in tropics
- K.E. flux small
- D.S.E. and latent components 'compensate' in tropics

4.5.11 Division into monthly and sub-monthly

[see figure 1, Trenberth and Stepaniak]

- Transient (sub-monthly) is poleward
- Longer than monthly → large compensation in Tropics

4.5.12 Ocean – atmosphere division

[see figs. from Czaja and Marshall]

- Ocean important at low latitudes, atmosphere at middle and high latitudes.
- Here infer ocean fluxes from atmospheric fluxes and TOA radiative fluxes.

4.6 Vertical transport of energy

Neglecting $\overline{\mathcal{F}^D_{H\,p}}$, $\overline{\mathcal{F}^D_{q}}_{\,p}$ and $\overline{\underline{\tau}\cdot\underline{c}}$ (small outside PBL),

$$\frac{\partial}{\partial t}\overline{[E]} = -\frac{1}{R\cos\phi}\frac{\partial}{\partial\phi}\Big(\overline{[\mathcal{F}_{E\phi}]}\cos\phi\Big) - \frac{\partial}{\partial p}\Big[\overline{\mathcal{F}_{Ep}} + g\overline{F}_{rad}\Big]$$

For a steady state, we can define a streamfunction ψ_E through

$$-\frac{\partial\psi_E}{\partial p} = 2\pi R\cos\phi\Big[\overline{\mathcal{F}_{E\phi}}\Big]$$
$$\frac{1}{R}\frac{\partial\psi_E}{\partial\phi} = 2\pi R\cos\phi\Big(\overline{[\mathcal{F}_{Ep}]} + g\overline{[F}_{rad}]\Big)$$

To evaluate ψ_E we need $\overline{F}_{rad}$ at the TOA, then integrate from pole at the TOA, then integrate down. (We *don't* need F_{rad} or $\mathcal{F}_E$ in the interior).

4.6.1 Fig. 13.15: annual

- inflow at TOA between -30° and 30 °.
- Much passes through to surface of tropical oceans
- Further poleward, much is fluxed polewards by circulation and out through extratropical OLR

4.6.2 Fig. 13.15: DJF and JJA

- Large inflow into summer hemisphere and outflow in winter hemisphere.
- Ocean heat storage as streamlines reach surface
- Tilting → role of circulation

5 Forcing of the zonal mean circulation

Refer to Section 14.5 of Peixoto and Oort (1992).

5.1 Introduction

The goal is to investigate the effect of eddies on the zonal-mean state of the atmosphere (by eddies here, we mean departure from zonal mean). Specifically, we will study the impact of the meridional eddy heat and momentum fluxes on the zonal mean velocities and potential temperature.

We will see that an efficient way to represent eddy fluxes is a fictitious vector called the Eliassen Palm flux (EP flux, named after Eliassen and Palm (1961)). Its meridional component is proportional to the eddy momentum flux, and its vertical component is proportional to the eddy heat flux.

The EP flux is a very powerful tool to display the impact of eddies on the zonal-mean fields; the direction of EP flux vector gives the relative contribution of eddy momentum and heat fluxes, and its divergence indicates the strength of the eddy-induced forcing on the mean flow (see, e.g., figure 14.9).

5.2 Basic equations in spherical coordinates (λ, ϕ, p, t)

We will use the quasi-geostrophic approximation, although the theoretical development can be generalized to the full primitive equations in the case of small amplitudes eddies. We start with the basic equations in pressure coordinate:

$$
\begin{aligned}
0 &= \frac{1}{R\cos\phi}\frac{\partial u}{\partial \lambda} + \frac{1}{R\cos\phi}\frac{\partial}{\partial \phi}\left(v\cos\phi\right) + \frac{\partial \omega}{\partial p} \\
\frac{du}{dt} &= \frac{\tan\phi}{R}uv + fv - \frac{g}{R\cos\phi}\frac{\partial Z}{\partial \lambda} + F_\lambda \\
\frac{dv}{dt} &= -\frac{\tan\phi}{R}u^2 - fu - \frac{g}{R}\frac{\partial Z}{\partial \phi} + F_\phi \\
c_p\frac{T}{\theta}\frac{d\theta}{dt} &= Q
\end{aligned}
$$

Since we are interested in the zonal mean flow, we take zonal averages of the above

equations. The continuity equation becomes:

$$\frac{1}{R\cos\phi}\frac{\partial}{\partial\phi}\big([v]\cos\phi\big)+\frac{\partial[\omega]}{\partial p}=0$$

In the QG approximation, $\omega=\mathcal{O}(Ro)$, while u,v are $\mathcal{O}(1)$. In addition, it follows from the continuity equation that the zonal mean $[v]=\mathcal{O}(Ro)$, and hence to first order can be neglected in the equations.

The zonally averaged u equation can be written

$$\begin{aligned}\frac{\partial}{\partial t}[u]+\frac{1}{R\cos^2\phi}\frac{\partial}{\partial\phi}\big([u][v]\cos^2\phi\big)+\frac{\partial}{\partial p}\big([u][\omega]\big)\\ =-\frac{1}{R\cos^2\phi}\frac{\partial}{\partial\phi}\big([u^*v^*]\cos^2\phi\big)-\frac{\partial}{\partial p}\big([u^*\omega^*]\big)+f[v]+[F_\lambda]\end{aligned}$$

Using the fact that the zonal mean $[v]=\mathcal{O}(Ro)$, as well as the QG scaling $\omega=\mathcal{O}(Ro)$, this equation becomes

$$\frac{\partial}{\partial t}[u]=f[v]+[F_\lambda]-\frac{1}{R\cos^2\phi}\frac{\partial}{\partial\phi}\big([u^*v^*]\cos^2\phi\big)$$

The v equation to first order yields the geostrophic relation for $[u]$, which we write in its thermal wind form so as not to introduce the geopotential as unknown

$$f\frac{\partial[u]}{\partial p}=\frac{1}{R\rho[\theta]}\frac{\partial[\theta]}{\partial\phi}$$

We can not neglect the term involving ω in the θ equation, because of the large static stability of the atmosphere. Nevertheless, we can approximate this term by

$$\frac{d([\omega][\theta]}{dp}\sim[\omega]\frac{d[\theta_s]}{dp}$$

where $\theta_s(p)$ is the global mean potential temperature profile. Thus the θ eqn becomes

$$\frac{\partial}{\partial t}[\theta]+[\omega]\frac{\partial\theta_s}{\partial p}=\Big(\frac{p_0}{p}\Big)^\kappa\frac{[Q]}{c_p}-\frac{1}{R\cos\phi}\frac{\partial}{\partial\phi}\big([v^*\theta^*]\cos\phi\big)$$

We therefore have 4 equations for 4 unknowns $[u],[v],[\omega],[\theta]$. Note that the eddy fluxes are forcing the mean flow, along with $[F]$ (dissipation) and $[Q]$ (diabatic heating).

5.3 Eliassen-Palm flux

5.3.1 An interesting special case: steady, adiabatic, non-dissipative flow

If the flow is steady, adiabatic and non-dissipative, the equations yield

$$\begin{aligned}f[v]&=\frac{1}{R\cos^2\phi}\frac{\partial}{\partial\phi}\big([u^*v^*]\cos^2\phi\big)\\ [\omega]&=-\frac{1}{R\cos\phi}\frac{\partial}{\partial\phi}\left(\frac{[v^*\theta^*]\cos\phi}{\frac{\partial\theta_s}{\partial p}}\right)\end{aligned}$$

(The continuity equation and thermal wind balance are unchanged.)

Thus in that case, the eddies do not influence $[u]$ and $[\theta]$, but they do influence $[\omega]$ and $[v]$. In fact, the effect of the eddies is simply to *balance the mean meridional circulation.*

We can now state a result known as the Eliassen-Palm theorem:

> In a steady, adiabatic, non-dissipative system, $\nabla \cdot \mathcal{F} = 0$, where
>
> $$\mathcal{F} = \begin{pmatrix} \mathcal{F}_\phi \\ \mathcal{F}_p \end{pmatrix} = \begin{pmatrix} -R\cos\phi\big[u^*v^*\big] \\ fR\cos\phi\big[v^*\theta^*\big]\left(\frac{\partial\theta_s}{\partial p}\right)^{-1} \end{pmatrix}$$
>
> The vector $\mathcal{F}$ is called the Eliassen-Palm flux.

5.3.2 Proof of EP theorem

For a steady, adiabatic, non-dissipative flow ($\frac{\partial}{\partial t} = [F] = [Q] = 0$), the equations yield

$$[v] = \frac{1}{fR\cos\phi}\frac{\partial}{\partial\phi}\Big(\big[u^*v^*\big]\cos^2\phi\Big)$$
$$[\omega] = -\frac{1}{\frac{\partial\theta_s}{\partial p}}\frac{1}{R\cos\phi}\frac{\partial}{\partial\phi}\Big(\big[v^*\theta^*\big]\cos\phi\Big)$$

Plugging these into the continuity equation yields

$$\frac{1}{R\cos\phi}\frac{\partial}{\partial\phi}\left(\frac{1}{fR\cos^2\phi}\frac{\partial}{\partial\phi}\Big(\big[u^*v^*\big]\cos^2\phi\Big)\cos\phi\right) + \frac{\partial}{\partial p}\left(\frac{-1}{\frac{\partial\theta_s}{\partial p}}\frac{1}{R\cos\phi}\frac{\partial}{\partial\phi}\Big(\big[v^*\theta^*\big]\cos\phi\Big)\right) = 0$$

$$\frac{1}{fR^2\cos\phi}\frac{\partial}{\partial\phi}\left(\frac{1}{\cos\phi}\frac{\partial}{\partial\phi}\Big(\big[u^*v^*\big]\cos^2\phi\Big)\right) - \frac{1}{R\cos\phi}\frac{\partial^2}{\partial p\partial\phi}\left(\frac{\big[v^*\theta^*\big]\cos\phi}{\frac{\partial\theta_s}{\partial p}}\right) = 0$$

$$\frac{\partial}{\partial\phi}\left[\left(\frac{1}{\cos\phi}\frac{\partial}{\partial\phi}\Big(\big[u^*v^*\big]\cos^2\phi\Big)\right) - \frac{\partial}{\partial p}\left(\frac{fR\big[v^*\theta^*\big]\cos\phi}{\frac{\partial\theta_s}{\partial p}}\right)\right] = 0$$

Integrating in ϕ, we see that the expression inside the square brackets is a function of p only. But at the poles, $v = [v] = v^* = 0$, whence

$$\frac{\partial}{\partial p}\left(\frac{\big[v^*\theta^*\big]}{\frac{\partial\theta_s}{\partial p}}\right) = 0$$

Furthermore, it follows from above that at the poles,

$$\frac{\partial}{\partial\phi}\Big(\big[u^*v^*\big]\cos^2\phi\Big) = 0$$

Therefore the integrand is zero at the pole and

$$\frac{1}{R\cos\phi}\frac{\partial}{\partial\phi}\Big(-R\big[u^*v^*\big]\cos^2\phi\Big) + \frac{\partial}{\partial p}\left(\frac{fR\cos\phi\big[v^*\theta^*\big]}{\frac{\partial\theta_s}{\partial p}}\right) = 0$$

or $\nabla \cdot \mathcal{F} = 0$.

5.3.3 Consequence: The non-acceleration theorem

Non-acceleration theorem: If the flow is adiabatic, non-dissipative, and if the divergence of the EP flux is zero, then there is a trivial solution:

$$\frac{\partial u}{\partial t} = \frac{\partial \theta}{\partial t} = 0$$

with $[v], [\omega]$ given above.

Proof: plug into the equations.

Thus $\nabla \cdot \mathcal{F}$ is the total explicit internal eddy forcing of the $[u]$ and $[\theta]$ fields. Note that there could be implicit effects of eddies on the boundary conditions, or eddy modifications of $[Q]$ and $[F]$.

5.3.4 Steady (or stationary mean) motion with heat and friction

More generally, if $[F]$ and $[Q]$ are non zero, then the equations for $[v]$ and $[\omega]$ become

$$[v] = \frac{1}{fR\cos^2\phi}\frac{\partial}{\partial\phi}\left([u^*v^*]\cos^2\phi\right) - \frac{1}{f}[F_\lambda]$$

$$[\omega] = -\frac{1}{R\cos\phi\frac{\partial\theta_s}{\partial p}}\frac{\partial}{\partial\phi}\left([v^*\theta^*]\cos\phi\right) + \left(\frac{p_0}{p}\right)^\kappa \frac{[Q]}{c_p\frac{\partial\theta_s}{\partial p}}$$

In that case, the continuity equation yields a relation between the diabatic forcing, the friction forcing, and the divergence of the EP flux:

$$\frac{\partial}{\partial p}\left(\left(\frac{p_0}{p}\right)^\kappa \frac{[Q]}{c_p}\left(\frac{\partial\theta_s}{\partial p}\right)^{-1}\right) - \frac{1}{R^2\cos\phi}\frac{\partial}{\partial\phi}\left(\frac{1}{f}[F_\lambda]R\cos\phi + \frac{1}{f}\nabla\cdot\mathcal{F}\right) = 0$$

Figure 11.7 on p.256 of Peixoto and Oort (1992) shows the eddy momentum fluxes. Transient eddies dominate in the upper levels, with convergence in midlatitudes → equatorward $[v]$ → upper branch of the Ferrel cell, and divergence in tropical and subtropical latitudes → poleward $[v]$ → upper branch of the Hadley cell.

At low levels, friction dominates; Midlatitude westerlies imply $[F] < 0$ → poleward $[v]$ → lower branch of the Ferrel cell, and low latitude easterlies yield $[F] > 0$ → equatorward $[v]$ → lower branch of the Hadley cell.

Figure 13.5 shows eddy heat fluxes. In midlatitudes, eddy heat flux convergence yields upward motion ($[\omega] < 0$). Divergence at subtropical latitudes yields subsiding motion → downward branch of Ferrel and Hadley cells. In the ITCZ, diabatic heating dominates (fig 13.2) and yields upward motion (ascending branch of the Hadley cell). All those results put together yield the 3 cell structure observed on fig 7.19.

Instead of looking at eddy momentum and heat fluxes separately, one can investigate the net effects of eddies on the mean circulation by studying the EP flux vector and its divergence. We will discuss this further in the following sections.

5.4 Modified momentum and energy equations

We saw earlier that in the thermodynamic equation, there can be a strong cancellation between the eddy heat flux and the adiabatic cooling $[\omega]\partial\theta_s/\partial p$.

This motivates the definition of a residual mean circulation defined by

$$\tilde{v} = [v] - \frac{\partial}{\partial p}\left(\frac{[v^*\theta^*]}{\partial\theta_s/\partial p}\right)$$
$$\tilde{\omega} = [\omega] + \frac{1}{R\cos\phi}\frac{\partial}{\partial\phi}\left(\frac{[v^*\theta^*]\cos\phi}{\partial\theta_s/\partial p}\right)$$

In other words, $\tilde{\omega}$ is the departure from the vertical velocity induced by eddy heat fluxes, and $\tilde{v}$ is such that the residual circulation $(\tilde{v}, \tilde{\omega})$ satisfies the continuity equation.

With these new variables, the equations become

$$\begin{aligned}
0 &= \frac{1}{R\cos\phi}\frac{\partial}{\partial\phi}\left(\tilde{v}\cos\phi\right) + \frac{\partial\tilde{\omega}}{\partial p} \\
\frac{\partial[u]}{\partial t} &= f\tilde{v} + [F_\lambda] + \frac{1}{R\cos\phi}\nabla\cdot\mathcal{F} \\
\frac{\partial[\theta]}{\partial t} + \tilde{\omega}\frac{\partial\theta_s}{\partial p} &= \left(\frac{p_0}{p}\right)^\kappa\frac{[Q]}{c_p} \\
f\frac{\partial[u]}{\partial p} &= \frac{1}{R\rho[\theta]}\frac{\partial[\theta]}{\partial\phi}
\end{aligned}$$

This set of equations makes it clear that the net effect of the eddies in the forcing of $[u]$ and $[\theta]$ can be described by the divergence of the EP flux. In other words, the eddies force $[u]$ and $[\theta]$ ONLY where $\nabla\cdot\mathcal{F}$ is non zero. If $\nabla\cdot\mathcal{F} = 0$, we recover the original equations without the eddy terms.

The residual circulation has a simple interpretation in steady state; the thermodynamic equation implies that $\tilde{\omega}$ is the vertical velocity corresponding to the mean diabatic heating, and $\tilde{v}$ follows from the continuity equation. Therefore $(\tilde{v}, \tilde{\omega})$ represents the circulation arising from the zonal mean heating $[Q]$.

5.5 Forcing of the mean meridional circulation

One can define a streamfunction for (v, ω), as well as for the residual circulation $(\tilde{v}, \tilde{\omega})$

$$\begin{aligned}
[v] &= \frac{g}{2\pi R\cos\phi}\frac{\partial\psi}{\partial p} \\
[\omega] &= -\frac{g}{2\pi R^2\cos\phi}\frac{\partial\psi}{\partial\phi} \\
\tilde{v} &= \frac{g}{2\pi R\cos\phi}\frac{\partial\tilde{\psi}}{\partial p} \\
\tilde{\omega} &= -\frac{g}{2\pi R^2\cos\phi}\frac{\partial\tilde{\psi}}{\partial\phi}
\end{aligned}$$

and the two streamfunctions are related by

$$\tilde{\psi} = \psi - \frac{2\pi R\cos\phi}{g}\frac{[v^*\theta^*]}{\partial\theta_s/\partial p}$$

From the equations of motion, the residual streamfunction satisfies the diagnostic equation

$$\frac{f^2 g}{2\pi R\cos\phi}\frac{\partial^2\tilde{\psi}}{\partial p^2} - \frac{g}{2\pi R^2\cos\phi\rho[\theta]}\frac{\partial}{\partial\phi}\Big(\frac{1}{R}\frac{\partial\theta_s}{\partial p}\frac{\partial\tilde{\psi}}{\partial\phi}\Big) = \frac{1}{R\rho[T]}\frac{\partial}{\partial\phi}\frac{[Q]}{c_p} - f\frac{\partial[F_\lambda]}{\partial p} - \frac{f}{R\cos\phi}\frac{\partial}{\partial p}\nabla\cdot\mathcal{F}$$

The strength of the forcing thus depends on the eddies through the divergence of the EP flux.

Similarly, one can derive an equation for ψ

$$\frac{f^2 g}{2\pi R\cos\phi}\frac{\partial^2\psi}{\partial p^2} - \frac{g}{2\pi R^2\cos\phi\rho[\theta]}\frac{\partial}{\partial\phi}\Big(\frac{1}{R}\frac{\partial[\theta]}{\partial p}\frac{\partial\psi}{\partial\phi}\Big) = \frac{1}{R\rho[T]}\frac{\partial}{\partial\phi}\frac{[Q]}{c_p} - f\frac{\partial[F_\lambda]}{\partial p} - \frac{1}{R\rho[\theta]}\frac{\partial}{\partial\phi}\left(\frac{1}{R\cos\phi}\frac{\partial}{\partial\phi}\big([v^*\theta^*]\cos\phi\big)\right) + \frac{f}{R\cos^2\phi}\frac{\partial^2}{\partial p\partial\phi}\big([u^*v^*]\cos^2\phi\big)$$

This equation is frequently written in terms of $[\omega]$ and is known as the omega equation.

5.6 Transformed Eulerian Mean

ψ is known as the Eulerian mean streamfunction, whille $\tilde{\psi}$ is the 'Transform Eulerian Mean' (TEM) streamfunction. The transformed streamfunction is similar to the (dry) isentropic streamfunction everywhere except near the surface. This makes sense as both have vertical motion directly related to diabatic heating. Both fields are plotted in Fig. 5.1 from ERA-40 data. (See e.g. Vallis, 2006, for more details.)

Near the surface, boundary layer fluxes are important and $\partial\theta_s/\partial p$ may be small, also surface intersections of isentropes are important. Note: $\tilde{\omega}$ not zero at surface unless no-slip condition applies so that $[v^*\theta^*] = 0$.

5.7 Example of EP flux diagram

Figure 14.9 of Peixoto and Oort (1992) shows cross sections of EP flux represented by arrows, and contours of its divergence (note that an upward pointing $\mathcal{F} \rightarrow$ its p-component is negative $\rightarrow$ poleward eddy heat flux).

- The direction of the arrow indicates the relative importance of the meridional eddy heat flux (vertical) and momentum flux (horizontal). The divergence contours indicate the strength of the eddy forcing on the mean flow.

- Stationary eddy EP fluxes are typically smaller than EP fluxes associated with transient eddies. The divergence is larger at low levels at mid and high latitudes.

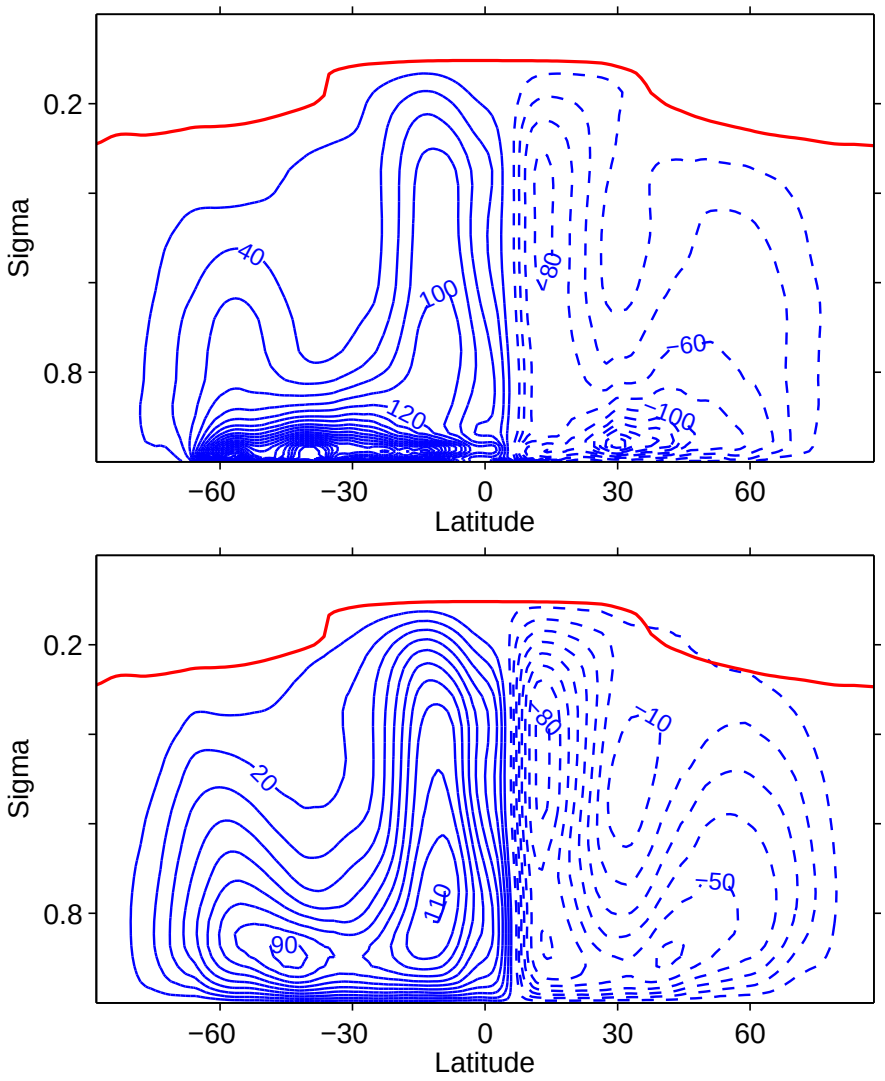

Figure 5.1: Transformed Eulerian Mean streamfunction $\tilde{\psi}$ (upper) and isentropic streamfunction (lower), both in units of 10^9 kg s^{-1}.

- The EP flux is upward for transient eddies and stationary eddies in winter, indicating that poleward eddy heat fluxes and baroclinic energy conversion dominate.
- The EP flux tilts equatorward at upper levels, indicating momentum flux convergence near the jet.

6 Available energy and the atmospheric energy cycle

6.1 Heat engine

Have seen that the kinetic energy is less than $\frac{1}{10}\%$ of the total energy in the atmosphere. Also, less than 1% of heat absorbed in the atmosphere is converted to K.E.

We can view the atmosphere as a heat engine:

- Transports heat poleward and upward
- High temperatures near surface and in tropics
- Cold temperatures at high latitudes and in upper atmosphere
- Heat flows from warm source to cold sink

Carnot engine efficiency is defined as the ratio of work to energy input. As a very rough estimate for the atmosphere, consider

$$h = \frac{T_w - T_c}{T_w} = \frac{\Delta T}{T_w} \sim \frac{40}{290} \sim 10 - 15\%$$

where we've used the vertical $\Delta T \sim 290 - 250 \sim 40$ K; we might also take the horizontal $\Delta T \sim 35$ K. The actual efficiency is lower than this crude estimate – see later for entropy analysis.

We need a more nuanced analysis of energy cycle.

6.2 Available potential energy (Lorenz, 1955, 1978, 1979)

6.2.1 Definition

Total energy $= \int dm(I + \Phi + LH + KE)$, where we can denote $(I + \Phi + LH)$ as the non-kinetic energy (NKE).

Total energy is conserved under adiabatic, frictionless flows $\rightarrow \Delta KE = -\Delta(I + \Phi + LH)$. What part of NKE could be converted to KE?

An intuitive argument: If we have a stably stratified fluid with no horizontal temperature gradients, *there is no energy available* for conversion to KE.

The available potential energy (APE) is the biggest possible ΔKE achievable under a reversible adiabatic transformation. It thus corresponds to the most negative ΔNKE, that is

$$APE = \int dm \Big(\big(I + \Phi + LH\big) - \big(I + \Phi + LH\big)_{ref} \Big)$$

where ref refers to the reference state, i.e. the state with lowest NKE achievable by rearrangement of the mass of the atmosphere using reversible adiabatic processes.

We could in principle calculate APE by brute force approach:

- evaluate NKE of all possible adiabatic transformations, and choose the largest $(-\Delta NKE)$
- such an approach may be needed in moist, conditionally unstable case – no completely general algorithm devised yet.

Note we don't require that the rearrangement is dynamically possible (i.e. satisfying momentum equations): only thermodynamic constraints enter.

6.2.2 What properties does the reference state have?

1. Isobaric surfaces must be horizontal
   - otherwise could impose a zero wind field and allow the system to evolve under the dynamic equations with no friction or external heating
   - this would lead to acceleration and production of KE and reduction of NKE
2. Reference state must be in hydrostatic balance
   - same reasoning as for point 1
   - implies ρ must be horizontally uniform (and same for θ, T, etc.)
3. Reference state must be statically stable
   - otherwise could impose weak wind field and produce more KE
   - In dry case, this implies θ increases with height
   - In moist case, θ_e^* can't increase with height in saturated air

In conclusion:

- For a dry atmosphere, the reference field has horizontal θ surfaces, with θ increasing upwards (and θ conserved by parcels in rearrangement).
- For a moist atmosphere, θ constant in reference state (w.r.t horiztonal) when unsaturated, θ_e^* and θ constant where saturated.

6.3 Computing APE

We will derive a formula for the APE (following Lorenz) in the dry case ($LH = 0$), and then derive an approximate version of it that involves the temperature variance.

6.3.1 Exact formula for dry APE

$$\begin{aligned} APE &= \int c_p\big(T - T_r\big)dm \\ &= \int c_p T\big(1 - T_r/T\big)dm \end{aligned}$$

where $(T - T_r)$ is known as the efficiency factor.

Useful to change to θ coordinates as dry adiabatic parcel motions conserve θ (note that if θ was truly conserved, this would imply $APE = 0$!)

Potential energy per unit area is

$$\begin{aligned} \int_0^{p_0} \frac{dp}{g} c_p T &= \int_0^{p_0} \frac{dp}{g} c_p \theta \Big(\frac{p}{p_{00}}\Big)^\kappa \\ &= \frac{c_p}{g(1+\kappa)p_{00}^\kappa} \int_0^{p_0} \theta dp^{\kappa+1} \end{aligned}$$

Now integrate by parts:

$$= \frac{c_p}{g(1+\kappa)p_{00}^\kappa} \left(\Big[\theta p^{\kappa+1}\Big]_{TOA}^{SFC} - \int_{\theta_{TOA}}^{\theta_{SFC}} p^{\kappa+1} d\theta \right)$$

Note that at TOA $p = 0$ implies $\theta \to \infty$.

$$= \frac{c_p}{g(1+\kappa)p_{00}^\kappa} \left(\int_{\theta_0}^{\infty} p^{\kappa+1} d\theta + \theta_0 p_0^{\kappa+1} \right)$$

Use convention that $p = p_0$ for θ below surface

$$= \frac{c_p}{g(1+\kappa)p_{00}^\kappa} \int_0^{\infty} p^{\kappa+1} d\theta$$

So potential energy is related to pressure distribution on θ surfaces.

To evaluate APE need to know how p and θ are related in the reference state. See Fig. 6.1. Under an adiabatic transformation, θ surfaces act as material surfaces. (We are assuming a statically stable state).

In particular the amount of mass above a given isentropic surface remains constant, that it

$$\tilde{p}(\theta) = \frac{\int\int p(x, y, \theta) dx dy}{\int\int dx dy}$$

remains constant. Here $\widetilde{(\cdot)}$ denotes a global mean.

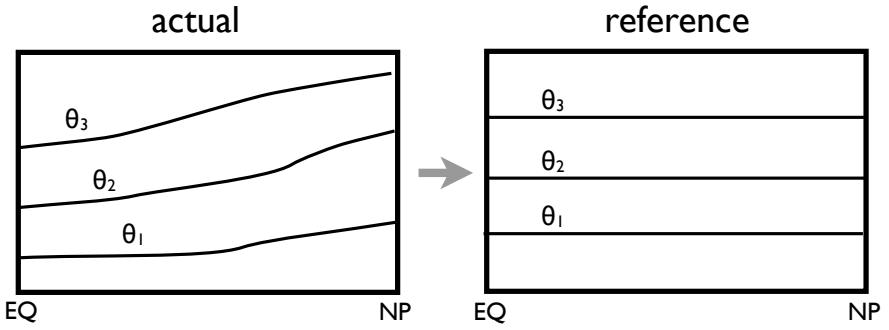

Figure 6.1: Schematic of the actual and reference states of the isentropic surfaces.

The reference state has θ constant on pressure surfaces, implying pressure constant on θ surfaces:

$$p_r = \tilde{p}_r(\theta) = \tilde{p}(\theta)$$

Therefore,

$$APE = \frac{c_p}{g(1+\kappa)p_{00}^{\kappa}} \int_0^{\infty} \left(\widetilde{p^{\kappa+1}} - \tilde{p}^{\kappa+1} \right) d\theta$$

No approximations have been made thus far. Note the following

$$\kappa + 1 > 1 \rightarrow \widetilde{p^{\kappa+1}} - \tilde{p}^{\kappa+1} \geq 0$$

$$APE = 0 \rightarrow p \equiv \tilde{p}$$

6.3.2 Approximate form: APE in terms of pressure variance along isentropes

We now make an approximation that leads to the 'quadratic' formula of Lorenz.

Define the deviation from global mean

$$p = \tilde{p} + p'$$

and assume that $\left| \frac{p'}{\tilde{p}} \right|$ is small. (A similar approximation is made in Q.G. – related to slope of isentropes).

$$\begin{aligned} \left(\tilde{p} + p' \right)^{1+\kappa} &\simeq \tilde{p}^{(1+\kappa)} \left(1 + \frac{p'}{\tilde{p}} \right)^{1+\kappa} \\ &= \tilde{p}^{(1+\kappa)} \left(1 + \frac{p'}{\tilde{p}}(1+\kappa) + \frac{p'^2}{\tilde{p}^2} \frac{\kappa(1+\kappa)}{2} + \dots \right) \end{aligned}$$

which implies

$$\widetilde{p^{\kappa+1}} - \tilde{p}^{\kappa+1} \simeq \frac{p'^2}{\tilde{p}^2} \frac{\kappa(1+\kappa)}{2} \tilde{p}^{(1+\kappa)}$$

and therefore

$$APE \simeq \frac{c_p \kappa}{2g p_{00}^{\kappa}} \int_0^{\infty} d\theta \tilde{p}^{(1+\kappa)} \widetilde{\left(\frac{p'}{\tilde{p}} \right)^2}$$

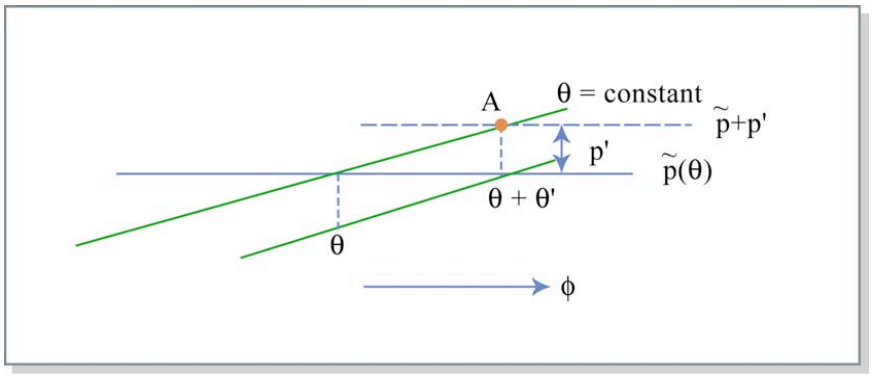

Figure 6.2: Figure by MIT OCW.

giving APE in terms of pressure variance on isentropes.

Note that the next term in the expansion is

$$\mathcal{O}\Big(\frac{p'}{\tilde{p}}\frac{\kappa-1}{3}\Big) \sim 0.05$$

6.3.3 APE in terms of temperature variance on constant pressure surfaces

If θ and p surfaces are quasi-horizontal, then

$$p \simeq \tilde{p}\big(\tilde{\theta}(p)\big)$$

[Insert little sketch] where $\tilde{\theta}(p)$ is the average θ on a p surface.

At a given point with pressure p and potential temperature θ

$$\begin{aligned} p' &= p - \tilde{p} \\ &= \tilde{p}(\tilde{\theta}) - \tilde{p}(\theta) \\ &= \tilde{p}(\theta - \theta') - \tilde{p}(\theta) \\ &\simeq -\theta' \frac{\partial \tilde{p}}{\partial \theta} \end{aligned}$$

Alternatively, consider isentrope θ with average pressure $= \tilde{p}(\theta)$

Consider a point A on θ at latitude ϕ_1, corresponds to pressure $p = \tilde{p} + p'$.

At $p = \tilde{p}(\theta)$ at latitude ϕ_1, have potential temperature $\tilde{\theta} + \theta' = \theta + \theta'$. (This assumes $\tilde{\theta}\big(\tilde{p}(\theta)\big) = \theta$).

Given quasi-horizontal surfaces,

$$\theta' \simeq -\frac{\partial \theta}{\partial p}p' \simeq -\frac{\partial \tilde{\theta}}{\partial p}p'$$

(see Fig. 6.2).

$$APE = \frac{c_p\kappa}{2gp_{00}^{\kappa}}\int_0^{\infty} d\theta\tilde{p}^{1+\kappa-2}\widetilde{\theta'^2}\Big(\frac{\partial\tilde{p}}{\partial\theta}\Big)^2$$
$$= \frac{c_p\kappa}{2gp_{00}^{\kappa}}\int_0^{p_0} d\tilde{p}\tilde{p}^{(\kappa-1)}\Big(-\frac{\partial\tilde{p}}{\partial\theta}\Big)\widetilde{\theta'^2}$$

where $\tilde{p}$ is now an integration variable.

Alternatively, we can use (for hydrostatic states)

$$\frac{\partial\theta}{\partial p} = \frac{\kappa\theta}{p}\frac{(\Gamma_d - \Gamma)}{\Gamma_d} = -\frac{\kappa\theta c_p}{gp}\big(\Gamma_d - \Gamma\big)$$

where $\Gamma = -\partial T/\partial z, \Gamma_d = g/c_p$. This implies

$$-\frac{\partial\tilde{p}}{\partial\theta} \simeq \frac{g\tilde{p}}{\kappa\tilde{\theta}c_p}\frac{1}{(\Gamma_d - \tilde{\Gamma})}$$

and

$$\frac{\widetilde{\theta'^2}}{\tilde{\theta}}\frac{\tilde{p}^{\kappa}}{p_{00}^{\kappa}} = \frac{\widetilde{T'^2}}{\tilde{T}}$$

giving

$$APE = \frac{1}{2}\int_0^{p_0}\frac{\widetilde{T'^2}}{\tilde{T}}\frac{1}{(\Gamma_d - \tilde{\Gamma})}dp$$

6.3.4 What fraction of potential energy is available?

Now consider that

$$I + \Phi = \int_0^{p_0}\frac{dp}{g}c_p\tilde{T} = \frac{1}{\Gamma_d}\int_0^{p_0} dp\tilde{T}$$

so that

$$\frac{APE}{I+\Phi} \sim \frac{1}{2}\Gamma_d\big(\Gamma_d - \tilde{\Gamma}\big)^{-1}\frac{\widetilde{T'^2}}{\tilde{T}^2}$$

If $\tilde{\Gamma} \sim \frac{2}{3}\Gamma_d$ and $\widetilde{T'^2} \sim (15\text{ K})^2$, then

$$\frac{APE}{I+\Phi} \sim \frac{3}{2}\frac{15^2}{250^2} = \frac{1}{2}\%$$

showing that less than 1% of potential energy is available for conversion to kinetic energy.

Earlier we had $KE/(\Phi + I) \sim 10^{-3}$. Putting these together,

$$\frac{KE}{APE} \sim \frac{0.001}{0.005} = \frac{1}{5}$$

Note we have ignored horizontal variations in the static stability factor; this is an acceptable approximation in the present climate.

More generally,

$$\begin{aligned} APE &\sim \frac{(\text{horizontal temperature fluctuations})^2}{\text{static stability}} \\ &\sim \frac{(\text{horizontal temperature gradients})^2 L^2}{\text{static stability}} \\ &\sim (\text{isentropic slope})^2 \times (\text{static stability}) \times L^2 \end{aligned}$$

Globally find dry APE of zonal mean state ~ 3 MJ/m^2, and eddy kinetic energy ~ 0.7 MJ/m^2.

Including moisture increases global available energy by $\sim 30\%$ for the current climate. The difference is considerable smaller if the tropics is excluded.

6.4 Decomposing APE into eddy and mean components

$$\begin{aligned} APE \text{ per unit area} &= \frac{1}{2}\int_0^{p_0} dp \frac{\widetilde{T'^2}}{\tilde{T}} \frac{1}{(\Gamma_d - \tilde{\Gamma})} \\ \text{(Total) } APE &= \frac{1}{2}\int_0^{p_0} \frac{dp}{g} \int dxdy \frac{g(T^2 - \tilde{T}^2)}{\tilde{T}(\Gamma_d - \tilde{\Gamma})} \end{aligned}$$

and using $T' = T - \tilde{T}$, we can write

$$\begin{aligned} T'^2 &= T^2 + \tilde{T}^2 - 2T\tilde{T} \\ \widetilde{T'^2} &= \widetilde{T^2} - \tilde{T}^2 \end{aligned}$$

giving

$$\begin{aligned} APE &= \frac{c_p}{2} \int \frac{\Gamma_d}{(\Gamma_d - \tilde{\Gamma})} \frac{(T^2 - \tilde{T}^2)}{\tilde{T}} dm \\ APE &= \frac{c_p}{2} \int s(T^2 - \tilde{T}^2) dm \end{aligned}$$

where

$$s = s(p) = \frac{\Gamma_d}{\tilde{T}} \frac{1}{(\Gamma_d - \tilde{\Gamma})}$$

Work with eddies defined w.r.t. zonal mean

For kinetic energy, $K = K_M + K_E$, where

$$\begin{aligned} K_M &= \frac{1}{2} \int \left([u]^2 + [v]^2\right) dm \\ K_E &= \frac{1}{2} \int \left[u^{*2} + v^{*2}\right] dm \end{aligned}$$

For available potential energy,

$$\big[T^2\big] = \big[T\big]^2 + \big[T^{*2}\big] \rightarrow APE = APE_M + APE_E$$

$$\rightarrow APE_M = \frac{c_p}{2}\int s\big([T]^2 - \tilde{T}^2\big)dm$$
$$APE_E = \frac{c_p}{2}\int s\big[T^{*2}\big]dm$$

6.4.1 Aside: incompressible limit of ideal gas

In the incompressible limit, the sound speed $\rightarrow \infty$. Thus

$$\frac{c_p}{c_v} \rightarrow \infty$$
$$1 + \frac{R}{c_v} \rightarrow \infty$$
$$\kappa = \frac{R}{c_p} = \frac{R}{c_v + R} = \frac{1}{\frac{c_v}{R} + 1} \rightarrow 1$$
$$\theta = T\Big(\frac{p_{00}}{p}\Big)^{\kappa} \sim \frac{1}{\rho} \text{ is conserved}$$
$$APE = \frac{c_p}{g(1+\kappa)p_{00}^{\kappa}}\int_0^{\infty} \widetilde{p^{(\kappa+1)}} - \tilde{p}^{(\kappa+1)}d\theta$$
$$APE = \frac{c_p}{2gp_{00}}\int_0^{\infty}\big(\widetilde{p^2} - \tilde{p}^2\big)d\theta$$

So in the incompressible limit, APE can be expressed as a variance without the need to make an approximation. For the ocean, one can express APE in terms of variance of height in density surfaces, or density on height surfaces.

6.4.2 Time evolution of kinetic and available potential energy

Now we will derive the equations governing the evolution of mean and eddy kinetic and available potential energy. Begin by considering a generic variable A.

$$\frac{\partial A}{\partial t} = -\underline{v}\cdot\nabla A - \omega\frac{\partial A}{\partial p} + s$$
$$A = [A] + A^*$$
$$\frac{\partial [A]}{\partial t} = -\big[\underline{v}\cdot\nabla A\big] - \big[\omega\frac{\partial A}{\partial p}\big] + [s]$$

Multiply by $[A]$:

$$\frac{1}{2}\frac{\partial}{\partial t}[A]^2 = -[A]\big[\underline{v}\cdot\nabla A\big] - [A]\big[\omega\frac{\partial A}{\partial p}\big] + [A][s]$$

Expand the advective terms

$$\big[\underline{v}\cdot\nabla A\big] = [\underline{v}]\cdot\nabla[A] + \big[v^*\cdot\nabla A^*\big] \text{ etc.}$$

to get

$$\frac{1}{2}\frac{\partial}{\partial t}[A]^2 = -\frac{1}{2}[\underline{v}]\cdot\nabla[A]^2 - \frac{1}{2}[A]\big[\underline{v}^*\cdot\nabla A^*\big] - \frac{1}{2}[\omega]\frac{\partial[A]^2}{\partial p} - [A]\big[\omega^*\frac{\partial A^*}{\partial p}\big] + [A][s]$$

Now use continuity

$$\nabla\cdot\underline{v} + \frac{\partial\omega}{\partial p} = 0$$
$$\nabla\cdot\underline{v}^* + \frac{\partial\omega^*}{\partial p} = 0$$
$$\nabla\cdot[\underline{v}] + \frac{\partial[\omega]}{\partial p} = 0$$

$$\begin{aligned}\frac{1}{2}\frac{\partial}{\partial t}[A]^2 = &-\frac{1}{2}\frac{1}{R\cos\phi}\frac{\partial}{\partial\phi}\Big([v][A]^2\cos\phi\Big) - \frac{1}{2}\frac{\partial}{\partial p}\Big([\omega][A]^2\Big)\\ &+ [A][s] - [A]\frac{1}{R\cos\phi}\frac{\partial}{\partial\phi}\Big[v^*A^*\cos\phi\Big] - [A]\frac{\partial}{\partial p}\big[\omega^*A^*\big]\end{aligned}$$

or

$$\begin{aligned}\frac{1}{2}\frac{\partial}{\partial t}[A]^2 = &-\frac{\partial\big([v]\frac{1}{2}[A]^2\cos\phi\big)}{R\cos\phi\partial\phi} - \frac{\partial}{\partial p}\Big([\omega]\frac{1}{2}[A]^2\Big) && \textit{flux divergence terms}\\ &+ [A][s] && \textit{source / sink term}\\ &- \frac{\partial\big([v^*A^*][A]\cos\phi\big)}{R\cos\phi\partial\phi} - \frac{\partial}{\partial p}\Big(\big[\omega^*A^*\big][A]\Big) && \textit{flux divergence terms}\\ &+ \big[v^*A^*\big]\frac{\partial[A]}{R\partial\phi} + \big[\omega^*A^*\big]\frac{\partial[A]}{\partial p} && \textit{conversion from eddy to mean}\end{aligned}$$

and note that all the flux divergence terms vanish in the global integral.

Similarly, multiply $\partial A/\partial t$ equation by A^*:

$$\begin{aligned}A^*\frac{\partial A}{\partial t} &= -\underline{v}A^*\cdot\nabla A - \omega A^*\frac{\partial A}{\partial p} + A^*s\\ &= -\underline{v}A^*\cdot\nabla[A] - \omega A^*\frac{\partial[A]}{\partial p} + A^*s - \underline{v}A^*\cdot\nabla A^* - \omega A^*\frac{\partial A^*}{\partial p}\end{aligned}$$

Now take the zonal average

$$\begin{aligned}\Big[A^*\frac{\partial A^*}{\partial t}\Big] = &-\big[v^*A^*\big]\frac{\partial[A]}{R\partial\phi} - \big[\omega^*A^*\big]\frac{\partial[A]}{\partial p} + \big[A^*s^*\big]\\ &- \big[\underline{v}\cdot\nabla\frac{1}{2}A^{*2}\big] - \Big[\omega\frac{\partial}{\partial p}\big(\frac{1}{2}A^{*2}\big)\Big]\end{aligned}$$

or using the continuity equation

$$\begin{aligned}\frac{\partial}{\partial t}\frac{1}{2}\big[A^{*2}\big] = &-\frac{1}{R\cos\phi}\frac{\partial}{\partial\phi}\big[v\frac{1}{2}A^{*2}\cos\phi\big] - \frac{\partial}{\partial p}\big[\omega\frac{1}{2}A^{*2}\big] && \textit{flux divergence terms}\\ &+\big[A^{*}s^{*}\big] && \textit{source / sink term}\\ &-\big[v^{*}A^{*}\big]\frac{\partial[A]}{R\partial\phi} - \big[\omega^{*}A^{*}\big]\frac{\partial[A]}{\partial p} && \textit{conversion from mean to eddy}\end{aligned}$$

Apply this approach to quadratic quantities – kinetic energy $K = K_M + K_E$ and available potential energy $P = P_M + P_E$ (use P instead of APE for brevity).

We will integrate over the mass of the atmosphere and disregard boundary terms.

From the momentum equations:

$$\begin{aligned}\frac{\partial}{\partial t}K_M = C\big(P_M, K_M\big) + C\big(K_E, K_M\big) - D\big(K_M\big)\\ C\big(A, B\big) : \text{conversion from A to B}\\ D\big(K_M\big) : \text{dissipation of } K_M\end{aligned}$$

In particular,

$$\begin{aligned}C\big(P_M, K_M\big) &= -\int [\omega][\alpha]dm\\ &= -\int [v]g\frac{\partial[Z]}{R\partial\phi}dm\end{aligned}$$

which says that kinetic energy in zonal-mean flows can be generated by mean meridional motion down the meridional pressure gradient, or symmetric circulations involving the rising of less dense air and the sinking of dense air.

$$\begin{aligned}D\big(K_M\big) &= -\int \big([u][F_\lambda] + [v][F_\phi]\big)dm\\ C\big(K_E, K_M\big) &= \int [v^{*}u^{*}]\cos\phi\frac{\partial}{\partial\phi}\frac{[u]}{R\cos\phi}dm\\ &\quad + \int [\omega^{*}u^{*}]\frac{\partial[u]}{\partial p}dm\\ &\quad + \int [v^{*2}]\frac{\partial[v]}{R\partial\phi}dm - \int [v]\frac{\tan\phi}{R}[u^{*2}]dm\\ &\quad + \int [\omega^{*}v^{*}]\frac{\partial[v]}{\partial p}dm\end{aligned}$$

→ Conversion from eddy to mean when transports of momentum (vertical and meridional) are *up gradient*.

In general, up-gradient fluxes remove eddy variance and strengthen the mean gradient while down-gradient fluxes (e.g. diffusive fluxes) generate eddy variance and weaken the mean gradient.

For the eddy kinetic energy K_E

$$\begin{aligned}\frac{\partial K_E}{\partial t} =& C\big(P_E, K_E\big) - C\big(K_E, K_M\big) - D\big(K_E\big)\\ C\big(P_E, K_E\big) =& -\int [\omega^* \alpha^*] dm\\ D\big(K_E\big) =& -\int \big[u^* F_\lambda^*\big] dm - \int \big[v^* F_\phi^*\big] dm\end{aligned}$$

→ Positive conversion from P_E to K_E when vertical wind anomalies along a latitude circle are correlated with density anomalies, such that light air rises and dense air sinks.

For the mean available potential energy

$$P_M = \frac{c_p}{2} \int s\big([T]^2 - \tilde{T}^2\big) dm$$

Begin with

$$\frac{\partial T}{\partial t} = -\underline{v} \cdot \nabla T - \omega \frac{T}{\theta} \frac{\partial \theta}{\partial p} + \frac{Q}{c_p}$$

and multiply by $c_p s\big([T] - \tilde{T}\big)$, then integrate over the domain.

$$\begin{aligned}\frac{\partial P_M}{\partial t} =& G\big(P_M\big) - C\big(P_M, P_E\big) - C\big(P_M, K_M\big)\\ G\big(P_M\big) =& \int s\big([T] - \tilde{T}\big)\big([Q] - \tilde{Q}\big) dm\end{aligned}$$

→ Generation of P_M by heating of warm air and cooling of cold air (e.g. high vs. low latitudes)

$$\begin{aligned}C\big(P_M, P_E\big) =& -c_p \int s\big[v^* T^*\big] \frac{\partial [T]}{R \partial \phi} dm\\ & - c_p \int p^{-\kappa} \big[\omega^* T^*\big] \frac{\partial}{\partial p} \Big(s p^\kappa \big([T] - \tilde{T}\big)\Big) dm\end{aligned}$$

→ Conversion from mean to eddy APE by poleward or upward heat transport down the mean temperature gradients.

An equation for P_E can also be derived by multiplying $\partial T / \partial y$ by $c_p s T^*$ and averaging. We'll skip straight to the answer:

$$\begin{aligned}\frac{\partial P_E}{\partial t} =& G\big(P_E\big) + C\big(P_M, P_E\big) - C\big(P_E, K_E\big)\\ G\big(P_E\big) =& \int s\big[T^* Q^*\big] dm\end{aligned}$$

→ generation by heating anomalies and temperature anomalies that are correlated along a latitude circle. Such heating could be radiative damping or latent heating.

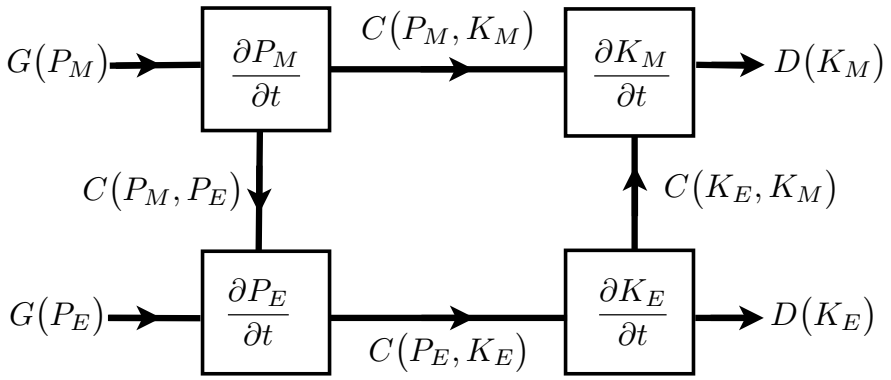

Figure 6.3: Schematic of the Lorenz energy cycle.

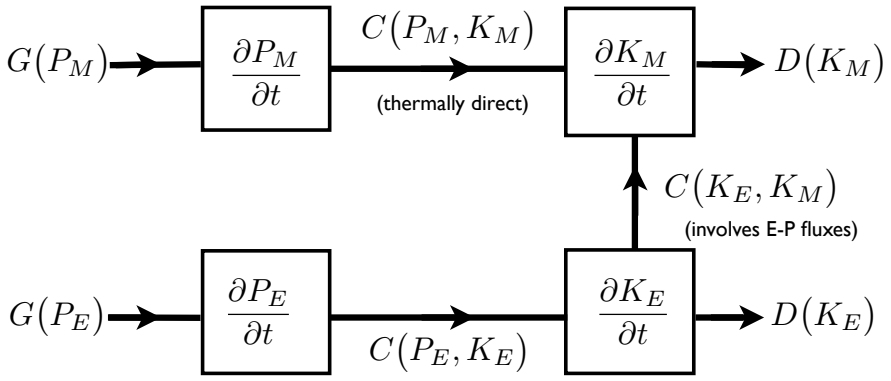

Figure 6.4: Lorenz energy cycle in TEM (Plumb, 1983).

These results are summarized schematically in Fig. 6.3 (see also Peixoto and Oort 14.3). Note the connection to the heat engine concept: generation of $P_M + P_E$ requires heating of warm regions and cooling of cold regions.

The interpretation depends on one's choice of mean. For TEM, one finds a different picture, shown in Fig. 6.4 (Plumb, 1983) (note K_E, K_M, P_E, P_M definitions unchanged in Plumb analysis).

In QG we have

$$\frac{\partial [u]}{\partial t} = f[v] - \frac{1}{R\cos^2\phi}\frac{\partial}{\partial \phi}\left([u^* v^*]\cos^2\phi\right)$$
$$\frac{\partial [\theta]}{\partial t} = -[\omega]\frac{\partial \theta_s}{\partial p} - \frac{1}{R\cos\phi}$$

while in TEM

$$\frac{\partial [u]}{\partial t} = f\tilde{v} + \frac{1}{R\cos\phi}\nabla \cdot F$$
$$\frac{\partial [\phi]}{\partial t} = -\tilde{\omega}\frac{\partial \theta_s}{\partial p}$$

In this form, K_E to K_M is now proportional to $[u]\nabla \cdot F$ (where F is the Eliassen-Palm flux vector).

6.5 Observed energy cycle

We will refer to several figures from Peixoto and Oort (1992)

6.5.1 Fig. 14.4: Contributions to APE and KE vs. latitude

- Since APE is not defined locally, these must be interpreted with caution
- The APE curves using annual statistics are not very meaningful as they include the seasonal cycle
- Higher P_M in S.H. due to larger pole-to-equation temperature difference.

6.5.2 Fig. 14.6: Contributions to energy conversions vs. latitude

- Other than the seasonal cycles, both the hemispheres are similar
- $C\big(P_M, P_E\big)$ is generally positive and peaks in midlatitudes where the meridional temperature gradient and poleward heat flux are maximum
- $C\big(K_E, K_M\big)$ is generally positive – eddy fluxes of momentum act to maintain the jet structure
- $C\big(P_M, K_M\big)$ is positive for the thermally direct Hadley cells and negative for the thermally indirect Ferrel cells.

6.5.3 Horizontal spectral distributions of energy conversions

Can also look at spectral energy budgets for each spherical wavenumber n.
See Fig.1 and Fig. 6b from Koshyk and Hamilton (2001).

- From a high resolution GCM (smallest length scale $\sim$ 35 km
- Nonlinear advection transfer from medium wavenumbers to high and low wavenumbers
- Conversion from PE to KE important at all scales
- Dissipation important at all scales
- $\rightarrow$ simple inertial range picture inapplicable!

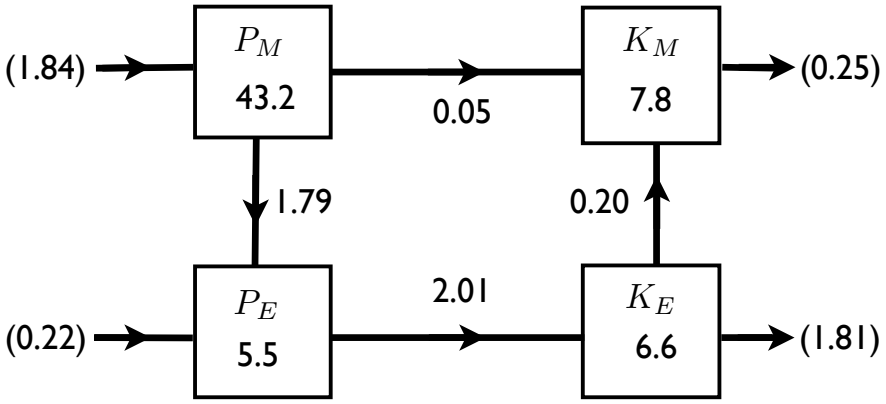

Figure 6.5: Observed global energy cycle. Units are W m^{-2} (conversions) and 10^5 J m^{-2} (reservoirs). G and D values are residuals, all other quantities are calculated directly. Computed from ERA40 data by Li et al. (2007).

6.5.4 Global energy cycle

An estimate of the global energy cycle is shown in Fig. 6.5, based on Li et al. (2007) – from ERA40 data.

We can now describe the energy cycle of the atmosphere:

1. Radiative heating and cooling maintain a largely zonally symmetric north-south gradient of temperature in each hemisphere
   - $G\big(P_M\big) = 1.84$ W/m^2
2. Midlatitude eddies deform the zonal symmetry and generate eddy variance
   - $C\big(P_M, P_E\big) = 1.79$ W/m^2
   - the dominant (QG) contribution is $\big[v^*T^*\big]\frac{\partial T}{\partial \phi}$
3. Through mechanisms such as baroclinic instability and convection, some of the P_E is converted to kinetic energy of disturbances
   - $C\big(P_E, K_E\big) = 2.01$ W/m^2
   - note subgrid contribution not included in Li et al. analysis, Steinheimer et al. (2008) suggest 50% more conversion globally from convection scheme $\big([\omega^*\alpha^*]\big)$.
4. Eddies transport momentum and convert K_E to K_M
   - $C\big(K_E, K_M\big) = 0.2$ W/m^2
   - $\big[v^*u^*\big]\frac{\partial}{\partial \phi}\Big(\frac{[u]}{R\cos\phi}\Big)$
5. Mean meridional circulations convert between P_M and K_E. Positive conversion in Tropics (Hadley cells), negative in midlatitudes (Ferrel cells). Net is small and positive.

- $C\big(P_M, K_E\big) = 0.05$ W/m^2
- (Peixoto and Oort found -0.15 W/m^2)

6. Kinetic energy of eddies is dissipated in boundary layer and by a cascade to small scale turbulence (c.f. spectral discussion earlier)
   - 1.81 W/m^2
   - (most of conversion $C\big(P_E, K_E\big) = 2.01$ W/m^2)
7. Some of the kinetic energy of zonal mean flow dissipated (primarily near surface)
   - 0.25 W/m^2
   - (small fraction actually goes into ocean circulation)

In summary:

- Total $KE \sim 14 \times 10^5$ J/m^2
- Total dissipation ~ 2 W/m^2
- $\rightarrow$ timescale $\sim \frac{1.4\times10^6}{2}$ s $\sim 10^6$ s ~ 10 days

6.5.5 Table 14.1, Peixoto and Oort

- Ratio of KE to $KE + APE$ roughly constant, $\sim 20\%$
  - use to understand changes with climate change?
- Rough equipartition between K_E and P_E.
- Efficiency of heat engine (taking the absorbed incoming solar radiation as 240 W/m^2):

$$\frac{2 \text{ W/m}^2}{240 \text{ W/m}^2} \sim 1\%$$

- APE and KE higher in winter, also dissipation and conversion, but generation of APE bigger in summer.

7 Entropy budget of the atmosphere

The 2nd law says

$$\Delta s = \frac{Q_{ext}}{T} + \Delta s_{irr} \qquad\qquad \Delta s_{irr} \geq 0$$

with Q_{ext} the external heating, and $s = c_p \log\theta +$ const, a state variable.

For the Earth system as a whole, the external heating is purely radiative. Solar radiation peaks at wavelength $\lambda \simeq 0.5$ μm (shortwave), corresponding to a temperature of $T \sim 5760$ K. On the other hand, terrestrial radiation is emitted at temperature $T \sim 250$ K, corresponding to a wavelength of $\lambda \simeq 10\mu$m (longwave).[1]

The Earth thus receives radiation low in entropy and emits radiation high in entropy. This implies than the Earth system generates entropy by irreversible processes.

The simplest analysis views dry atmosphere as acted on by external heating (e.g. latent heating, radiative heating).

In the Energetics sections we defined the heating rate

$$Q_h = -\frac{1}{\rho}\Big(\nabla \cdot \underline{F}_{rad} + \nabla \cdot \underline{J}^D_H\Big) - L(e-c)$$

Regard this as external.

Frictional dissipation is irreversible work, with associated entropy generation Q_f/T. Recall that

$$Q_f = -\frac{1}{\rho}\underline{\underline{\tau}} : \nabla \times \underline{c}$$

Key point: in long-term mean, atmosphere does not accumulate entropy (remember that entropy is a state variable).

$$\int_V \rho \overline{\frac{ds}{dt}} dV = 0$$

which implies that

$$\int_V \rho \overline{\frac{Q_h + Q_f}{T}} dV = 0$$

But $Q_f \geq 0$ and $rho, T > 0$, so

$$\int_V \overline{\frac{\rho Q_h}{T}} dV \leq 0$$

[1] These values can be computed using Wien's law $\lambda_{max} = \frac{b}{T}$, where λ_{max} is the wavelength of peak blackbody intensity, and $b = 2.9 \times 10^{-3}$ m K^{-1}.

So Q_h and T must have positive correlation.

Thus we must heat warm areas and cool cold areas in order to do work and have dissipation. This is the same conclusion we reached from APE analysis.

Note in long-term mean

$$\int_V \overline{\rho Q_h} dV \simeq 0$$

(energy balance)

Can make more nuanced analysis by only taking sensible heating as external at the boundaries. Take the example of diffusive (sensible) heat flux $\underline{J}_H^D$.

$$\rho \frac{ds}{dt} = -\frac{\nabla \cdot \underline{J}_H^D}{T} + ...$$

$$\begin{aligned}
\frac{\partial}{\partial t} \int_V \rho s dV &= -\int_V \frac{1}{T} \nabla \cdot \underline{J}_H^D dV + ... \\
&= -\int_V \nabla \cdot \Big(\frac{1}{T} \underline{J}_H^D \Big) dV - \int_V \frac{1}{T^2} \underline{J}_H^D \cdot \nabla T dV \\
&= -\int_S \frac{1}{T} \underline{J}_H^D \cdot \underline{n} dS - \int_V \frac{1}{T^2} \mathcal{J}_H^D \cdot \nabla T dV
\end{aligned}$$

where the first term is transport of entropy into the atmosphere, and the second term represents internal generation.

For a diffusive heat flux

$$\underline{J}_H^D = -K \nabla T$$

we can write

$$-\int_V \frac{1}{T^2} \mathcal{J}_H^D \cdot \nabla T dV = \int_V \frac{K}{T^2} \big(\nabla T \big)^2 dV \geq 0$$

As expected, diffusion of heat in the atmosphere leads to entropy production.

Can also try to evaluate entropy budget of atmosphere as a control volume. It is difficult to correctly treat the radiative fluxes. Peixoto and Oort treat entropy fluxes as (energy flux / T), and entropy production associated with irreversible absorption of radiation as

$$\Big(-\frac{\nabla \cdot F_{rad}}{T_{rad}} + \frac{\nabla \cdot F_{rad}}{T_{air}} \Big)$$

Characteristic temperatures are also assigned to each term. Results roughly consistent with balance between entropy production in the atmosphere and net flux out of atmosphere. (Note that latent heating is viewed as external heating).

See Fig. 15.2 in Peixoto and Oort (1992).

8 Hydrological cycle

The hydrological cycle is critical for energy transport, cloud and water vapor radiative effects, influences ocean circulation, agriculture, groundwater supplies, etc.

8.1 Basics

8.1.1 Some definitions

$$
\begin{aligned}
q &= \text{specific humidity} = \frac{\text{mass vapor}}{\text{total mass}} \\
q &= \frac{\epsilon e}{p - (1-\epsilon)e} \\
\epsilon &= \frac{R_d}{R_v} = \frac{m_v}{m_d} \simeq 0.622 \\
e &= \text{vapor pressure}
\end{aligned}
$$

where m_v, m_d are molecular weights of vapor and dry air. (Note also $R_d \simeq 287$ J/kg/K).

8.1.2 Clausius-Clapeyron relation

Relates saturation vapor pressure to temperature. Approximately,

$$
e_s \simeq e_o \exp\Big(-\frac{\epsilon L}{R_d}(\frac{1}{T} - \frac{1}{T_0})\Big)
$$

where

$$
\begin{aligned}
e_0 &= 611\text{Pa} \\
T_0 &= 273\text{K} \\
\frac{\epsilon L}{R_d} &= 5420\text{K}
\end{aligned}
$$

To gain intuition, let $T = 288\text{K} + T'$. Thus

$$\begin{aligned} q_s &\simeq \frac{\text{constant}}{p} \exp\Big(- \frac{5420}{288 + T'}\Big) \\ &\simeq \frac{\text{constant}}{p} \exp\Big(- \frac{5420}{288}(1 - \frac{T'}{288})\Big) \\ &\simeq \frac{\text{constant}}{p} \exp\big(0.065 T'\big) \end{aligned}$$

So taking $T' = \pm 11$ K implies a doubling or halving of q_s. (Recall $\log 2 = 0.69$, and $\frac{1}{q_s}\frac{\partial q_s}{\partial T}$ increases with decreasing temperatures).

Thus, temperature variations are more important than pressure variations for specific humidity, and q_s falls off quickly with height and latitude.

Now calculate a scale height for q near the surface:

If $T' = -\Gamma z$ and $\Gamma = 5$ K/km, then

$$q_s \sim \exp\Big(- \frac{z}{H}\Big) \sim \exp\Big(\frac{T'}{\Gamma H}\Big)$$

$$\Rightarrow \frac{1}{\Gamma H} = 0.065$$

$$\Rightarrow H = \frac{1}{\Gamma 0.065} \simeq \frac{1}{0.065 \times 5\text{km}^{-1}} \simeq 3\text{km}$$

Review the zonal mean plots of specific and relative humidity from earlier in the course (ERA40). Recall relative humidity is defined

$$r = \frac{e}{e_s}$$

8.1.3 Some global values

Will derive water budgets for the atmosphere, and then discuss the 'temperature of last saturation' approach to understanding mean relative humidity distributions.

But first a few numbers to improve intuition on the atmospheric water cycle:

1. Global-mean precipitable water vapor (column integral of water vapor) = 25 kg/m^2, whereas for liquid water and ice in the atmosphere $\simeq 0.1$ kg/m^2 (Trenberth and Smith, 2005). We thus don't expect horizontal fluxes of condensate to be important on large scales.

2. Global-mean precipitation ~ 1 m/year.

$$\Rightarrow \text{residence time} = \frac{\text{water vapor}}{\text{precip. rate}} = \frac{\frac{25}{1000}\text{m}}{\frac{1\text{m}}{365\text{ days}}} = \frac{25\text{mm}}{2.7\text{mm/day}} \sim 10 \text{ days}$$

So water vapor is cycled through the atmosphere every 10 days or so.

3. Amount of water vapor in column of atmosphere:

$$\sim \frac{25\text{kg/m}^2}{\rho = 1000\text{kg/m}^3} \sim 25 \text{ mm} \sim 1 \text{ inch}$$

(e.g. for midlatitudes), and storms convert only a fraction of this precipitation (<30%) (see Trenberth 2003) [WHAT IS THIS SUPPOSED TO REFERENCE??].

But it often rains much more than this in a day (conditional rain rate $\sim$ 45 mm/day). Evaporation $\sim$ mean precip. $\sim$ 2.7 mm/day. So source of moisture for precipitation is not primarily evaporation during a storm, but rather nonlocal water vapor in the atmosphere. Also it doesn't rain very often (but this depends on threshold and spatial scale).

The record daily rain rate is 1825 mm/day (in one day – roughly 70 inches) at La Reunion Island off Madagascar (1966).

See Fig. 12.2 in Peixoto and Oort, an overview of reservoirs and fluxes between land, ocean and atmosphere.

Before turning to the atmosphere, consider water balance on land:

$$S = P - E - R_o - R_u$$

where S is the rate of storage, E is evapotranspiration (and sublimation over ice), R_o is surface runoff, and R_u is subterranean runoff.

For long times ($\overline{S} = 0$) and large regions ($\overline{R_u} = 0$),

$$\overline{P} - \overline{E} = \overline{R_o}$$

In the atmosphere, precipitable water is

$$W(\lambda, \phi, t) = \int_0^{p_0} \frac{dp}{g} q$$

Conservation of water gives

$$\frac{\partial q}{\partial t} + \nabla \cdot \left(q \underline{v}\right) + \frac{\partial q_w}{\partial p} = s(q) + D$$

with

$$s = e - c$$

$$D = -\alpha \nabla \cdot J_q^D \simeq -\alpha \frac{\partial}{\partial z} J_{qz}^D$$

Similarly for condensate

$$\frac{\partial q_c}{\partial t} + \nabla \cdot \left(q_c \underline{v}_c\right) + \frac{\partial q_c}{\partial p} \omega_c = -(e - c)$$

where $\underline{v}_c$ and ω_c are suitable net velocities of the condensate (this implies some kind of bulk description for the droplets or ice particles).

Adding the equations,

$$\frac{\partial}{\partial t}\big(q + q_c\big) + \nabla \cdot \big(q_c \underline{v}_c + q\underline{v}\big) + \frac{\partial}{\partial p}\big(q_c\omega_c + q\omega\big) = D$$

Integrating vertically yields

$$\frac{\partial}{\partial t}\big(W + W_c\big) + \nabla \cdot \big(\underline{Q} + \underline{Q}_c\big) = E - P$$

with terms defined as

$$W_c = \int_0^{p_0} q_c \frac{dp}{g} \qquad P = \omega_c q_c\big|_{sfc}$$
$$\underline{Q} = \int_0^{p_0} q\underline{v} \frac{dp}{g} \qquad E = J^D_{qz}\big|_{sfc}$$
$$\underline{Q}_c = \int_0^{p_0} q_c \underline{v} \frac{dp}{g}$$

But

$$\frac{\partial W_c}{\partial t} \ll \frac{\partial W}{\partial t}$$

and

$$\underline{Q}_c \ll \underline{Q}$$

so that

$$\frac{\partial \overline{W}}{\partial t} + \nabla \cdot \overline{Q} = \overline{E} - \overline{P}$$

We can also link to the terrestrial budget for long times and large regions

$$\overline{R_o} = -\nabla \cdot \overline{Q}$$

(i.e., the runoff balances the convergence of atmospheric water vapor fluxes).

Averaging zonally (and in time) yields

$$\frac{\partial}{\partial t}[\overline{W}] + \frac{1}{R\cos\phi}\frac{\partial}{\partial \phi}\Big([\overline{Q}_\phi]\cos\phi\Big) = [\overline{E} - \overline{P}]$$

and

$$[\overline{Q}_\phi] = \frac{1}{g}\int dp\Big([\overline{q}][\overline{v}] + [\overline{q}^*\overline{v}^*] + [\overline{q'v'}]\Big)$$

But we often care about zonal fluxes of water vapor since they contribute to regional convergence and divergence.

8.2 Observed vapor transport

Refer to figures in Peixoto and Oort (1992).

8.2.1 Fig. 12.7 and 12.9: Vertically integrated zonal transport of water vapor

These largely follow the circulation near the surface, but note the structure of the transient eddy fluxes (often associated with land-ocean contrast ⇒ dry winds from land vs. moist winds from the ocean).

8.2.2 Fig. 12.10, 12.11: Meridional flux of water vapor

- Transient meridional flux is generally poleward and intensified in the midlatitude storm tracks.
- In contrast to the zonal flux, the transient eddy flux is a major component of the total meridional flux.
- The flux associated with the mean circulation is strongly equatorward in the tropics in the annual mean. The upper branches of the Hadley cells contribute little.

8.2.3 Fig. 12.12: Seasonality of meridional water vapor fluxes

- Strong seasonal cycle associated with the mean meridional circulation in the tropics. There is a much smaller seasonal cycle in the midlatitudes, which are dominated by the transient flux.
- In long term, atmospheric fluxes must be balanced by opposite flows in the oceans and rivers.

8.2.4 Fig. 12.14: Vertical flux of water vapor (and condensate)

- The flux associated with the mean meridional circulation is upward in the ascending branch of the Hadley cell and downward in the subtropics (as expected).
- Stationary eddies transport water vapor upwards (as do transient eddies – see next plot).
- The total and transient fluxes include condensate transport (calculated as a residual – and the transient fluxes include convection).
- Eddy and mean fluxes oppose each other in the subtropics

8.2.5 Streamfunction for water vapor and condensate

Neglecting horizontal transport of condensate and taking the time and zonal mean,

$$\frac{1}{R\cos\phi}\frac{\partial}{\partial\phi}\Big([\overline{qv}]\cos\phi\Big)+\frac{\partial}{\partial p}\Big[\overline{q\omega}+\overline{q_c\omega_c}\Big]=0$$

whence we define a streamfunction ψ_q through the relations

$$\frac{\partial \psi_q}{\partial p} = \frac{2\pi R}{g} \cos\phi[\overline{qv}]$$
$$-\frac{1}{R}\frac{\partial \psi_q}{\partial \phi} = \frac{2\pi R}{g} \cos\phi\left[\overline{q\omega} + \overline{q_c\omega_c}\right]$$

Contours of ψ_q are plotted in Fig. 12.18:

- Water vapor primarily circulates in the lower troposphere
- Streamlines leaving the surface $\Rightarrow E > P$
- Streamlines entering the surface $\Rightarrow P > E$
- Low-level circulations in the tropics feed the ITCZ (although some water leaving the winter subtropics is fluxed to the summer midlatitudes).

8.2.6 Distribution of $E - P = \nabla \cdot \overline{Q}$

Fig. 12.16: Zonal-mean $E - P$

- Net divergence in subtropics, intensifies in winter (due to cross-equatorial Hadley cells)
- Net convergence in equatorial and mid- to high latitudes.

ERA40: $E - P$ vs. lat. and lon.

See Fig. 8.1

- Convergence and divergence generally stronger over oceans than land.
- Convergence over land often associated with drainage basins of large rivers.
- Divergence in subtropics coincide with arid regions, e.g. Sahara, Gobi (China), Kalahari (southern region of Africa), Arabian, Great Australian, etc.
- Matching patterns in surface salinity in ocean
- Sometimes divergence over land – either implies error or surface and underground flow.

8.2.7 Fig. 12.7: Streamlines vs. lat. and lon. of the water vapor flux

DJF shown. In JJA get bigger flux from gulf into North America.

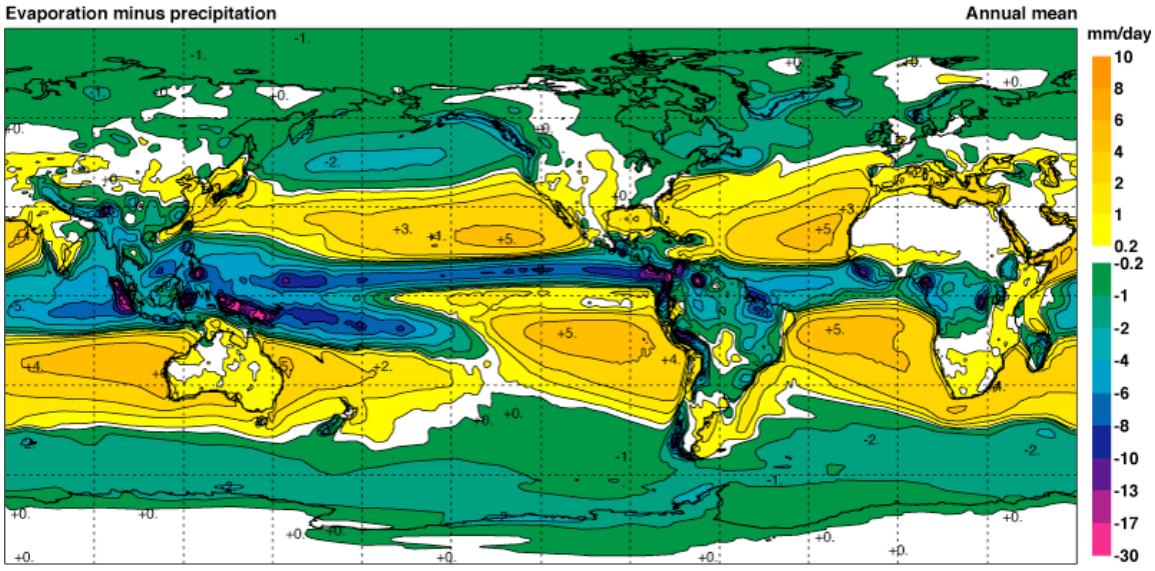

Figure 8.1: Annual mean evaporation minus precipitation in mm / day. Source: ERA-40 atlas.

8.3 Estimates of precipitation and evaporation rates

8.3.1 Precipitation

- Estimation of precipitation globally is a difficult task.
- Precipitation is intermittent in space and time (little correlation for distances > 100 km).
- In situ measurement of precip. over ocean is difficult. Coastal and island measurements are not very representative, and different rates are generally observed when ship data are available. (Ships and buoys gives estimates).

Figure 4 from Béranger et al. (2006) shows a comparison of different datasets over the ocean. Note, although the maximum is located at the same latitude, there is a fairly big range of values, with the two reanalysis estimates giving the highest (ERA15) and one of the lowest values (NCEP), a discrepancy of $\sim$30%.

Reanalysis does not assimilate precipitation observations (although, e.g. ERA40 does assimilate water vapor measurements from satellites). Thus, precipitation in reanalysis can be viewed as the model forecast from the previous analysis time 6 hours earlier. This will depend on the convective and large-scale precipitation parameterizations used in the model.

Figure 2 from Andersson et al. (2005) shows that in the ECMWF operational forecasting system the initial tropical precipitation is too large, reducing to a different value after 12-24 hours. This leads to too low a relative humidity after day 1 and day 5 compared with a verifying analysis, and the additional latent heating leads to too strong a Hadley cell after day 1.

The alternative is to use satellite measurements of microwave and infrared emissions to infer rain rates. The data are calibrated (e.g. trained using a neural net) against ground-based radar and gauge measurements. Note that these methods often do not measure precipitation directly – passive microwave can be emission based (cloud liquid water) or scattering (scattering of surface emissions by large ice particles). IR brightness temperatures are related to the existence and top-altitude of clouds. In general these physical properties should be regarded as only statistically related to the precipitation rate.

Fig. 1 of Adler et al. (2003) shows the GPCP algorithm, and Fig. 4 shows the long-term mean. GPCP is a merged product of several types of satellite data and in-situ observations. The figure from OCW compares the zonal-mean of GPCP with older (ground and ship based) estimates – there is reasonable agreement. Figs. 14 and 15 from Adler et al. (2003) compare the GPCP final product with independent rain-gauge measurements. For the comparison with Pacific atolls there is a large bias, but this may also be due to the non-representativeness of atoll precip. for a GPCP grid box.

8.3.2 Evaporation

Direct measurements of evaporation are sparse and insufficient to create a climatology (using pans to measure evaporation is also difficult). Over ocean, evaporation rates are estimated using a bulk aerodynamic formalism. (Similar formulae can be written for the surface sensible heat and momentum fluxes).

Bulk aerodynamic formula for evaporation

$$E = -\rho C_w |\underline{v}(z)| \big(q(z) - q(0)\big)$$

with C_w an empirical transfer coefficient that depends on wind (shear), static stability.

- z is often taken as 10 m.
- In calm conditions ($|\underline{v}(z)|$ small), often add a 'gustiness factor' to $|\underline{v}(z)|$ to avoid C_w becoming large.
- Can try to estimate C_w based on theory of boundary layer turbulence.
- Often $-\big(q(z) - q(0)\big) \simeq (1 - r) q_s(0)$, so that near-surface relative humidity is very important (and tightly constrained by the surface energy budget).
- Over land this only gives an estimate of the *potential* evapotranspiration. The actual rate depends on soil moisture, plant activity, etc. $\Rightarrow$ need to rely on more complicated models (e.g. a land model or a reanalysis) or estimate from the energy budget at the surface, or measure runoff and precip., etc.

Estimate of evaporation rate from ERA40 reanalysis

THIS FIGURE IS MISSING!

Shown for the long-term mean vs. latitude and longitude. The highest values occur over the subtropical oceans. The effects of ocean boundary currents are also evident. The zonal-mean (P&O Fig. 7.27) reveals a local minimum near the equator, and greater rates in winter than summer. Both these features are related to the magnitudes of surface winds.

8.4 Note on surface energy budget

$$F_{rad}^{sfc} = F_{SH}^{\uparrow} + L_c E + F_G^{\downarrow} + L_M\big(M_s - F_s\big)$$

where

$$F_{SH}^{\uparrow} = -\rho c_p C_H |\underline{v}(z)|\big(\theta(z) - \theta(0)\big)$$
$$F_{rad}^{sfc} = F_{SW}^{\downarrow}(1 - A_{sfc}) - \epsilon\sigma T_{sfc}^4 + F_{LW}^{\downarrow}$$

and we have defined

$$F_G^{\downarrow} = \text{heat flux into subsurface layers}$$
$$L_M M_s = \text{energy used in melting snow or ice}$$
$$L_M F_s = \text{energy released by freezing water}$$

F_{SH} and E are strongly related to the surface winds, boundary layer stability and the land/ocean – air temperature difference.

8.5 Importance of upper-tropospheric water vapor

Radiative effects of water vapor provide a motivation to study the amount of water vapor in the upper troposphere (even though there is relatively little there).

Consider the change in OLR (R) for a given change in temperature δT_k in each layer of the atmosphere (keeping clouds, aerosols, etc. fixed)

$$\delta R = \sum_{k=1}^{N} \Big(\frac{\partial R}{\partial T_k}\delta T_k + \frac{\partial R}{\partial e_k}\delta e_k \Big)$$

where k indexes 100 hPa thick layers.

If constant relative humidity is assumed, then

$$\delta e = H\frac{de_s}{dT}\delta T$$

We therefore write

$$\delta R = \sum_{k=1}^{N} \Big(Q_T^k + Q_e^k \Big)\delta T$$

with

$$Q_T^k = \frac{\partial R}{\partial T_k} \qquad\qquad Q_e^k = \frac{\partial R}{\partial e_k} H \frac{de_s}{dT}$$

following Held and Soden (2000).

This allows us to compare water vapor and temperature effects in the same units ($\mathrm{W/m^2/K}$). For reference, a doubling of $CO_2 \simeq 4$ $\mathrm{W/m^2}$.

Held and Soden (2000) fig. 9 shows $Q_{e,T}^k$ based on temperature and humidity from ECMWF and cloud data from the International Satellite Cloud Climatology Project (ISCCP). Clouds are important – for clear sky conditions, low level temperatures are important in Q_T^k, but upper levels matter in cloudy conditions. Similarly, Q_e^k maximizes in the deep tropics if clouds are omitted. Mid- and upper-level water vapor is most important: this makes sense as emission near water vapor spectral lines comes primarily from upper levels. Upper levels also have a stronger greenhouse effect because they are colder.

Fig. 8 from Held and Soden (2000) shows some processes that may be important for the water vapor distribution. The phase changes of water mean that particular approaches are needed to understand the maintenance and control of the water vapor distribution. An example is offered in the following section.

8.6 Last-saturation analysis of the mean relative humidity field

Assume that evaporation of condensate is unimportant, and that the relative humidity is set to one following condensation. Then, when condensation is not occurring,

$$\frac{dq}{dt} = e - c = 0$$

(also neglecting diffusion). And when condensation occurs $q = q_s$.

Since q is conserved by an air parcel since its last saturation, then

$$\begin{aligned} q &= q_s\big(T_{\text{last sat.}}, p_{\text{last sat.}}\big) \\ &\simeq \frac{\epsilon e(T_{\text{last sat.}})}{p_{\text{last sat.}}} \end{aligned}$$

The relative humidity is given by

$$r = \frac{e}{e_s} \simeq \frac{q}{q_s} \simeq \frac{q_s\big(T_{\text{last sat.}}, p_{\text{last sat.}}\big)}{q_s(T,p)}$$

or using an approximate form for q_s

$$r \simeq \frac{e_s(T_{\text{last sat.}})p}{e_s(T)p_{\text{last sat.}}} \simeq \frac{p}{p_{\text{last sat.}}} \exp\left(-\frac{\epsilon L}{R_v}\Big(\frac{1}{T_{\text{last sat.}}} - \frac{1}{T}\Big)\right)$$

Thus, relative humidity will be much less than one if the temperature of last saturation is much lower than the current temperature.

Writing $T_{\text{last sat.}} = T - \Delta T$, we get

$$\exp\Big(-\frac{L}{R_v}\frac{1}{T}\Big(\frac{T}{T-\Delta T}-1\Big)\Big) = \exp\Big(-\frac{L}{R_vT}\Big(\frac{1}{1-\frac{\Delta T}{T}}-1\Big)\Big) = \exp\Big(-\frac{L}{R_vT^2}\Delta T\Big)$$

so that

$$r \simeq \frac{p}{p_{\text{last sat.}}}\exp\Big(-\frac{L}{R_vT^2}\Delta T\Big)$$

For a uniform global warming and no change in the distribution of where last saturation occurs, we find that relative humidity doesn't change as much as saturation vapor pressure:

$$\begin{aligned}\frac{\delta r}{r} &= \frac{2L_v}{R_vT^3}\Delta T\delta T\\ \frac{\delta e_s}{e_s} &= \frac{L_v}{R_vT^2}\delta T\\ \frac{\delta r}{r}\frac{e_s}{\delta e_s} &= \frac{2\Delta T}{T} \ll 1\end{aligned}$$

Some air parcels have not been saturated since they last left the boundary layer.

$$q = q_{\text{boundary layer}}$$

Galewsky et al. (2005) (and others) exploit this property to determine the controls on free-tropospheric relative humidity.

Divide global domain into sub-domains $\mathcal{D}_i, i = 1, ..., N$, and define corresponding tracers $\mathcal{T}_i(\phi, p, \lambda)$. The domains typically contain many grid-cells.

1. If saturation occurs in a grid cell we set

   $$\mathcal{T}_i(\phi, p, \lambda) = 1 \text{ and } \mathcal{T}_j(\phi, p, \lambda) = 0$$

   where the grid cell is in $\mathcal{D}_i$ and $j = 1, ..., N$ excluding $j = i$.

2. Otherwise advect tracers with vertical and horizontal winds.

3. If all air in a given grid-cell was saturated at least once then

   $$\sum_{i=1}^{N}\mathcal{T}_i = 1$$

This last point is not true since some air parcels not saturated since they left the surface. Define 'source tracer' S. In layer near surface, $S = q, \mathcal{T}_i = 0$.

Then, if have steady axisymmetric fields

$$q(\phi, p) \simeq \sum_{i=1}^{N}\mathcal{T}_i(\phi, p)q_{si} + S(\phi, p)$$

This is accurate so long as the sub-domains are not very large. (q_{si} is an average of q_s over the sub-domain).

For the general unsteady and asymmetric case replace all fields and tracers with their zonal and time means – introduces an error, but can check accuracy of reconstruction a posteori. (Galewski et al. do some further refinements of approach to improve accuracy).

Interpretation of $\mathcal{T}_i$: probability that air in grid cell was last saturated in sub-domain $\mathcal{D}_i$ (mixing and averaging mean each grid cell has contributions of air from many trajectories).

First apply to idealized GCM with dry dynamics and a moisture tracer that is advected and reset to saturation whenever advection would otherwise cause super-saturation. Evaporation is prescribed, no latent heating.

Fig. 2 shows zonal mean relative humidity, θ and Eulerian mean meridional streamfunction.

Fig. 3 shows $\mathcal{T}_i$ for 28 sub-domains. The sub-domains are evident as the rectangular areas with largest values in each case (the grid boxes most likely to be last saturated in a given sub-domain are in that sub-domain).

Interpretation:

- Air reaches saturation in adiabatic ascent.
- Deep tropical air remains saturated throughout its ascent.
- Descending air in subtropics last saturated at higher levels, but often swept poleward and upwards by midlatitude eddies which bring the air to saturation. This is made clear by the plumes along mean-isentropic surfaces.

Fig. 4 shows the pdf for location of last saturation for a reference point in the subtropics at low levels. The value in each sub-domain i are the value of $\mathcal{T}_i$ at the reference point. Last saturation was generally higher and poleward along isentropic surfaces (with a small contribution from cross-isentropic transport, although this analysis neglects the contribution of the source traces).

Fig. 5 shows the temperature at last saturation. This differs from the dewpoint depression as $p \neq p_{\text{last sat.}}$ and because of the source tracer. (The dewpoint is the temperature at which saturation is reached under isobaric cooling).

Fig. 7 shows the reconstruction of relative humidity is reasonably accurate.

The approach was also applied to observations using NCEP winds and temperatures and the MATCH (Model of Atmospheric Transport and Chemistry) for tracers and water vapor. MATCH's convective parameterization does not remove tracers during convection.

Assume saturation when relative humidity reaches 90%.

Fig. 9 shows the MATCH mean relative humidity and the reconstruction. Both have a minimum on subtropics at lower levels than in ERA40. The poor reconstruction at upper levels relates to not allowing convection to rain out water vapor.

Figs. 10 and 12 emphasize the role isentropic transports in setting subtropical relative humidity.

Fig. 11 shows the relative contributions of the isentropic extratropical path and the tropical subsidence path at 633 hPa and vs. lat. and lon.

8.7 Water vapor budget in isentropic coordinates

A different perspective on subtropical water vapor comes from analysis of the water vapor budget on dry isentropes in ERA40 reanalysis data. (see Schneider et al., 2006).

At the location of the minimum of relative humidity in the subtropics (Fig. 2), there is large isentropic eddy flux of water vapor from the tropics to the extratropics, but its divergence is small, and the main balance is between subsidence drying and subgrid (convective) moistening (the latter is only from certain longitudes) (Fig. 8).

9 Angular momentum of the atmosphere

9.1 Conservation of angular momentum

Consider a particle at position $\underline{r}$ in an interial frame. Angular momentum of the particle is defined as

$$\underline{M} = \underline{r} \times \underline{c}$$

and when acted on by a force $\underline{F}$, evolves according to

$$\frac{d\underline{M}}{dt} = \underline{r} \times \underline{F}$$

where $\underline{r} \times \underline{F}$ is the torque.

Let $\hat{\underline{n}}$ be the unit vector along the axis of rotation of the Earth, so that a parcel rotating with the Earth has velocity $\Omega(\hat{\underline{n}} \times \underline{r})$, and its total angular momentum about the axis of rotation is

$$\underline{M} = \underline{r} \times \Big(\Omega\big(\hat{\underline{n}} \times \underline{r}\big) + \underline{c}\Big)$$

(here $\underline{r}$ is the vector from the axis of rotation to the particle).

The component in the direction of $\hat{\underline{n}}$ is $\underline{M} \cdot \hat{\underline{n}}$, which we write as

$$M \equiv \underline{M} \cdot \hat{\underline{n}} = \Omega r^2 \cos^2\phi + ur\cos\phi$$

where $u = r\cos\phi\dot{\lambda}$ and r, ϕ, λ are the usual spherical coordinates. Note that

$$|\underline{r}| = r\cos\phi \neq r$$

We make the thin-shell approximation

$$r = R + r' \qquad\qquad r' \ll R$$

(since $R = 6400$ km and $r' \leq 12$ km), giving

$$M = \Omega R^2 \cos^2\phi + uR\cos\phi$$

where the first term is the planetary angular momentum M_Ω, and the second term is the relative angular momentum M_r.

In the absence of forces

$$\frac{dM}{dt} = 0$$

As an air parcel moves away from the equator, ϕ changes and u must change (in the absence of forces). Since $\cos\phi$ decreases, u must increase.

For example, if a parcel has $u = 0$ at the equator, then

$$M = \Omega R^2$$

which must remain constant as ϕ changes, thus

$$M = \Omega R^2 = \Omega R^2 \cos^2\phi + uR\cos\phi$$

$$\Rightarrow \Omega R^2 \sin^2\phi = uR\cos\phi$$

$$\Rightarrow u = \Omega R \tan\phi \sin\phi$$

9.2 Variations in atmospheric angular momentum

The total relative angular momentum of the atmosphere is

$$\widetilde{M_r} = \int M_r dm = \int uR\cos\phi dm$$

This varies seasonally and on longer and shorter timescales. See Peixoto and Oort, Fig. 11.2.

The seasonal cycle of the zonal wind is a little greater in the N.H. than the S.H., so that $\widetilde{M_r}$ is greater in DJF than JJA. Since the angular momentum of the Earth system is conserved, there must be a corresponding change in Ω. This implies that the length of the sidereal day (and solar day)[1] must vary, as shown in Fig. 11.2 of P&O.

If all parts of the Earth's interior rotate at some angular velocity and if the density of the Earth were constant (though note iron denser than rock, which is denser than water, so actually core denser than crust etc.),

$$\widetilde{M_\Omega} = \int \Omega r^2 \cos^2\phi dm = \int \Omega \rho_e r^4 \cos^3\phi dr d\phi d\lambda$$

since the mass element is

$$dm = \rho_e dr r d\phi r\cos\phi d\lambda$$

Thus

$$\widetilde{M_\Omega} = \frac{2}{5} M_e R^2 \Omega \sim 6 \times 10^{33} \text{ kg m}^2 \text{ s}^{-1}$$

where M_e is the mass of the earth. (We could also write $M_\Omega = I\Omega$ with the moment of interia $I = \int r^2 \cos^2\phi dm$)

We used

$$\int r^2 \cos\phi dr d\phi d\lambda = \frac{R^3}{3} 2\pi \left[\sin\phi\right]_{-\pi/2}^{\pi/2} = \frac{4\pi R^3}{3}$$

[1]The solar day is the time it takes for the sun to return to the same point in the sky, and is 24 hours. The sidereal day is measured against the fixed stars and is roughly 23 hours, 56 minutes (there is one less solar day per year). The Earth's rotation rate is $\Omega = \frac{2\pi}{1 \text{ sidereal day}}$

and

$$\begin{aligned}\int r^4 \cos^3\phi dr d\phi d\lambda &= \frac{R^5}{5} 2\pi \int_{-\pi/2}^{\pi/2} d\phi \cos^3\phi \\ &= \frac{2\pi R^5}{5} \int_{-\pi/2}^{\pi/2} d(\sin\phi)\big(1-\sin^2\phi\big) \\ &= \frac{2\pi R^5}{5} \int_{-1}^{+1} dx(1-x^2) \\ &= \frac{2\pi R^5}{5}\Big(2-\frac{2}{3}\Big) \\ &= \frac{8\pi R^5}{15}\end{aligned}$$

Fig. 11.2 suggests changes in $\widetilde{M_r}$ of $10^2 6$ kg m^2 s^{-2}. We can work out the corresponding change in the rotation rate

$$\Delta\widetilde{M_\Omega} \sim \frac{2}{5} M_e R^2 \Delta\Omega \sim \widetilde{M_\Omega}\frac{\Delta\Omega}{\Omega} \sim -\widetilde{M_\Omega}\frac{\Delta T}{T}$$

where T is the length of day. Thus

$$\Delta T \sim -T\frac{\Delta\widetilde{M_r}}{\widetilde{M_\Omega}} \sim -86400\frac{10^{26}}{6\times 10^{33}} \sim 10^{-3}\text{s}$$

which is what is also shown in Fig. 11.2.

- The secular trend in Fig. 11.2 may be related to changes in rotation of core relative to the mantle.
- Also would expect a slowing of rotation due to tidal forcing (tidal friction with the moon).

9.3 Surface stress and mountain torque

Now return to consideration of M in the atmosphere alone:

$$\frac{dM}{dt} = -\frac{1}{\rho}\frac{\partial p}{\partial\lambda} + R\cos\phi F$$

using $\hat{\underline{n}} \cdot (\underline{r} \times \underline{F}) = R\cos\phi F_x$ and setting $F_x = F$ for convenience (here F is the frictional force).

Note that

$$\frac{\partial u}{\partial t} = -\frac{1}{\rho}\frac{\partial p}{\partial x} + ... = -\frac{1}{\rho R\cos\phi}\frac{\partial p}{\partial\lambda} + ...$$

But

$$\rho F = -\Big(\frac{\partial\tau_{xx}}{\partial x} + \frac{\partial\tau_{yx}}{\partial y} + \frac{\partial\tau_{zx}}{\partial z}\Big) \simeq -\frac{\partial\tau_{zx}}{\partial z}$$

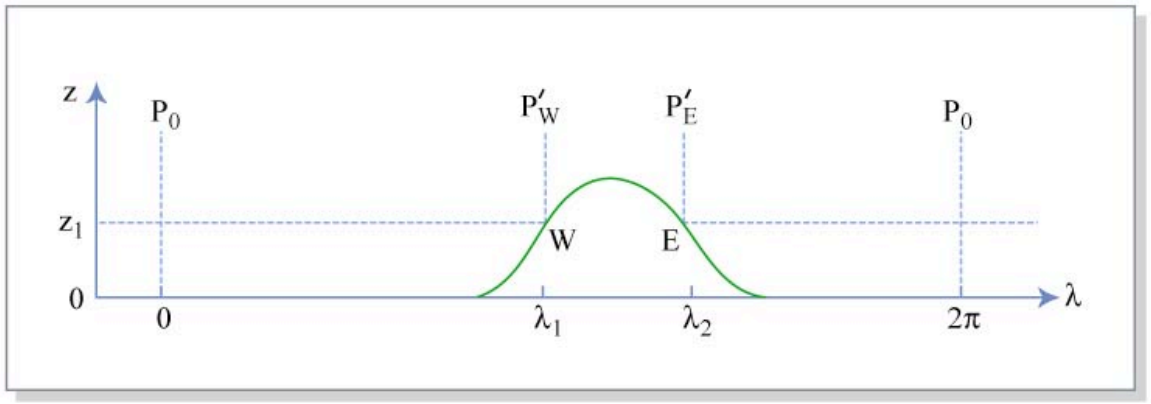

Figure 9.1: Figure by MIT OCW.

where $\underline{\underline{\tau}}$ is the stress tensor and we neglect the horizontal components since they are much smaller than the vertical component in the planetary boundary layer.

$$\rho \frac{dM}{dt} = -\frac{\partial p}{\partial \lambda} - R\cos\phi \frac{\partial \tau_{zx}}{\partial z}$$

but

$$\begin{aligned}\rho \frac{dM}{dt} &= \rho \frac{\partial M}{\partial t} + \rho \underline{c} \cdot \nabla M \\ &= \frac{\partial}{\partial t}(\rho M) + \nabla \cdot (\rho M \underline{c})\end{aligned}$$

by continuity.

Integrating over the atmosphere we find

$$\int \nabla \cdot (\rho M \underline{c}) dV = \int \rho M \underline{c} \cdot \underline{ds} = 0$$

$$-\int_{z_s}^{\infty} \frac{\partial \tau_{zx}}{\partial z} dz = \tau_0 = \text{surface wind stress}$$

and

$$\int_0^{2\pi} \frac{\partial p}{\partial \lambda} d\lambda = 0 \text{ if } z > z_s \text{ for all } \lambda$$

where $z_s = z_s(x, y)$ is the surface topography, but otherwise is non-zero (mountain torque).

Consider a single mountain, sketched in Fig. 9.1. At height z,

$$\begin{aligned}\int \frac{\partial p}{\partial \lambda} d\lambda &= \int_0^{\lambda_1} \frac{\partial p}{\partial \lambda} d\lambda + \int_{\lambda_2}^{2\pi} \frac{\partial p}{\partial \lambda} d\lambda \\ &= p(\lambda_1) - p_0 + p_0 - p(\lambda_2) \\ &= p_W(z) - p_E(z)\end{aligned}$$

In general,

$$\frac{\partial}{\partial t}\int \rho M dV = T_m + T_f$$

where

$$T_f = \int R\cos\phi\tau_0 dA = \int_{-\pi/2}^{\pi/2} d\phi \int_0^{2\pi} d\lambda R^3 \cos^2\phi\tau_0$$

using

$$dA = Rd\phi R\cos\phi d\lambda$$

and the mountain torque term is

$$\begin{aligned} T_m &= -\int\int \frac{\partial p}{\partial\lambda} dA dz \\ &= \int_{-\pi/2}^{\pi/2} d\phi R^2\cos\phi \int dz \sum_i \left(P_E^i - P_W^i\right) \end{aligned}$$

where the sum is taken over all mountains reaching a height of z.[2]

The total angular momentum of the atmosphere changes by mountain torques or surface frictional stresses. For a stationary system, these must sum to zero. Note τ_0 is in opposite direction to surface winds.

9.4 Torques and meridional transport of angular momentum

We next consider the torques and transports at a given latitude.

Writing $M = \Omega R^2\cos^2\phi + M_r$

$$\begin{aligned} \frac{dM}{dt} &= -\Omega R^2 2\cos\phi\sin\phi\frac{d\phi}{dt} + \frac{dM_r}{dt} \\ &= -2\Omega\sin\phi R\cos\phi R\frac{d\phi}{dt} + \frac{dM_r}{dt} \\ &= -fvR\cos\phi + \frac{dM_r}{dt} \end{aligned}$$

Note we neglected $f'w$ term. Is this a useful step? See P&O.

$$\frac{dM_r}{dt} = -\frac{1}{\rho}\frac{\partial p}{\partial\lambda} + R\cos\phi\big(fv + F\big)$$

Substituting $M_r = R\cos\phi u$ would give us the usual zonal momentum equation (including metric and Coriolis terms).

Multiplying by ρ and using continuity,

$$\begin{aligned} \frac{\partial}{\partial t}\big(\rho M_r\big) + \frac{1}{R\cos\phi}\frac{\partial}{\partial\lambda}\big(\rho u M_r\big) + \frac{1}{R\cos\phi}\big(\rho v\cos\phi M_r\big) + \frac{\partial}{\partial z}\big(\rho w M_r\big) \\ = -\frac{\partial p}{\partial\lambda} + R\cos\phi\Big(\rho f v - \frac{\partial\tau_{zx}}{\partial z}\Big) \end{aligned}$$

[2]Note that one can avoid sums by working in σ coordinates. $p_s\frac{\partial z_s}{\partial x}$ then enters the problem.

The assumption of stationarity implies $\frac{\partial}{\partial t} = 0$ in the time mean. Now integrate vertically and use $w = 0$ at $z = z_s, \infty$:

$$\frac{1}{R\cos\phi}\frac{\partial}{\partial\lambda}\int_{z_s}^{\infty}\overline{\rho u M_r}dz + \frac{1}{R\cos\phi}\frac{\partial}{\partial\phi}\int_{z_s}^{\infty}\overline{\rho v M_r}dz$$
$$= -\int_{z_s}^{\infty}\overline{\frac{\partial p}{\partial\lambda}}dz + R\cos\phi f\int_{z_s}^{\infty}\overline{\rho v}dz + R\cos\phi\overline{\tau_0}$$

Integrate zonally, using $u = 0$ at the side of mountains and

$$\int_0^{2\pi}d\lambda\int_{z_s}^{\infty}\overline{\rho v}dz = 0$$

by mass conservation. (Thus the Coriolis term has no effect in the zonal, time and vertical mean).

$$\frac{1}{R\cos\phi}\frac{\partial}{\partial\phi}\int_0^{2\pi}d\lambda\int_{z_s}^{\infty}\overline{\rho v M_r}\cos\phi dz$$
$$= \int_{z_s}^{\infty}\sum_i\Big(\overline{p_E^i} - \overline{p_W^i}\Big)dz + R\cos\phi\int_0^{2\pi}\overline{\tau_0}(\lambda)d\lambda$$

If we set $v = 0$ for $z < z_s$ then

$$\frac{1}{R\cos\phi}\int_0^{p_0}\frac{\partial}{\partial p}\big(\overline{vM_r}\cos\phi\big)dp = \frac{g}{2\pi}\int_{z_s}^{\infty}\sum_i\Big(\overline{p_E^i} - \overline{p_W^i}\Big)dz + Rg\cos\phi[\overline{\tau_0}]$$

- Three-way balance between transport, mountain torques and surface frictional stress.
- Globally, transport term drops out.

9.5 Observed angular momentum transport

The transport term

$$[\overline{vM_r}] = R\cos\phi[\overline{uv}]$$
$$= R\cos\phi\Big([\overline{u}][\overline{v}] + [\overline{u^*v^*}] + [\overline{u'v'}]\Big)$$

is shown in Fig. 11.7 of Peixoto and Oort (1992).

It is quite antisymmetric w.r.t hemisphere, dominated by the transient part, largest in the upper troposphere, and poleward except at high latitudes (equatorward wave breaking).

Vertically averaged, Fig. 11.8 shows the strong seasonal cycle in the mean component, and the importance of the stationary component in N.H. winter.

Fig. 11.12 shows the mountain torque is greatest in the N.H., and contributes a significant component to the angular momentum balance there. (It is calculated from p_s and z_s, and is correlated with $\overline{u}_{sfc}$.

The left hand side of Fig. 11.12 shows the torque on the atmosphere (calculated from the divergence of the dynamical transport in the atmosphere assuming stationarity). The units of torque used are Hadleys:

$$1 \text{ Hadley} = 10^{18} \text{ kg m}^2 \text{ s}^{-2}$$

Note that the unresolved component of the mountain drag (due to smaller scale orography and its generation of vertically propagating gravity waves) is not included in Fig. 11.12.

Bibliography

Robert F. Adler, George J. Huffman, Alfred Chang, Ralph Ferraro, Ping-Ping Xie, John Janowiak, Bruno Rudolf, Udo Schneider, Scott Curtis, David Bolvin, Arnold Gruber, Joel Susskind, Philip Arkin, and Eric Nelkin. The version-2 global precipitation climatology project (GPCP) monthly precipitation analysis (1979-present). *J. Hydrometeor.*, 4:1147–1167, 2003.

Erik Andersson, Peter Bauer, Anton Beljaars, Frederic Chevallier, Elías Hólm, Marta Janisková, Per Kållberg, Graeme Kelly, Philippe Lopez, Anthony Mcnally, Emmanuel Moreau, Adrian J. Simmons, Jean-Noël Thépaut, and Adrian M. Tompkins. Assimilation and modeling of the atmospheric hydrological cycle in the ECMWF forecasting system. *Bull. Amer. Meteor. Soc.*, 86:387–402, 2005.

Karine Béranger, Bernard Barnier, Sergei Gulev, and Michel Crépon. Comparing 20 years of precipitation estimates from different sources over the world ocean. *Ocean Dynamics*, 56:104–138, 2006.

G. J. Boer. Diagnostic equations in isobaric coordinates. *Mon. Wea. Rev.*, 110(12): 1801–1820, 12 1982.

Jule G. Charney. Geostrophic turbulence. *J. Atm. Sci.*, 28(6):1087–1095, 9 1971.

Arnt Eliassen and Enok Palm. On the transfer of energy in stationary mountain waves. *Geofysiske Publikasjoner*, 22(3):1–23, 1961.

Kerry Emanuel. *Atmospheric Convection*. Oxford University Press, 1994.

Joseph Galewsky, Adam Sobel, and Isaac Held. Diagnosis of subtropical humidity dynamics using tracers of last saturation. *J. Atm. Sci.*, 62:3353–3367, 2005.

Dennis L. Hartmann. *Global Physical Climatology*, volume 56 of *International Geophysics Series*. Academic Press, San Diego, 1994.

Isaac M. Held and Brian J. Soden. Water vapor feedback and global warming. *Ann. Rev. Energy Environ.*, 25:441–475, 2000.

M. N. Juckes. The static stability of the midlatitude troposphere: The relevance of moisture. *J. Atm. Sci.*, 57:3050–3057, 2000.

John N. Koshyk and Kevin Hamilton. The horizontal kinetic energy spectrum and spectral budget simulated by a high-resolution troposphere–stratosphere–mesosphere GCM. *J. Atm. Sci.*, 58:329–348, 2001.

L. Li, A.P. Ingersoll, X. Jiang, D. Feldman, and Y.L. Yung. Lorenz energy cycle of the global atmosphere based on reanalysis datasets. *Geophys. Res. Lett.*, 34(L16813), 2007.

Edward N. Lorenz. Available potential energy and the maintenance of the general circulation. *Tellus*, 7:271–281, 1955.

Edward N. Lorenz. Available energy and the maintenance of a moist circulation. *Tellus*, 30:15–31, 1978.

Edward N. Lorenz. Numerical evalution of moist available energy. *Tellus*, 31:230–235, 1979.

Edward N. Lorenz. A history of prevailing ideas about the general circulation of the atmosphere. *Bull. Amer. Meteor. Soc.*, 64(7):730–734, 1983.

Abraham H. Oort and Jose P. Peixoto. Global angular momentum and energy balance requirements from observations. *Adv. Geophys.*, 25:355–490, 1983.

Olivier Pauluis, Arnaud Czaja, and Robert Korty. The global atmospheric circulation on moist isentropes. *Science*, 321(5892):1075–1078, 8 2008.

Jose P. Peixoto and Abraham H. Oort. *Physics of Climate*. Springer-Verlag, New York, 1992.

R. Alan Plumb. A new look at the energy cycle. *J. Atm. Sci.*, 40:1669–1688, 1983.

Tapio Schneider. The tropopause and the thermal stratification in the extratropics of a dry atmosphere. *J. Atm. Sci.*, 61(12):1317–1340, 6 2004.

Tapio Schneider. Self-organization of atmospheric macroturbulence into critical states of weak nonlinear eddy-eddy interactions. *J. Atm. Sci.*, 63:1569–1586, June 2006.

Tapio Schneider and Paul A. OGorman. Moist convection and the thermal stratification of the extratropical troposphere. *J. Atm. Sci.*, 65(11):3571–3583, 11 2008.

Tapio Schneider, Karen L. Smith, Paul A. O'Gorman, and Christopher C. Walker. A climatology of tropospheric zonal-mean water vapor fields and fluxes in isentropic coordinates. *J. Clim.*, 19:5918–5933, 2006.

Dian J. Siedel, Qiang Fu, William J. Randel, and Thomas J. Reichler. Widening of the tropical belt in a changing climate. *Nature Geoscience*, 1:21–24, 2008.

Martin Steinheimer, Michael Hantel, and Peter Bechtold. Convection in lorenz's global energy cycle with the ecmwf model. *Tellus A*, 60:1001–1022, 2008.

Peter H. Stone. Baroclinic adjustment. *J. Atm. Sci.*, 35(4):561–571, April 1978.

Kevin E. Trenberth and Lesley Smith. The mass of the atmosphere: A constraint on global analyses. *J. Clim.*, 18:864–875, 2005.

Geoffrey K. Vallis. *Atmospheric and Oceanic Fluid Dynamics: fundamentals and large-scale circulation*. Cambridge University Press, 2006.

Shuntai Zhou and Peter H. Stone. The role of large-scale eddies in the climate equilibrium. part ii: Variable static stability. *J. Clim.*, 6(10):1871–1881, 10 1993.